

ISSN 1023-0149

*Yarmouk University Publications
Deanship of Research and
Graduate Studies*

ABHATH AL-YARMOUK

Basic Sciences and Engineering

Refereed Research Journal

Vol. 17

No. 2

1429/2008

ISSN 1023-0149

ABHATH AL-YARMOUK

Basic Sciences and Engineering

Refereed Research Journal

Vol. 17

No. 2

1429/2008

**© Copyright 2008 by Yarmouk University
All rights reserved.
No part of this publication may be reproduced without the prior written
permission of the Editor-in-Chief.**

*Opinions expressed in this Journal are those of the authors and do not necessarily reflect
the opinions of the Editorial Board or the policy of Yarmouk University*

Proof Reading:

Prof. Ibrahim Jibril,

Chemistry Dept. Yarmouk University

Typesetting and Layout

Fatima Yousef Atrooz

Cover Design

Ahmad Al-Tamimi

EDITORIAL BOARD

Editor-in-Chief
Professor Abdul Rahman S. Attiyat

Members

Professor Omar Rimawi	Professor Mashhoor Al-Refai
Professor Mohmmad Abu-Saleh	Dr. Mohammad Sheboul
Professor Hamed Zraiqat	Dr. Mohammad Belal Al-Zoubi

Editorial Secretary
Kamilia Adel Al-Haj

In the Name of God Most Gracious Most Merciful

Abhath al-Yarmouk: is a refereed research journal
Basic Sciences and Engineering
Abbreviated: A.Y. (Basic Sci. & Eng.)

NOTES TO CONTRIBUTORS

Only original unpublished articles will be considered.

LANGUAGE: Manuscripts may be written in Arabic or English.

FORMAT:

Manuscripts should be submitted in quadruplicate and typed double-spaced, on one side of the paper only, and with 2.5cm margins. The size of the paper should be (27x21.5cm).

- The total number of pages on the manuscript should not exceed 30 pages, including figures, illustrations, references, tables, and appendices.
- Each manuscript should be accompanied by two abstracts, one in Arabic and one in English, of approximately 200 words each, typed on two separate sheets.
- The title of the manuscript, the author's name, academic rank and affiliation should appear on a separate sheet. The title should also appear on the first page of the manuscript and on each abstract.
- Manuscripts should be sent in print and on a floppy 3.5 computer disk compatible with **IBM (Ms Word)**.

FIGURES AND ILLUSTRATIONS:

- Figures and illustrations should be drawn on tracing paper. Their dimensions should not exceed 19 x 12cm.

FOREIGN NAMES:

When foreign names are mentioned in an Arabic manuscript, they should be written in Arabic, followed by the English transcription in parentheses.

DOCUMENTATION:

- A) Documentation of published references:** This should be done within the text by numbers [5], reference should be listed at the end of the manuscripts.

For a reference to a book:

[] Franson N., Clesceri L., Greenberg A. and Eaton A.(eds.), *Standard methods for the examination of water and wastewater*, 20th Edition, American Public Health Association, Washington, D.D., USA.(1998).

For a reference to an article in a Periodical:

[] Smith P. D., 'On tuning the Boyer-Moore-Horspool string searching algorithm', *Software-Practice and Experience*, 24(4) (1994) 435-436.

For a reference to an article in a book:

[] Gordan A.J. & Ford R.A., A Handbook of Practical Data, Techniques, and References, *Properties of the Elements*. Canada: John Wiley and Sons, Inc, 1972.

- B) Documentation of notes and unpublished references:** This should be done within the text by writing the word “note” followed by the succession number of the note in brackets, as follows: (Note 1). Then every note is explained in further detail at the end of the manuscript, before the references, under the title **Notes**, as follows:

Note 1: Al-Nijjar, Tariq H., Levels of Trace Elements in Freshwater fishes of Azraq Oasis-Jordan, Unpublished M.S Thesis, Yarmouk University, 1991.

BOOK REVIEWS: Book reviews of recent academic publications may be considered for inclusion in the Journal.

EDITORIAL CHANGES: The Editor-in-Chief reserves the right to make any editorial changes he deems necessary.

OFFPRINTS: Twenty offprints will be sent free of charge to the principal author of the published manuscript, in addition to one copy of the journal issue in which the manuscript is published.

SUBMISSION OF MANUSCRIPTS AND CORRESPONDENCE:

Manuscripts and Correspondence should be sent to:

The Editor-in-Chief
Abhath al-Yarmouk (Basic Sciences and Engineering)
Deanship of Research and Graduate Studies
Yarmouk University, Irbid, Jordan

SUBSCRIPTION INFORMATION:

ABHATH AL-YARMOUK may be obtained through the Exchange Division of the Yarmouk University Library or through the Deanship of Research and Graduate Studies at JD 1.000 per single copy. Annual subscription rates for individuals and institutions: Jordan: JD2. 500; Arab World: JD 8.000 or US\$ 12.00; countries outside the Arab World: US\$ 18.00 or equivalent.

TABLE OF CONTENTS

Articles in English

* The Witten –Reshetikhin- Turaev Invariants of Lens Spaces	Khaled Qazaqzeh	425
* On Fibrewise τ – Paracompact Spaces	Abedallah D. AL-Momany	437
* Radon Measurements in Caves and Houses in Umm- Qais, Jordan	Khitam Khasawinah and Khalid Abumurad	459
* Critical Current Enhancement by Iron Doping in $Y_1Ba_2Cu_3O_{7-\delta}$ Superconducting System	Abdul Raouf El Ali (Al-Dairy) and Khitam Khasawinah	467
* Introducing English-Arabic Dictionary-Based Cross Language Information Retrieval	Awni Hammouri	477
* Parallel Graph Colouring Based on Saturated Degree Ordering	Ahmad Sharieh and Khair Eddin Sabri	489
* Automated Global Prayer Calls Using GPS	Zakaria Saleh	505
* Bayesian Prediction Interval from Grouped Data: Exponential Distribution	Moh'd Alodat, Khaled Aludaat and Tareq Alodat	517
* Up-Crossing Rates of Particular Non-Gaussian Processes	Moh'd Alodat and Khaled Aludaat	525
* Analysis of Rainfall in Southern Area of Jordan	Suleiman Tashtoush	533
* Petrographical and Mineralogical Study of the Travertine in Deir Abu Said Area, NW Jordan	Nazem El- Radaideh and Hakam Mustafa	565

The Witten-Reshetikhin-Turaev Invariants of Lens Spaces

Khaled Qazaqzeh*

Received on Jan, 15, 2007

Accepted for publication on June, 28, 2007

Abstract

We derive an explicit formula for the Witten-Reshetikhin-Turaev $SO(3)$ -invariants of lens spaces. We use the representation of the mapping class group of the torus corresponding to the Witten-Reshetikhin-Turaev $SO(3)$ -TQFT to give such formula.

Keywords: Lens spaces, TQFT, $SO(3)$ -quantum invariant.

1. Introduction

We consider a variation of the $(2 + 1)$ cobordism category that was studied in [1]. The variation consists of replacing the p_1 structure by integers that are called weights. This notion was first introduced by [9, 10]. This weighted category can be described roughly as follows. The objects of this category C are closed surfaces Σ equipped with a Lagrangian subspace $\lambda \subset H_1(\Sigma, \mathbb{R})$. We will denote objects by pairs (Σ, λ) . A cobordism from (Σ, λ) to (Σ', λ') is a 3-manifold with an orientation preserving homeomorphism (called its boundary identification) from its boundary to $-\Sigma \sqcup \Sigma'$. Here and elsewhere, $-\Sigma$ denotes Σ with the opposite orientation. Two cobordisms are equivalent if there is an orientation preserving homeomorphism between the underlying 3-manifolds that commutes with the boundary identifications. A morphism $M : (\Sigma, \lambda) \rightarrow (\Sigma', \lambda')$ is an equivalence class of cobordisms from (Σ, λ) to (Σ', λ') together with an integer weight. We denote morphisms by $(M, w(M))$, where $w(M)$ denotes the weight of M . The gluing of 3-manifolds represents the composition and the weight of the composed morphism is given by [3, Equation(1.6)] which was derived from [9, Thm.(4.1.1)].

The version of the WRT invariant that we study here is the invariant that is obtained from the $SO(3)$ -TQFT-functor for $r \equiv 1 \pmod{4}$ on C over a commutative ring K_r that was given in [1]. The $SO(3)$ -TQFT-functor (V_r, Z_r) is a functor from C to the category of finitely generated free k_r -modules. It is defined as follows: $V_p(\Sigma)$ is a quotient of the k_r -module generated by all cobordisms with boundary Σ , and $Z_r(M)$ is the k_r -linear map from $V_r(\Sigma)$ to $V_r(\Sigma')$ (where $\partial M = -\Sigma \sqcup \Sigma'$) induced by gluing

Qazaqzeh

representatives of elements of $V_r(\Sigma)$ to M along Σ via the identification map. The ring is $K_r = \mathbb{Q}[\zeta_{2r}, i]$ with $A = \zeta_{2r}$, and $\kappa = iA^{-1}$ where $\zeta_{2r} = e^{\frac{2\pi i}{2r}}$. This invariant is recovered from the representation of the gluing map between the two parts of the Heegaard splitting of the 3-manifold on the $SO(3)$ -TQFT-vector space $V_r(\Sigma)$ of the boundary surface.

2. The $SO(3)$ -TQFT-Representation of $SL(2, \mathbb{Z})$

The $SO(3)$ -TQFT associates to a surface Σ , a representation of the mapping class group on the vector space $V_r(\Sigma)$. We consider the case where the surface is the torus. The mapping class group of the torus is known to be $SL(2, \mathbb{Z})$. Hence, we obtain a representation of the group $SL(2, \mathbb{Z})$ on the vector space $V_r(S^1 \times S^1)$.

The group $SL(2, \mathbb{Z})$ is specified in terms of two generators $\mathbf{S} = \begin{pmatrix} 0 & -1 \\ 1 & 0 \end{pmatrix}$, and

$\mathbf{T} = \begin{pmatrix} 1 & 1 \\ 0 & 1 \end{pmatrix}$ with the relations $\mathbf{S}^4 = (\mathbf{ST})^6 = 1$. So any representation is specified in terms of these two generators satisfying the relations.

We adopt the following notation of [5] that has been used also in [4]:

$$e(\alpha) \stackrel{\text{def}}{=} \exp(2\pi i\alpha), \quad e_n(\alpha) \stackrel{\text{def}}{=} \exp(2\pi i\frac{\alpha}{n}). \quad \text{Also, } \zeta \stackrel{\text{def}}{=} \exp \frac{i\pi}{4}.$$

The representation is given explicitly by the assignments $\mathbf{S} \mapsto \mathcal{D}^{-1}S$ and $\mathbf{T} \mapsto T^{-1}$ as given in [9, Page 98]. This assignments define a projective representation because of the factor $\Delta\mathcal{D}^{-1} \in K$. This factor is expressed in terms of κ in the following lemma.

Lemma 1 *Let $\kappa \in K$ be as above, then $\mathcal{D}\Delta^{-1} = \kappa^3 = -iA^{-3}$.*

Proof :-

$$\begin{aligned} \kappa^3 &= \kappa^3 \mathcal{D} \langle S^3, 0 \rangle = \mathcal{D} (\kappa^3 \langle S^3, 0 \rangle) \\ &= \mathcal{D} \langle S^3, 1 \rangle \\ &= \mathcal{D} (\mathcal{D}\Delta^{-1}) \langle S^3, 0 \rangle \\ &= \mathcal{D} (\mathcal{D}\Delta^{-1}) \mathcal{D}^{-1} = \mathcal{D}\Delta^{-1}. \end{aligned}$$

Hence the assignments $\mathbf{S} \mapsto \mathcal{D}^{-1}S$ and $\mathbf{T} \mapsto \kappa^{-1}T^{-1}$ give a linear representation as stated in the following proposition whose proof can be found in [9, §2.3].

Proposition 2 *The representation of $SL(2, \mathbb{Z})$ on the vector space $V_r(S^1 \times S^1)$ obtained from the $SO(3)$ -TQFT-representation is given by*

$$\begin{aligned} S_{jl} &= \frac{1}{i\sqrt{r}} [e_r(jl) - e_r(-jl)] = \frac{2}{\sqrt{r}} \sin\left(\frac{jl\pi}{r}\right), \\ T_{jl} &= \delta_{jl} T_j, \quad T_j = ie_{2r}(j^2), \end{aligned}$$

for $1 \leq j, l \leq \frac{r-1}{2}$.

The Witten-Reshetikhin-Turaev Invariants of Lens Spaces

Remark 3 In the above two matrices, we should have $j, l \in \{0, 2, 4, \dots, r - 3\}$ since the last set represents the set of simple objects in the $SO(3)$ -modular category. However, the above two matrices and the actual matrices are similar by the same permutation matrix, i.e

$$S = PS_aP^{-1}, \quad T = PT_aP^{-1}$$

where S_a, T_a are the actual matrices.

Lemma 4 The entries of S_{jl} , and T_j satisfy the following symmetries:

$$S_{jl} = S_{j(r+l)} = -S_{j(r-l)}, \quad T_j = T_{(j+r)} = T_{(r-j)}.$$

Proof :- It is clear for the entries of the S -matrix. For the entries of the T -matrix, we know that $e_{2r}(1) = -e_r(n)$ for some integer n . Therefore, $T_j = -ie_r(nj^2) = -ie_r(n(j+r)^2) = -ie_r(n(r-j)^2)$.

Now, we wish to give an explicit formula for the representation of any element of $SL(2, \mathbb{Z})$ independent from the way we write that element in terms of the generators **S**, and **T**. But before we do that, we would like to quote the Gauss sum reciprocity formula in one dimension from [4].

Proposition 5 If $\lambda, n, m \in \mathbb{Z}$ with nm is even and $n\psi \in \mathbb{Z}$, then:

$$\sum_{\lambda \pmod{n}} e_{2n}(m\lambda^2)e(\psi\lambda) = \sqrt{\frac{in}{m}} \sum_{\lambda \pmod{m}} e_{2m}(-n(\lambda + \psi)^2). \quad (1)$$

2.1 The formula of the Representation

Let $U = \begin{pmatrix} a & b \\ c & d \end{pmatrix} \in SL(2, \mathbb{Z})$, we want to give a formula for the representation of U in terms of its entries.

Definition 6 A continued fraction expansion for U is a tuple of integers $\mathcal{C} = (m_1, \dots, m_t)$ such that

$$U = T^{m_t} S T^{m_{t-1}} \dots T^{m_1} S.$$

We would like to quote the following proposition from [4].

Proposition 7 [4, Prop.(2.5)] Suppose U , and \mathcal{C} as above. Then

$$(i) \quad a/c = m_t - \frac{1}{m_{t-1} - \frac{1}{\dots - \frac{1}{m_1}}}$$

(ii) $b/a = -\left(\frac{1}{a_1} + \frac{1}{a_2 a_1} + \dots + \frac{1}{a_t a_{t-1}}\right)$. Moreover, define a_i, b_i, c_i, d_i by the partial evaluation of this product:

Qazaqzeh

$$\begin{pmatrix} a_i & b_i \\ c_i & d_i \end{pmatrix} = \mathbf{T}^{m_i} \mathbf{S} \mathbf{T}^{m_{t-1}} \dots \mathbf{T}^{m_1} \mathbf{S},$$

with the convention that:

$$a_0 = d_0 = 1, \quad b_0 = c_0 = 0.$$

Then these satisfy the recurrence relations (for $t \geq 2$)

$$\begin{aligned} (iii) \quad & a_t = m_t a_{t-1} - c_{t-1}, & c_t &= a_{t-1}; \\ (iv) \quad & b_t = m_t a_{t-1} - d_{t-1}, & d_t &= b_{t-1}. \end{aligned}$$

Lemma 8 Denote by \mathfrak{S}_t the sum

$$\mathfrak{S}_t = \sum_{j_1, \dots, j_t=1}^{\frac{r-1}{2}} S_{j_{t+1}j_t} T_{j_t}^{m_t} S_{j_t j_{t-1}} T_{j_{t-1}}^{m_{t-1}} \dots T_{j_1}^{m_1} S_{j_1 j_0}. \quad (2)$$

Then in terms of the previous proposition

$$\mathfrak{S}_t = C_t \sum_{\substack{\gamma \pmod{2ra_t} \\ \gamma \equiv j_{t+1} \pmod{r}}} \left\{ e_{2ra_t} \left(-c_t \left(\gamma + \frac{j_0}{c_t} \right)^2 \right) - e_{2ra_t} \left(-c_t \left(\gamma - \frac{j_0}{c_t} \right)^2 \right) \right\},$$

where

$$C_t = -i^{(t-1)} \zeta^{t-1} \zeta^{\text{sign}(a_t)} \frac{i^{(m_t + \dots + m_1)}}{\sqrt{r |a_t|}} e_{2r} \left\{ - \left(\frac{1}{a_0 a_1} + \dots + \frac{1}{a_{t-2} a_{t-1}} \right) j_0^2 \right\}.$$

Proof :- We observe that each of the indices j_1, \dots, j_t appears twice for the entries of S in (2), so we may divide by 2 and replace the sum over j_1, \dots, j_t from 1 to r (using the symmetries in Lemma (4)). To prove the result, we use induction on t . For $t = 1$:

$$\begin{aligned} \mathfrak{S}_1 &= \frac{1}{2} \sum_{j_1=1}^r S_{j_2 j_1} T_{j_1}^{m_1} S_{j_1 j_0} \\ &= \frac{1}{2} \frac{-1}{r} i^{m_1} \sum_{j_1=1}^r e_{2r} (m_1 j_1^2) \{ e_r (j_2 j_1) - e_r (-j_2 j_1) \} \{ e_r (j_1 j_0) - e_r (-j_1 j_0) \} \\ &= \frac{-1}{2r} 2i^{m_1} \sum_{j \pmod{r}} e_{4r} (2m_1 j^2) \{ e_r ((j_2 + j_0) j) - e_r ((j_2 - j_0) j) \} \\ &= \frac{-1}{r} i^{m_1} \sqrt{\frac{2ir}{2m_1}} \\ &\times \sum_{\beta \pmod{2m_1}} \left\{ e_{4m_1} \left(-2r \left(\beta + \frac{j_2 + j_0}{r} \right)^2 \right) - e_{4m_1} \left(-2r \left(\beta + \frac{j_2 - j_0}{r} \right)^2 \right) \right\} \end{aligned}$$

The Witten-Reshetikhin-Turaev Invariants of Lens Spaces

$$\begin{aligned}
 &= -i^{m_1} \zeta^{\text{sign}(a_1)} \frac{1}{\sqrt{r|a_1|}} \\
 &\times \sum_{\beta \pmod{2a_1}} e_{2ra_1} \left(-(r\beta + j_2 + j_0)^2 \right) - e_{2ra_1} \left(-(r\beta + j_2 - j_0)^2 \right)
 \end{aligned}$$

Two terms in the third equality corresponding to the complex conjugates of the terms shown have been removed, and the overall expression was multiplied by 2: this results from the substitution $j \rightarrow -j$. The fourth equality was obtained by applying the reciprocity formula (1). We obtain the required result by substituting $\gamma = r\beta + j_2$. Hence, this confirms the first step of the induction. Now, we assume that the result holds inductively for $t - 1$. To prove the result for \mathfrak{S}_t , we use the symmetries in Lemma (4) to expand the sum over j_t from 1 to r .

$$\begin{aligned}
 \mathfrak{S}_t &= \frac{1}{2} \sum_{j_t=1}^r S_{j_{t+1}j_t} T_{j_t}^{m_t} \mathfrak{S}_{t-1} \\
 &= \frac{1}{2} \frac{i^{m_t}}{i\sqrt{r}} C_{t-1} \sum_{j_t \pmod{r}} \sum_{\substack{\gamma \pmod{2ra_{t-1}} \\ \gamma \equiv j_t \pmod{r}}} e_{2ra_{t-1}}(m_t a_{t-1} j_t^2) e_{2ra_{t-1}}(-c_{t-1} \gamma^2) \\
 &\quad e_{2ra_{t-1}c_{t-1}}(-j_0^2) \{e_{ra_{t-1}}(-\gamma j_0) - e_{ra_{t-1}}(\gamma j_0)\} \{e_r(j_{t+1}j_t) - e_r(-j_{t+1}j_t)\}
 \end{aligned}$$

Now, we replace j_t by γ and we combine the coefficients of the γ^2 factors using Proposition 7(iii), so we get:

$$\begin{aligned}
 \mathfrak{S}_t &= \frac{i^{m_t}}{2i\sqrt{r}} C_{t-1} e_{2ra_{t-1}c_{t-1}}(-j_0^2) \sum_{\gamma \pmod{2rc_t}} e_{2ra_{t-1}}(a_t \gamma^2) \\
 &\quad \times \{e_r(j_{t+1}\gamma) - e_r(-j_{t+1}\gamma)\} \{e_{ra_{t-1}}(-\gamma j_0) - e_{ra_{t-1}}(\gamma j_0)\}.
 \end{aligned}$$

Now the substitution $\gamma \rightarrow -\gamma$ allows us to condense four terms to two and a factor of -2 in front of the sum, so this yields:

$$\begin{aligned}
 \mathfrak{S}_t &= \frac{-i^{m_t}}{i\sqrt{r}} C_{t-1} e_{2ra_{t-1}c_{t-1}}(-j_0^2) \sum_{\gamma \pmod{2rc_t}} e_{2rc_t}(a_t \gamma^2) \\
 &\quad \times \{e_{rc_t}(c_t j_{t+1} + j_0)\gamma) - e_{rc_t}(c_t j_{t+1} - j_0)\gamma)\}
 \end{aligned}$$

Qazaqzeh

$$\begin{aligned}
 &= \frac{-i^{m_t}}{i\sqrt{r}} C_{t-1} e_{2ra_{t-1}c_{t-1}}(-j_0^2) \sum_{\substack{\gamma \pmod{2rc_t} \\ \gamma \equiv j_0 \pmod{r}}} e_{4rc_t}(2a_t\gamma^2) \\
 &\times \{e_{rc_t}(c_t j_{t+1} + j_0)\gamma) - e_{rc_t}(c_t j_{t+1} - j_0)\gamma)\}.
 \end{aligned}$$

Now, we use the reciprocity formula (1) to obtain:

$$\begin{aligned}
 \mathfrak{S}_t &= \frac{-i^{m_t}}{i\sqrt{r}} C_{t-1} e_{2ra_{t-1}c_{t-1}}(-j_0^2) \sqrt{\frac{2irc_t}{2a_t}} \sum_{\beta \pmod{2a_t}} \\
 &\left\{ e_{4a_t} \left(-2rc_t \left(\beta + \frac{c_t j_{t+1} + j_0}{rc_t} \right)^2 \right) - e_{4a_t} \left(-2rc_t \left(\beta + \frac{c_t j_{t+1} - j_0}{rc_t} \right)^2 \right) \right\} \\
 &= \frac{-i^{m_t}}{i\sqrt{r}} C_{t-1} e_{2ra_{t-1}c_{t-1}}(-j_0^2) \sqrt{\frac{irc_t}{a_t}} \sum_{\beta \pmod{2a_t}} \\
 &\left\{ e_{2ra_t} \left(-c_t \left(r\beta + j_{t+1} + \frac{j_0}{c_t} \right)^2 \right) - e_{2ra_t} \left(-c_t \left(r\beta + j_{t+1} + \frac{-j_0}{c_t} \right)^2 \right) \right\}.
 \end{aligned}$$

Now, the main formula holds using the substitution $\gamma = r\beta + j_{t+1}$. Finally, we use induction for C_t :

$$C_t = \frac{-i^{m_t}}{i\sqrt{r}} C_{t-1} e_{2ra_{t-1}c_{t-1}}(-j_0^2) \sqrt{\frac{irc_t}{a_t}} = i^{m_t} e_{2ra_{t-1}a_{t-2}}(-j_0^2) \sqrt{\frac{ic_t}{a_t}} C_{t-1}.$$

Hence, the formula for C_t holds from the induction hypothesis for C_{t-1} .

Proposition 9 *The representation of $SL(2, \mathbb{Z})$ on $V_r(S^1 \times S^1)$ is given by*

$$\mathcal{R}(U)_{jl} = (-iK_t) \frac{1}{\sqrt{r|c|}} e_{2rc}(dl^2) \sum_{\substack{\gamma \pmod{2rc} \\ \gamma \equiv j_t \pmod{r}}} e_{2rc}(a\gamma^2) \{e_{rc}(\gamma l) - e_{rc}(-\gamma l)\},$$

where $K_t = i^{(t-1)} \zeta^{t-2} \zeta^{\text{sign}(a_{t-1})} i^{(m_t + \dots + m_1)}$ for $t \geq 2$ and $K_1 = i^{m_1}$.

Proof :- We prove the case for $t \geq 2$, we have

$$\begin{aligned}
 \mathcal{R}(U)_{j_t j_0} &= T_{j_t}^{m_t} \mathfrak{S}_{t-1} \\
 &= i^{m_t} C_{t-1} \sum_{\substack{\gamma \pmod{2rc_t} \\ \gamma \equiv j_t \pmod{r}}} e_{2r}(m_t \gamma^2)
 \end{aligned}$$

The Witten-Reshetikhin-Turaev Invariants of Lens Spaces

$$\begin{aligned}
 & \times \left\{ e_{2ra_{t-1}} \left(-c_{t-1} \left(\gamma + \frac{j_0}{c_{t-1}} \right)^2 \right) - e_{2ra_{t-1}} \left(-c_{t-1} \left(\gamma - \frac{j_0}{c_{t-1}} \right)^2 \right) \right\} \\
 & = i^{m_t} C_{t-1} e_{2ra_{t-1}c_{t-1}}(-j_0^2) \sum_{\substack{\gamma \pmod{2rc_t} \\ \gamma \equiv j_t \pmod{r}}} e_{2ra_{t-1}}(m_t a_{t-1} \gamma^2) \\
 & \times e_{2ra_{t-1}}(-c_{t-1} \gamma^2) \left\{ e_{ra_{t-1}}(-\gamma j_0) - e_{ra_{t-1}}(\gamma j_0) \right\}.
 \end{aligned}$$

We combine the coefficients of the γ^2 factors using Proposition 7(iii), to obtain:

$$\begin{aligned}
 \mathcal{R}(U)_{j_t j_0} & = -i^{m_t} C_{t-1} e_{2ra_{t-1}a_{t-2}}(-j_0^2) \sum_{\substack{\gamma \pmod{2rc_t} \\ \gamma \equiv j_t \pmod{r}}} \\
 & e_{2ra_{t-1}}(a_t \gamma^2) \left\{ e_{ra_{t-1}}(\gamma j_0) - e_{ra_{t-1}}(-\gamma j_0) \right\} \\
 & = -i^{m_t} C_{t-1} e_{2ra_{t-1}a_{t-2}}(-j_0^2) e_{2ra_t a_{t-1}}(-j_0^2) \sum_{\substack{\gamma \pmod{2rc_t} \\ \gamma \equiv j_t \pmod{r}}} \\
 & \left\{ e_{2ra_{t-1}} \left(a_t \left(\gamma + \frac{j_0}{a_t} \right)^2 \right) - e_{2ra_{t-1}} \left(a_t \left(\gamma - \frac{j_0}{a_t} \right)^2 \right) \right\}.
 \end{aligned}$$

We substitute the value of C_{t-1} from the previous lemma, to get:

$$\begin{aligned}
 \mathcal{R}(U)_{j_t j_0} & = i^{m_t} i^{(t-2)} \zeta^{t-2} \zeta^{\text{sign}(a_{t-1})} \frac{i^{(m_{t-1} + \dots + m_1)}}{\sqrt{r |a_{t-1}|}} \\
 & e_{2r} \left\{ - \left(\frac{1}{a_0 a_1} + \dots + \frac{1}{a_{t-3} a_{t-2}} \right) j_0^2 \right\} e_{2ra_{t-1}a_{t-2}}(-j_0) e_{2ra_t a_{t-1}}(-j_0^2) \\
 & \times \sum_{\substack{\gamma \pmod{2rc_t} \\ \gamma \equiv j_t \pmod{r}}} \left\{ e_{2ra_{t-1}} \left(a_t \left(\gamma + \frac{j_0}{a_t} \right)^2 \right) - e_{2ra_{t-1}} \left(a_t \left(\gamma - \frac{j_0}{a_t} \right)^2 \right) \right\}.
 \end{aligned}$$

Now, we use Proposition 7(ii) for the prefactor involving j_0^2 to obtain:

$$\begin{aligned}
 \mathcal{R}(U)_{j_t j_0} & = -i K_t \frac{1}{\sqrt{r |c|}} e_{2ra}(b j_0^2) \tag{3} \\
 & \sum_{\substack{\gamma \pmod{2rc_t} \\ \gamma \equiv j_t \pmod{r}}} \left\{ e_{2ra_{t-1}} \left(a_t \left(\gamma + \frac{j_0}{a_t} \right)^2 \right) - e_{2ra_{t-1}} \left(a_t \left(\gamma - \frac{j_0}{a_t} \right)^2 \right) \right\}
 \end{aligned}$$

$$\begin{aligned}
 &= -iK_t \frac{1}{\sqrt{r|c|}} e_{2rac}(bcj_0^2) e_{2rac}(j_0^2) \sum_{\substack{\gamma \pmod{2rc_t} \\ \gamma \equiv j_t \pmod{r}}} e_{2rc}(a\gamma^2) \{e_{rc}(\gamma j_0) - e_{rc}(-\gamma j_0)\} \\
 &= -iK_t \frac{1}{\sqrt{r|c|}} e_{2rc}(dj_0^2) \sum_{\substack{\gamma \pmod{2rc} \\ \gamma \equiv j_t \pmod{r}}} e_{2rc}(a\gamma^2) \{e_{rc}(\gamma j_0) - e_{rc}(-\gamma j_0)\}.
 \end{aligned}$$

Here $K_t = i^{(t-1)} \zeta^{t-2} \zeta^{\text{sign}(a_{t-1})} i^{(m_t + \dots + m_1)}$. The last equality follows from the equation $bc + 1 = ad$.

3. The Formula of the Invariant for Lens Spaces

The lens space $L(p, q)$ is specified by a pair of coprime integers p, q . We can assume that $0 < -q < p$ as it was shown in [8] that $L(p, q)$ is diffeomorphic to $L(p, q + np)$ for any integer n . The above lens space is obtained by doing a rational surgery on S^3 along the unknot with coefficient $-p/q$. Equivalently, it is obtained by an integer surgery on S^3 along a chain link L with successive framings by integers m_1, m_2, \dots, m_{t-1} such that $\mathcal{C} = (m_1, m_2, \dots, m_{t-1})$ is a continued fraction of $-p/q$ as in [7]. The rational surgery on S^3 means removing a solid torus around the unknot and gluing it back using the matrix:

$$A = \begin{pmatrix} p & d \\ -q & -b \end{pmatrix} \in SL(2, \mathbb{Z}).$$

Hence, the lens space $L(p, q)$ is obtained by gluing two solid tori by

$$U = \mathbf{S}A = \begin{pmatrix} q & b \\ p & d \end{pmatrix}.$$

Therefore, U has a continued fraction expansion $\mathcal{C} = (m_1, \dots, m_{t-1}, m_t = 0)$. Thus, according to the TQFT axioms, the WRT invariant of $L(p, q)$ with the weight obtained from the composition is given by

$$\langle L(p, q), w \rangle_r = \mathcal{R}(U)_{11},$$

where $w = \sum_{i=2}^t \text{sign}(c_{i-1}c_i)$ as computed in [2, Page. 415]. As $0 < -q < p$, we have $-p/q > 1$. We need to use a generalized version of [4, Lem. (3.1)].

Lemma 10 $-p/q$ has a unique continued fraction expansion with all $m_i \geq 2$.

Proof :- We know that any rational number has a continued fraction expansion. The construction of the required fraction expansion is given as follows: set $m_{t-1} = \lceil -p/q \rceil \geq 2$, so $-p/q = m_{t-1} - (p'/q')^{-1}$, where $1 \leq q' < p' = -q < p$, and $p'/q' > 1$. We repeat this process for p'/q' and since the denominators continue to decrease, this process will terminate. This gives a continued fraction expansion with $m_i \geq 2$. The idea of this construction is due to Jeffery in the her proof of [4, Lem. (3.1)]. To prove the

The Witten-Reshetikhin-Turaev Invariants of Lens Spaces

uniqueness, we assume that $\mathcal{C}' = (m_1, m_2, \dots, m_{r-1})$ is another continued fraction expansion of $-p/q$ with all $m_i \geq 2$. Let k be the first integer such that $m_{t-1-k} \neq m_{r-1-k}$. Hence, we would have $s/u = m_{r-1-k} - (s'/u')^{-1}$ with $s'/u' < 1$. Therefore, $(m_1, m_2, \dots, m_{r-2-k})$ is a continued fraction expansion for $(s'/u') < 1$ with $m_i \geq 2$ which contradicts the result of the next lemma.

Lemma 11 *If $s/u < 1$, then there is no continued fraction expansion for s/u with all $m_i \geq 2$.*

Proof :- Assume such a continued fraction expansion exists for s/u . We consider first the case $0 < s/u < 1$. If $s/u = m_{v-1} - (s'/u')^{-1}$ with $1 \leq s < u = s' < u'$ then it implies $0 < s'/u' < 1$. Now, if we repeat this process for s'/u' then it will never terminate as long as $m_i \geq 2$. For the second case, if $s/u < 0$ then it is enough to notice that $s/u = m_{v-1} - (s'/u')^{-1}$ where $0 < s'/u' < 1$. Now we can apply the first case to s'/u' to conclude that there is no continued fraction expansion with all $m_i \geq 2$.

Theorem 12 *There is a unique continued fraction expansion \mathcal{C} for any rational number $|s/u| \neq 1$ with*

1. $m_i \geq 2, 1 \leq i \leq t$ if $s/u > 1$.
2. $m_i \leq -2, 1 \leq i \leq t$ if $s/u < -1$.
3. $m_i \leq -2, 1 \leq i \leq t - 1$ and $m_t = 0$ if $0 \leq s/u < 1$.
4. $m_i \geq 2, 1 \leq i \leq t - 1$ and $m_t = 0$ if $-1 < s/u \leq 0$.

We need to use the next lemma whose proof can be found in [4].

Lemma 13 (4, Lem. (3.2)) *If A is given by the continued fraction with all $m_i \geq 2$ as above, then*

$$\Phi(U) = -3(t - 1) + \sum_{i=0}^{t-1} m_i.$$

Here and elsewhere, $\Phi(U)$ is the Rademacher phi function of U (see [4, 6] for more details about this function). Now, we have

$$\kappa^{3 \text{Sign}(W_L)} \langle L(p, q), 0 \rangle_r = \langle L(p, q), w \rangle_r = \kappa^{\text{Trace}(W_L)} \mathcal{R}(U)_{11}.$$

where W_L is the linking matrix of the link L . Hence, we have

$$\langle L(p, q), 0 \rangle_r = \kappa^{\Phi(U)} \mathcal{R}(U)_{11}. \tag{4}$$

Therefore, we can conclude the following theorem.

Theorem 14 *The Witten-Reshetikhin-Turaev invariant of the lens space $L(p, q)$ weighted zero is given by*

$$\langle L(p, q), 0 \rangle_r = -\frac{i\zeta^{t-1}}{\sqrt{rp}} e_{2r}(12s(q, p)) \sum_{\pm} \sum_{n=1}^p e_{rp}(\pm 1) e_p(2qrn^2) e_p(2n(q \pm 1)), \quad (5)$$

where the Dedekind sum $s(q, p)$ is defined in [4, Equation(2.16)].

Proof :- Using equation (3), we have

$$\begin{aligned} \mathcal{R}(U)_{11} &= -iK_t \frac{1}{\sqrt{rp}} e_{2rq}(b) \\ &\quad \sum_{\substack{\gamma \pmod{2rp} \\ \gamma \equiv 1 \pmod{r}}} \left\{ e_{2rp} \left(q \left(\gamma + \frac{1}{q} \right)^2 \right) - e_{2rap} \left(q \left(\gamma - \frac{1}{q} \right)^2 \right) \right\} \\ &= -iK_t \frac{1}{\sqrt{rp}} e_{2rq}(b) \sum_{n=1}^p \\ &\quad \{ e_{2rpq}(2rnq + q + 1)^2 - e_{2rpq}(2rnq + q - 1)^2 \} \\ &= -iK_t \frac{1}{\sqrt{rp}} e_{2rq}(b) \sum_{n=1}^p e_p(2qrn^2) \\ &\quad \{ e_p(2n(q + 1)) e_{2rpq}(q + 1)^2 - e_p(2n(q - 1)) e_{2rpq}(q - 1)^2 \}. \end{aligned}$$

Therefore by (4), we get:

$$\begin{aligned} \langle L(p, q), 0 \rangle_r &= -i \cdot \Phi(U) \zeta^{t-2} \zeta^{\text{sign}(p)} (i^{-1} e_{2r}(-1))^{\Phi(U)} \frac{1}{\sqrt{rp}} e_{2rq}(b) \\ &\quad \times \sum_{n=1}^p e_p(2qrn^2) \\ &\quad \times \{ e_p(2n(q + 1)) e_{2rpq}(q + 1)^2 - e_p(2n(q - 1)) e_{2rpq}(q - 1)^2 \}. \end{aligned}$$

Now,

$$e_{2rq}(b) e_{2rpq}(q \pm 1)^2 = e_{2rpq}(bp + q^2 \pm 2q + 1) = e_{2rp}(d + q \pm 2),$$

as $bp + 1 = dq$. Also, if we introduce the integer q^* solving $qq^* \equiv 1 \pmod{p}$ then we have

$$e_{2rp}(d + q \pm 2) (e_{2r}(-1))^{\Phi(U)} = e_{rp}(\pm 1) e_{2r}(12s(d, p)) = e_{rp}(\pm 1) e_{2r}(12s(q^*, p)),$$

as $\Phi(U) = \frac{d+q}{p} - 12s(d, p)$ and $q^* \equiv d \pmod{p}$. Finally, we obtain the result as $s(q^*, p) = s(q, p)$.

Summary and Acknowledgments:

The main conclusion of this work is to obtain formula (5) that gives the WRT-invariant of lens spaces in terms of a finite sum. As generalized version of [4, Lem (3.1)] was needed, we proved Theorem (12) which gives more information than what we needed.

I would like to acknowledge that the idea behind this work was inspired by Jeffery's work [4]. The main difference between the two is the TQFT that was considered. In particular, her work was based on the TQFT associated to the group $SU(2)$ where our work is based on the TQFT associated to the group $SO(3)$. Also, I would like to thank my Ph.D. adviser P. Gilmer for motivating and encouraging me to do this work.

متغيرات Witten-Reshetikhin-Turaev للفضاءات العدسية

خالد قزاقزة

ملخص

نقوم بإيجاد صيغة صريحة لمتغيرات Witten-Reshetikhin-Turaev للفضاءات العدسية في حالة الزمرة $SO(3)$. نستخدم تمثيل زمرة الاقتترانات للدولاب المرتبطة بنظرية حقول الكمية لـ Witten-Reshetikhin-Turaev في حالة الزمرة $SO(3)$ لإعطاء هذه الصيغة.

References

- [1] Blanchet C., Habegger N., Masbaum G. and Vogel P., Topological Quantum Field Theories derived from the Kauffman bracket., *Topology*, 34 (1995) 883-927.
- [2] Gilmer P., Skein Theory and Witten-Reshetikhin-Turaev Invariants of Links in Lens Spaces, *Commun. Math. Phys.*, 202 (1999) 411-419.
- [3] Gilmer P. and Qazaqzeh K., The parity of the Maslov index and the even cobordism category., *Fund. Math.*, 188 (2005) 95-102.
- [4] Jeffrey L., Chem-Simons-Witten Invariants of Lens Spaces and Torus Bundles and the Semiclassical Approximation, *Commun. Math. Phys.*, 147 (1992) 563-604.
- [5] Kirby R. and Melvin P., TiK-three-manifold invariants of Witten and Reshetikhin-Turaev, *Invent. Math.*, 105 (1991) 473-545.
- [6] Kirby R. and Melvin P., Dedekind sums, u-invariants, and the signature cocycle, *Math. Ann.*, 299 (1994) 231-267.
- [7] Prasolov V. and Sossinsky A., "Knots, links, braids and 3-manifolds. An introduction to the new invariants low-dimensional topology", *Transl. Math. Monogr.*, 154(1997).
- [8] Rolfsen D., "Knots and links, 2nd printing with corrections", Mathematics Lecture Series 7, Publish or Perish, Inc. (1990).
- [9] Turaev V., "Quantum invariants of knots and 3-manifolds", de Gruyter studies in mathematics, 18, (1994).
- [10] Walker K., "On Witten's 3-manifold invariants". Preprint (1991).

On Fibrewise τ – Paracompact Spaces

Abdallah D. AL-Momany *

Received on Dec. 20, 2006

Accepted for publication on Oct. 24, 2007

Abstract

In [2] and [3], Buhagiar defined paracompact mappings, subparacompact mappings, metacompact mappings, and collectionwise normal mappings which are fibrewise topological analogues of paracompact, subparacompact, and collectionwise normal spaces respectively.

In this paper we give new characterizations of fibrewise τ – Paracompact spaces.

2000 Mathematics subject classification: 54A25, 54C05, 54D20, 45D15.

Keywords: Fibrewise paracompact, Fibrewise countably paracompact, Fibrewise τ – paracompact, b -Locally finite.

Introduction

The fibrewise viewpoint is standard in the theory of fibre bundles, and some of the ideas of fibrewise topology originated in work of the ideas of that of theory. In fibrewise we work over a topological base space B . When B is a point space, the theory reduced to that ordinary topology. Most of the results obtained in this field can be found in [1], [2], [3] and [6].

1- Preliminaries:

Unless otherwise stated, B is a fixed topological space, τ denotes an ordinal number and \overline{O}^{X_w} denotes the closure of O in $X_w \dots$

Definition 1.1 [7]: Let $\mathcal{U} = \{U_\alpha \mid \alpha \in \Delta\}$ be a collection of subsets of space X . Then \mathcal{U} is called monotone increasing if $U_\alpha \subseteq U_\beta$ for any $\alpha < \beta$. \mathcal{U} is called closure – preserving (interior- preserving) if for any subcollection \mathcal{V} of \mathcal{U} , $\bigcup \{\overline{V} \mid V \in \mathcal{V}\}$ is

closed $(\cap \{Int(V) \mid V \in \mathcal{U}\})$ is open). \mathcal{U} is called locally finite if for every $x \in X$ there is nbhd O of x such that the cardinality of $\{U \in \mathcal{U} \mid U \cap O \neq \emptyset\}$ is finite. \mathcal{U} is called locally finite if for every $x \in X$ there is a nbhd O of x such that the cardinality of $\{U \in \mathcal{U} \mid O \cap U \neq \emptyset\}$ is finite. \mathcal{U} is called σ -locally finite if \mathcal{U} can be expressed as $\mathcal{U} = \{\mathcal{U}_n \mid n \in \mathbb{N}\}$, where each \mathcal{U}_n is locally finite. \mathcal{U} is called directed if \mathcal{U}^f is a partial refinement of \mathcal{U} where \mathcal{U}^f is the family of all finite unions of sets from \mathcal{U} .

Definition 1.2 [5]: let B be any set. Then a fibrewise over B consists of a set X together with a function $P: X \rightarrow B$, called the projection, where B is called a base set.

For each point b of B the fibre over b is the subset $X_b = p^{-1}(b)$ of X . also for each subset B' of B we regard $X_{B'} = p^{-1}(B')$ as fibrewise set over B' .

Definition 1.3[5]: If X and Y are fibrewise sets over B with projections P and q respectively, a function $\varphi: X \rightarrow Y$, is said to be fibrewise if $q \circ \varphi = p$. in other words $\varphi(X_b) \subseteq Y_b$ for each $b \in B$.

Definition 1.4[5]: let B be a topological space. Then a fibrewise topology on fibrewise set X over B is any topology on X for which the projection P is continuous.

A fibrewise topological space over B is defined to be a fibrewise set over B with fibrewise topology. If projection p closed then the fibrewise topology on X is called fibrewise closed.

Definition 1.5[2]: Let X be a fibrewise topological space over B . For $b \in B$, a collection \mathcal{U} of subsets of X is said to be b -locally finite if for every $x \in X_b$, there exists a nbhd V_x meets only finitely many elements of the collection \mathcal{U} .

If the collection $\mathcal{U} = \{U_\alpha \mid \alpha \in \Delta\}$ is a b -locally finite open (in X) collection, then \mathcal{U} is locally finite in $\bigcup \{V_x \mid x \in X_b\}$.

In particular, if X is fibrewise closed and \mathcal{U} covers X_b , then there exists a nbhd W of such that \mathcal{U} is a covered of X_w and is local finite in X_w that is for every $x \in X_w$ there

On Fibrewise τ -Paracompact Spaces

exists a nbhd of x in X_w (and so in X) such that it intersects only finitely many elements of \mathcal{U} .

Definition 1.6[2]: Let X be a fibrewise topological space over B . Then X is called fibrewise paracompact if for every $b \in B$ and every open (in X) over $\mathcal{U} = \{U_\alpha \mid \alpha \in \Delta\}$ of X_b there is a nbhd W of b in B such that X_w is covered by \mathcal{U} and $\{U_\alpha \cap X_b \mid \alpha \in \Delta\}$ has an open (in X) locally finite refinement in X_w .

Observe that if X is fibrewise paracompact then X is fibrewise closed.

Definition 1.7[1]: Let X be a fibrewise topological space over B . Then X is called fibrewise countable paracompact if for every countable $b \in B$ and every open (in X) over $\mathcal{U} = \{U_n \mid n \in N\}$ of X_b there exists a nbhd W of b in B such that X_w is covered by \mathcal{U} and $\{U_n \cap X_w \mid \alpha \in \Delta\}$ has an open (in X) locally finite refinement in X_w .

Theorem 1.8[1]: Let X be a fibrewise topological space over B . Then the following are equivalent:

- 1) X is fibrewise countably paracompact.
- 2) For every $b \in B$ and every open countable (in X) cover $\mathcal{U} = \{U_n \mid n \in N\}$ of X_b , there exists a nbhd W of b in B such that X_w is covered by \mathcal{U} and $\{U_n \cap X_w \mid U_n \in \mathcal{U}\}$ has a countable open (in X) locally finite refinement $\{V_n \mid n \in N\}$ in X_w such that $V_n \subseteq U_n \cap X_w$ for each n .

Theorem 1.9[1]: Let X be a fibrewise topological space over B . Then the following are equivalent:

- 1) X is fibrewise paracompact.
- 2) X is fibrewise countable paracompact and for every $b \in B$ and every open (in X) cover \mathcal{U} of X_b there exists a nbhd W of b in B such that X_w is covered by \mathcal{U} and $\{U \cap X_w \mid U \in \mathcal{U}\}$ has a σ -locally finite open (in X) refinement in X_w .

Definition 1.10[7]: Let \mathcal{U} and \mathcal{V} be collections of subsets of a space X . Then we say that \mathcal{V} is cushioned in \mathcal{U} if for every $V \in \mathcal{V}$ there exists $U(V) \in \mathcal{U}$ such that for every subcollection \mathcal{V}' of \mathcal{V} ,

$$\overline{\bigcup \{V \mid V \in \mathcal{V}'\}} \subseteq \bigcup \{U(V) \mid V \in \mathcal{V}'\}.$$

Definition 1.11[7]: A collection ζ of subsets of space X is said to be finitely closure - preserving in X if for any subcollection ζ' of ζ and any point $x \in X$ there exists a nbhd O of x and a finite subcollection ζ'' of ζ' such that $O \cap (\bigcup \zeta') \subseteq \overline{U\zeta''}$.

Note that local finiteness implies finitely closure – preserving property and finitely closure- preserving dose a closure- preserving property.

Lemma 1.12[7]: If $\{U_\alpha \mid \alpha \in \Delta\}$ is monotone increasing collection of a space X , then the following are equivalent:

- 1) $\{U_\alpha \mid \alpha \in \Delta\}$ is finitely closure- preserving in X .
- 2) For any $\alpha \in \Delta$ and any $x \in X$, there are a nbhd O of x and some $\alpha_1 < \alpha_0$ such that $O \cap (\bigcup \{U_\beta \mid \beta < \alpha_0\}) \subseteq U_{\alpha_1}$.

Definition 1.13[7]: Let \mathcal{A} and \mathcal{B} be collection of subsets of a space X and $x \in X$. we say that \mathcal{A} is local W - refinement of B at x if there exist some $C \in [\mathcal{B}]$, where $[\mathcal{B}]$ is the collection of all finite subsets of \mathcal{B} , and a nbhd U of x such that $\{A \in \mathcal{A} \mid U \cap A \neq \phi\}$ is a partial refinement of C . If C consists of a single element of \mathcal{B} and if $\bigcup \mathcal{A} = \bigcup \mathcal{B}$ and \mathcal{A} is a local W .refinement of B at each point of X then we say that \mathcal{A} is a local star - refinement of \mathcal{B} .

Lemma 1.14[7]: Let ζ be closure – preserving collection of closed subsets of a space X and A be a closed subset of X . then $\{F \cap A \mid F \in \zeta\}$ is closure- preserving.

Lemma 1.15[7]: If $\{\mathcal{U}_n \mid n \in N\}$ is a sequence of open covers of a space X such that \mathcal{U}_{n+1} is a W -refinement of \mathcal{U}_n for each $n \in N$, then \mathcal{U}_1 has a σ -locally finite open refinement.

Lemma 1.16[7]: For any interior – preserving open cover \mathcal{U} of a space X . the following are equivalent:

- 1) \mathcal{U}^f has a closure – preserving closed refinement whose interior is a cover of X .
- 2) \mathcal{U} has an interior- preserving open local W – refinement.
- 3) \mathcal{U}^f has an interior- preserving open local *star* – refinement.

2- Fibrewise τ – paracompact spaces

In this section we introduce fibrewise τ – paracompact spaces and give some characterizations of them.

Definition 2.1: Let X be fibrewise topological space over B . then X is called fibrewise τ – paracompact if for every $b \in B$ and every open (in X) cover $\mathcal{U} = \{U_\alpha \mid \alpha \in \Delta\}$ of X_b , with $|\Delta| \leq \tau$, there exists a nbhd W of b such that X_w is covered by \mathcal{U} and $\{U_\alpha \cap X_w \mid \alpha \in \Delta\}$ has a b -locally finite open (in X) refinement in X_w .

Example 2.2: Let α be an ordinal and $W_{\alpha+1}$ be the set of all ordinals less than $\alpha+1$ then $W_{\alpha+1}$ is α - paracompact (every open over of cardinality $\leq \alpha$ has a locally finite open refinement) but not $\alpha+1$ - paracompact (see[7]).

Let $B = \{b\}$ and the projection $p: W_{\alpha+1} \rightarrow B$ be the constant map. Then $W_{\alpha+1}$ is fibrewise α - paracompact but not fibrewise $\alpha+1$ - paracompact over B .

Theorem 2.3: Let X be fibrewise topological space over B . then the following are equivalent:

- 1) X is fibrewise τ – paracompact.
- 2) For every $b \in B$ and every open (in X) cover $\mathcal{U} = \{U_\alpha \mid \alpha \in \Delta\}$ of X_b , with cardinality $\leq \tau$, there exists a nbhd W of b such that X_w is covered by \mathcal{U} and $\{U_\alpha \cap X_w \mid \alpha \in \Delta\}$ has a locally finite open (in X) refinement in X_w .

- 3) For every $b \in B$ and every open (in X) cover $\mathcal{U} = \{U_\alpha \mid \alpha \in \Delta\}$ of X_b , with cardinality $\leq \tau$, there exists a nbhd W of b such that X_w is covered by \mathcal{U} and $\{U \cap X_w \mid \alpha \in \Delta\}$ has a locally finite open (in X) refinement $\mathcal{V} = \{V_\alpha \mid \alpha \in \Delta\}$ such that $V_\alpha \subseteq U_\alpha \cap X_w$ for each $\alpha \in \Delta$.

Proof:

(1) \rightarrow (2) Obvious.

(3) \rightarrow (1) Obvious.

- (2) \rightarrow (3) Let $b \in B$ and $\mathcal{U} = \{U_\alpha \mid \alpha \in \Delta\}$ be an open (in X) cover of X_b , with cardinality $\leq \tau$. Then there exists a nbhd W of b such that X_w is covered by \mathcal{U} and $\{U_\alpha \cap X_w \mid \alpha \in \Delta\}$ has a locally finite open (in X) refinement, say $\mathcal{T} = \{V_t \mid t \in T\}$. For each $t \in T$ choose $\alpha(t) \in \Delta$ such that $V_t \subseteq U_{\alpha(t)} \cap X_w$ and let $V_\alpha = \bigcup \{V_t \mid \alpha(t) = \alpha\}$. Then $\{V_\alpha \mid \alpha \in \Delta\}$ is an open (in X) locally finite cover of X_w such that $V_\alpha \subseteq U_\alpha \cap X_w$.

Theorem 2.4: Let X be fibrewise topological space over B . then the following are equivalent:

- 1) X is fibrewise τ - paracompact.
- 2) For every $b \in B$ and every open (in X) cover \mathcal{U} of X_b with cardinality $\leq \tau$, there exists a nbhd W of b such that X_w is covered by \mathcal{U} and $\{U \cap X_w \mid U \in \mathcal{U}\}$ has a locally finite open (in X) refinement in X_w .
- 3) For every $b \in B$ and every open (in X) cover $\mathcal{U} = \{U_\alpha \mid \alpha \in \Delta\}$ of X_b , with cardinality $\leq \tau$, there exists a nbhd W of b and a σ - locally finite open (in X) cover \mathcal{V} of X_w in X_w such that X_w is covered by \mathcal{U} and $\{\overline{V}^{X_w} \mid V \in \mathcal{V}\}$ is a refinement of $\{U \cap X_w \mid U \in \mathcal{U}\}$

Proof:

(1) \rightarrow (2) Obvious.

On Fibrewise τ -Paracompact Spaces

(2) \rightarrow (3) Let $b \in B$ and $\mathcal{U} = \{U_\alpha \mid \alpha \in \Delta\}$ be a monotone increasing open (in X) cover of X_b , with cardinality $\leq \tau$. Then there exists a nbhd W of b such that X_w is covered by \mathcal{U} and $\{U \cap X_w \mid U \in \mathcal{U}\}$ has a locally finite open (in X) refinement \mathcal{V} in X_w , where we may express \mathcal{V} as $\{V_\alpha \mid \alpha \in \Delta\}$ such that $V_\alpha \subseteq U_\alpha \cap X_w$ For each $\alpha \in \Delta$.

Let $H_\alpha = \bigcup \{O \mid O \text{ is open in } X_w, O \cap V_\beta = \emptyset \text{ for any } \beta > \alpha\}$. Then $\mathcal{H} = \{H_\alpha \mid \alpha \in \Delta\}$ is a monotone increasing open (in X) cover of X_w . Since $\overline{H_\alpha}^{X_w} \cap V_\beta = \emptyset$, for any $\beta > \alpha$ we have $\overline{H_\alpha}^{X_w} \subseteq X_w \setminus \bigcup \{V_\beta \cap X_w \mid \beta \leq \alpha\} \subseteq V_\beta \cap X_w \mid \beta > \alpha\} \subseteq U_\beta \cap X_w \mid \beta \leq \alpha\} \subseteq U_\alpha \cap X_w$. By (2), there exists a nbhd $W' \subseteq W$ such that X_w is covered by \mathcal{H} , so covered by \mathcal{U} , and $\{H_\alpha \cap X_w \mid H_\alpha \in \mathcal{H}\}$ has a locally finite open refinement \mathcal{K} for each $K \in \mathcal{K}$ there exists $\alpha \in \Delta$ such that $K \subseteq H_\alpha \cap X_w$, so $\overline{K}^{X_w} \subseteq \overline{H_\alpha \cap X_w}^{X_w} \subseteq \overline{H_\alpha}^{X_w} \subseteq U_\alpha \cap X_w$ and so (3) follows.

(3) \rightarrow (1) First we show that X is fibrewise countably paracompact.

Let $b \in B$ and $\mathcal{U} = \{U_n \mid n \in \mathbb{N}\}$ be a countable open (in X) cover of X_b . For $n \in \mathbb{N}$, let $O_n = \bigcup \{U_i \mid i = 1, 2, \dots, n\}$. Then $\mathcal{O} = \{O_n \mid n \in \mathbb{N}\}$ is a monotone increasing open (in X) cover of X_b , so there exists a nbhd W of b such that X_w is covered by \mathcal{O} and there exists a σ -locally finite open (in X) cover \mathcal{V} of X_w (in X) such that $\{\overline{V}^{X_w} \mid V \in \mathcal{V}\}$ is a refinement of $\{O \cap X_w \mid O \in \mathcal{O}\}$, where we may express \mathcal{V} as $\bigcup \{\mathcal{V}_n \mid n \in \mathbb{N}\}$ and each $\mathcal{V}_n = \{V_{n,i} \mid i \in \mathbb{N}\}$ is locally finite with $\overline{V_{n,i}}^{X_w} \subseteq O_n \cap X_w$ for each $i \in \mathbb{N}$.

For each $n \in \mathbb{N}$, let $H_n = \bigcup \{V_{i,j} \mid i,j < n\}$. Then $\mathcal{H} = \{H_m \mid m \in \mathbb{N}\}$ is a monotone increasing open cover of X_w such that $\overline{H_n}^{X_w} \subseteq O_n \cap X_w$ for each $n \in \mathbb{N}$.

Let $\mathcal{K} = \{U_1 \cap X_w, U_n \cap X_w \setminus \overline{H_{n-1}}^{X_w} \mid n \geq 2\}$. Then \mathcal{K} is a locally finite open refinement of $\{U_i \cap X_w \mid i \in \mathbb{N}\}$ in X_w , hence X is fibrewise countable paracompact.

Suppose that X is fibrewise γ -paracompact for all $\gamma \leq \tau$. Let $b \in B$ and $\mathcal{U} = \{U_\alpha \mid \alpha \in \Delta\}$ be an open (in X) cover of X_b , with cardinality $\leq \tau$. For each $\alpha \in \Delta$, let $O_\alpha = \bigcup \{U_\beta \mid \beta < \alpha\}$. Then $\mathcal{O} = \{O_\alpha \mid \alpha \in \Delta\}$ is a monotone increasing open (in X) cover of X_b , so there exists a nbhd W of b such that X_w is covered by \mathcal{O} and there exists a σ -locally finite open (in X) cover \mathcal{V} of X_w in X_w such that $\{\overline{V}^{X_w} \mid V \in \mathcal{V}\}$ is a refinement of $\{O_\alpha \cap X_w \mid \alpha \in \Delta\}$.

Let $\mathcal{V} = \bigcup \{\mathcal{V}_n \mid n \in \mathbb{N}\}$ and $V_n = \bigcup \{V \mid V \in \mathcal{V}_n\}$. Then $\{V_n \mid n \in \mathbb{N}\}$ is a countable open (in X) cover of X_b , so there exists a nbhd $W' \subseteq W$ of b such that $X_{w'}$ is covered by $\{V_n \mid n \in \mathbb{N}\}$ and $\{V_n \cap X_{w'} \mid n \in \mathbb{N}\}$ has a locally finite open (in X) refinement $\mathcal{H}' = \{H_n \mid n \in \mathbb{N}\}$ with $H_n \subseteq V_n \cap X_{w'}$. Hence $\{H_n \cap V \mid V \in \mathcal{V}_n, n \in \mathbb{N}\}$ is a locally finite open (in X) refinement of $\{V_n \cap X_{w'} \mid n \in \mathbb{N}\}$ in $X_{w'}$.

For each $V \in \mathcal{V}$, let $\alpha(V) \in \Delta$ such that $V \subseteq O_{\alpha(V)} \cap X_w$ and let $K_\alpha = \bigcup \{H_n \cap V \mid \alpha(V) = \alpha\}$. Then $\{K_\alpha \mid \alpha \in \Delta\}$ is a locally finite open cover of X_w such that $\overline{K_\alpha}^{X_{w'}} \subseteq \bigcup \{\overline{V}^{X_{w'} \cap X_w'} \mid V \in \mathcal{V}_w, \alpha(V) = \alpha\} \subseteq O_\alpha \cap X_{w'}$.

Therefore, by the transfinite induction, for each $\alpha \leq \tau$. There exists a nbhd $W_\alpha \subseteq W$ of b such that $(\overline{K_\alpha}^{X_{w'}})_{W_\alpha} = \overline{K_\alpha}^{X_{w_\alpha}}$ is covered by $\{U_\beta \cap X_w \mid \beta < \alpha\}$ and

$\{U_\beta \cap \overline{K_\alpha}^{X_{W_\alpha}} \mid \beta < \alpha\}$ has a locally finite open refinement \mathcal{S}_α that covers $\overline{K_\alpha}^{X_{W_\alpha}}$. Thus \mathcal{S}_α is a partial refinement of $\{U_\beta \cap X_{W'} \mid \beta < \alpha\}$ and is b -locally finite on $\overline{K_\alpha}^{X_{W_\alpha}}$ that covers $(K_\alpha)_b$.

Let $\mathcal{A}_\alpha = \{S \cap K_\alpha \mid S \in \mathcal{S}_\alpha\}$. Then \mathcal{A}_α is a locally finite (on $\overline{K_\alpha}^{X_{W_\alpha}}$) collection of open (in X) subsets that covers $(K_\alpha)_b$, and is a partial refinement of $\{U_\alpha \cap X_{W'} \mid \alpha \in \Delta\}$. Hence $\bigcup \{\mathcal{A}_\alpha \mid \alpha \in \Delta\}$ is a b -locally finite collection of open (in X) subset that covers $(K_\alpha)_b = X_b$ because $\{K_\alpha \mid \alpha \in \Delta\}$ covers $X_{W'}$, $X_b \subseteq X_{W'}$, and $\{K_\alpha \mid \alpha \in \Delta\}$ is a partial refinement of $\{U_\alpha \cap X_{W'} \mid \alpha \in \Delta\}$. Since p is closed, there exists a nbhd $W_b \subseteq W'$ of b such that $X_{W_b} \subseteq \bigcup \{\mathcal{A}_\alpha \mid \alpha \in \Delta\}$. Therefore $\mathcal{A} = \{A \cap X_{W_b} \mid A \in \bigcup \{\mathcal{A}_\alpha \mid \alpha \in \Delta\}\}$ is a b -locally finite (in X) refinement of $\{U_\alpha \cap X_{W'} \mid \alpha \in \Delta\}$ in X_{W_b} thus X is fibrewise τ - paracompact.

Theorem 2.5: Let X be fibrewise topological space over B . then the following are equivalent:

- 1) X is fibrewise τ - paracompact.
- 2) For every $b \in B$ and every open (in X) cover \mathcal{U} of X_b with cardinality $\leq \tau$, there exists a nbhd W of b such that X_W is covered by \mathcal{U} and $\{U \cap X_W \mid U \in \mathcal{U}\}$ has a locally finite open (in X) refinement in X_W .
- 3) For each $b \in B$ and every directed open (in X) cover of X_b , with cardinality $\leq \tau$, there exists a nbhd W of b such that X_W is covered by and $\{U \cap X_W \mid \alpha \in \Delta\}$ has a locally finite closed refinement in X_W .

Proof:

- (1) \rightarrow (2) Obvious.

(2) \rightarrow (3) Let $b \in B$ and $\mathcal{U} = \{U_\alpha \mid \alpha \in \Delta\}$ be a monotone increasing open (in X) cover of X_b , with cardinality $\leq \tau$. Where Δ is directed and if $\alpha < \beta$ in Δ , then $U_\alpha \subseteq U_\beta$. Then there exists a nbhd W of b in B such that X_b is covered by \mathcal{U} and $\{U_\alpha \cap X_w \mid \alpha \in \Delta\}$ has a locally finite open (in X) refinement $\mathcal{V} = \{V_\alpha \mid \alpha \in \Delta\}$ in X_w , with $V_\alpha \subseteq O_\alpha \cap X_w$ for each $\alpha \in \Delta$. For each $\alpha \in \Delta$, let $O_\alpha = X_w \setminus \bigcup \{\bar{V}_\beta \mid \beta \geq \alpha\}$. Then $\mathcal{O} = \{O_\alpha \mid \alpha \in \Delta\}$ is a directed collection of open (in X) subset that covers $\bar{O}_\alpha^{X_w} \subseteq U_\alpha \cap X_w$ for each $\alpha \in \Delta$, because if $x \notin U_\alpha \cap X_w$ then $x \in V_\beta$ for some $\beta > \alpha$. But $V_\beta \cap O_\alpha = \phi$, so $x \notin \bar{O}_\alpha^{X_w}$.

Now, we show that \mathcal{O} covers X_w . Let $x \in X_w$. then there exists a finite subset $\{\alpha_1, \alpha_2, \dots, \alpha_n\}$ of Δ such that $x \in \bigcap \{\bar{V}_\alpha^{X_w} \mid i=1,2,\dots,n\} \cup \{\bar{V}_\alpha \mid \alpha \notin \alpha_i, i=1,2,\dots, n\}$ because \mathcal{V} is locally finite. Since Δ is directed then there exist some $\alpha_0 \in \Delta$ such that $\alpha_0 > \alpha_i$ for any $i < n$, so $x \in X_w \setminus \bigcup \{\bar{V}_\beta^{X_w} \mid \beta \geq \alpha_0\} = O_{\alpha_0}$.

From (2), there exists a nbhd $W' \subseteq W$ of b such that $X_{W'}$ is covered by \mathcal{O} and $\{X_w \cap O_\alpha \mid \alpha \in \Delta\}$ has locally finite open refinement \mathcal{H} in $X_{W'}$, which is also a refinement of $\{X_w \cap U_\alpha \mid \alpha \in \Delta\}$ in X_w . Thus $\{\bar{H}^{X_w} \mid H \in \mathcal{H}\}$ is a locally finite closed refinement of $\{X_w \cap U_\alpha \mid \alpha \in \Delta\}$ in X_w .

(3) \rightarrow (1) Since every monotone increasing open is cover is directed then, by theorem 2.4, it suffices to show that (3) implies (2).

Let $b \in B$ and $\mathcal{U} = \{U_\alpha \mid \alpha \in \Delta\}$ be directed open (in X) cover of X_b . Then there exists a nbhd W of b such that X_w is covered by \mathcal{U} and $\{U_\alpha \cap X_w \mid \alpha \in \Delta\}$ has a

locally finite closed refinement $\zeta = \{F_\alpha \mid \alpha \in \Delta\}$ in X_w with $F_\alpha \subseteq U_\alpha \cap X_w$ for each $\alpha \in \Delta$.

For each $A \in [\Delta]$ (the collection of all finite subsets of Δ) let $V(A) = X_w \setminus \bigcup \{F_\alpha \mid \alpha \notin A\}$. Then $\mathcal{V} = \{V(A) \mid A \in [\Delta]\}$ is a direction open (in X_w), so in X , cover of X_b , with cardinality $\leq \tau$, so there exists a nbhd $W' \subseteq W$ of b such that $X_{W'}$ is covered \mathcal{V} and $\{V(A) \cap X_{W'} \mid A \in [\Delta]\}$ has a locally finite refinement \mathcal{H} in $X_{W'}$, where we may express \mathcal{H} as $\mathcal{H} = \{H(A) \mid A \in [\Delta]\}$ such that $H(A) \subseteq V(A) \cap X_{W'}$ for each $A \in [\Delta]$.

Let $O_\alpha = (U_\alpha \cap X_w) \cup \{H(A) \mid H(A) \cap F_\alpha = \emptyset\}$ for each $\alpha \in \Delta$. Then $\{O_\alpha \mid \alpha \in \Delta\}$ is an open cover of X_w with $O_\alpha \subseteq U_\alpha \cap X_w$.

Now, we show that is locally finite in $X_{W'}$. for any $x \in X_{W'}$. Since $\mathcal{H} = \{H(A) \mid A \in [\Delta]\}$ is locally finite in $X_{W'}$ for any $x \in X_{W'}$, we can choose a nbhd M of x such that $\{A \in [\Delta] \mid M \cap H(A) \neq \emptyset\}$ is finite. We denote this finite set by $\{A_1, A_2, \dots, A_k\}$. For any $\beta \notin \bigcup \{A_i \mid i=1,2,\dots,k\}$ we have $H(A_i) \cap F_\beta \subseteq V(A_i) \cap F_\beta = \emptyset$ so $H(A_i) \cap O_\beta = \emptyset$, hence $M \cap O_\beta \subseteq (\bigcup \{H(A_i) \mid i \leq k\}) \cap O_\beta = \emptyset$. Therefore M meets at most finitely many elements of $\{O_\alpha \mid \alpha \in \bigcup \{A_i \mid i \leq k\}\}$, and since A_i is finite for each $i \leq k$, than $\bigcup \{A_i \mid i \leq k\}$ is finite, so M meets at most finitely many elements of $\{O_\alpha \mid \alpha \in \Delta\}$, hence \mathcal{O} is locally finite in X .

Thus, by theorem 2.4 X is fibrewise τ -paracompact.

Remark 2.6: In the proof of (2) \rightarrow (3) of the last theorem, we have proved that: For every $b \in B$ and every monotone increasing directed open cover \mathcal{U} of X_b , with cardinality $\leq \tau$, there exists a nbhd W of b such that X_w is covered by \mathcal{U} and $\{U \cap X_w$

$\{ U \in \mathcal{U} \}$ has a locally finite open cover \mathcal{V} of X_w (in X_w) such that $\{ \bar{V}^{X_w} \mid V \in \mathcal{V} \}$ is a refinement of $\{ U \cap X_w \mid U \in \mathcal{U} \}$.

Therefore we have the following corollary.

Corollary 2.7: Let X be fibrewise topological over B . then the following are equivalent:

- 1) X is fibrewise τ – paracompact.
- 2) For every $b \in B$ and every monotone increasing open (in X_w) cover \mathcal{U} of X_b with cardinality $\leq \tau$, there exists a nbhd W of b and a locally finite open (in X_w) cover \mathcal{V} of X_w in X_w such that $\{ \bar{V}^{X_w} \mid V \in \mathcal{V} \}$ is a refinement of $\{ U \cap X_w \mid U \in \mathcal{U} \}$.
- 3) For every $b \in B$ and every directed open (in X_w) cover \mathcal{U} of X_b there exists a nbhd W of b and a locally finite open (in X) cover \mathcal{V} of X_w in X_w such that X_w covered by \mathcal{U} and $\{ \bar{V}^{X_w} \mid V \in \mathcal{V} \}$ is a refinement of $\{ U \cap X_w \mid U \in \mathcal{U} \}$.

Also from corollary 2.7 and theorem 2.4 we have the following.

Theorem 2.8: Let X be a fibrewise topological space over B . Then X is fibrewise τ – paracompact if and only if for every $b \in B$ and every directed open (in X_w) cover $\mathcal{U} = \{ U_\alpha \mid \alpha \in \Delta \}$ of X_b with cardinality $\leq \tau$, there exists a nbhd W of b and a σ – locally finite open (in X) cover \mathcal{V} of X_w in X_w such that X_w covered by \mathcal{U} and $\{ \bar{V}^{X_w} \mid V \in \mathcal{V} \}$ is a refinement of $\{ U_\alpha \cap X_w \mid \alpha \in \Delta \}$.

Theorem 2.9: Let X be a fibrewise topological space over B such that X_w is normal for every open subset of B . Then the following equivalent:

- 1) X is fibrewise τ – paracompact.
- 2) For every $b \in B$ and every monotone increasing open (in X) cover $\mathcal{U} = \{ U_\alpha \mid \alpha < \lambda \}$ of X_b with $\lambda \leq \tau$, there exists a nbhd W of b and a sequence $\{ \mathcal{V}_m \mid m \in \mathbb{N} \}$ of collections of open sets in X_w such that X_w is covered by \mathcal{U} , $\mathcal{V} =$

$\bigcup \{ \mathcal{V}_m \mid m \in N \}$ is refinement of $\{ U_\alpha \cap X_w \mid \alpha < \lambda \}$ in X_w and \mathcal{V}_m is cushioned in \mathcal{V}_{m+1} with respect to X_w , for any $m \in N$.

Proof:

- (1) \rightarrow (2) Let $b \in B$ and $\mathcal{U} = \{ U_\alpha \mid \alpha < \lambda \}$ be a monotone increasing open (in X) cover X_b with $\lambda \leq \tau$. there exists a nbhd W of b such that X_w is covered by \mathcal{U} and $\{ U_\alpha \cap X_w \mid \alpha < \lambda \}$ has a locally finite open (in X) refinement \mathcal{V} in X_w . Express \mathcal{V} as $\mathcal{V} = \{ V_\alpha \mid \alpha < \lambda \}$. Since X_w is normal and \mathcal{V} is locally finite then there exists a closed cover $\{ F_\alpha \mid \alpha \in \Delta \}$ of X_w with $F_\alpha \subseteq V_\alpha$ for each $\alpha < \lambda$. Also since X_w is normal then there exists a sequence $\{ V_{\alpha,m} \mid m \in N \}$ of open subsets of X_w such that $F_\alpha \subseteq V_{\alpha,m} \subseteq \overline{V_{\alpha,m}}^{X_w} \subseteq V_{\alpha,m+1} \subseteq V_\alpha$ for each $m \in N$. For each $m \in N$, let $\mathcal{V}_m = \{ V_{\alpha,m} \mid \alpha < \lambda \}$. Then the sequence $\{ \mathcal{V}_m \mid \alpha < \lambda \}$ satisfies statement (2).
- (2) \rightarrow (1) Let $b \in B$ and $\mathcal{U} = \{ U \mid \alpha < \lambda \}$, with cardinality $\leq \tau$, be a monotone increasing open (in X) cover of X_b . We show that there exists a nbhd W of b and a σ -locally finite open cover \mathcal{V} of X_w such that X_w is covered by \mathcal{U} and $\{ \overline{V}^{X_w} \mid V \in \mathcal{V} \}$ is a refinement of $\{ U_\alpha \cap X_w \mid \alpha \in \Delta \}$ and hence X is fibrewise τ -paracompact by 2.4.

From (2) there exists a nbhd W of b and sequence $\{ \mathcal{V}_m \mid m \in N \}$ of collections of open sets in X_w such that X_w is covered by \mathcal{U} , $\mathcal{V} = \bigcup \{ \mathcal{V}_m \mid m \in N \}$ is a refinement of $\{ U_\alpha \cap X_w \mid \alpha \in \Delta \}$ in X_w and \mathcal{V}_m is cushioned in \mathcal{V}_{m+1} with respect to X_w .

For ever $m \in N$ we may assume that \mathcal{V}_m is indexed by τ , that is, $\mathcal{V}_m = \{V_{m\alpha} \mid \alpha \in \Delta\}$, and \mathcal{V}_m is cushioned in \mathcal{V}_{m+1} with respect to $\alpha < \tau$, that is, for any $A \subseteq \Delta$, $\overline{\{V_{m\alpha} \mid \alpha \in A\}}^{X_w} \subseteq \bigcup \{V_{(m+1)\alpha} \mid \alpha \in A\}$.

For each $\alpha \in \Delta$, let $O_m \alpha = V_{m\alpha} \setminus \overline{\{V_{(m+1)\beta} \mid \beta \in \alpha\}}^{X_w}$ and $x \in X_w$, let α be the first of $\{\alpha \in \Delta \mid x \in U_\alpha\}$. Since $x \notin U_\beta$ for all $\beta < \alpha$ then $x \notin V_m \beta$ for all $\beta < \alpha$ and $m \in N$, so $x \notin \overline{\{V_{(m+1)\beta} \mid \beta \in \alpha\}}^{X_w}$ for all $m \in N$ because $\overline{\{V_{m\beta} \mid \beta \in \alpha\}}^{X_w} \subseteq \bigcup \{V_{(m+1)\beta} \mid \beta < \alpha\}$ and $x \notin \bigcup \{V_{(m+1)\beta} \mid \beta < \alpha\}$.

Since $x \in U_\alpha$ and \mathcal{V} covers X_w then $x \in V_k \alpha$ for some $k \in N$ then $x \in V_{ka}$ for some $K \in N$, hence $x \in V_{ka} \setminus \overline{\{V_{(k+1)\beta} \mid \beta \in \alpha\}}^{X_w} = O_{ka}$. then for $\mathcal{O} = \{O_{m\alpha} \mid \alpha \in \Delta, m \in N\}$ is an open cover of X_w which is a refinement of $\{U_\alpha \cap X_w \mid \alpha \in \Delta\}$.

Fix $m \in N$ and $x \in X$. if $x \in \bigcup \{V_{(m+1)\alpha} \mid \alpha < \tau\}$, let α be the first of $\{\beta < \tau \mid x \in V_{(m+1)\beta}\}$. Then $V_{(m+1)\alpha} \cap O_m \beta = \emptyset$ for any $\beta < \tau$, with $\alpha < \beta$, because $O_m \beta \cap \overline{\{V_{(m+1)\beta} \mid \beta \in \alpha\}}^{X_w} = \emptyset$ for all $\beta < \tau$. Also $x \notin \overline{\{V_{m\beta} \mid \beta \in \alpha\}}^{X_w}$ because $x \notin \bigcup \{V_{(m+1)\beta} \mid \beta < \alpha\}$ and $\overline{\{V_{m\beta} \mid \beta \in \alpha\}}^{X_w} \subseteq \bigcup \{V_m \beta \mid \beta < \alpha\}$. Therefore the open set $V_{(m+1)\alpha} \setminus \overline{\{V_{m\beta} \mid \beta \in \alpha\}}^{X_w}$ is a nbhd of x in X_w which intersects at most one member $O_m \beta$ of $\{O_m \beta \mid \beta \in \Delta\}$. If $x \notin \bigcup \{V_{(m+1)\alpha} \mid \alpha < \tau\}$ then $M = X_w \setminus \overline{\{V_{m\beta} \mid \beta \in \alpha\}}^{X_w}$ is nbhd of x in X_w which does not intersects any member of $\{O_m \beta \mid \alpha \in \Delta\}$. Therefore $\{O_m \beta \mid \alpha \in \Delta\}$ is discrete and locally finite in X_w for every $m \in N$, hence \mathcal{O} is a σ -locally finite open cover of X_w which is a refinement of $\{U_\alpha \cap X_w \mid \alpha \in \Delta\}$.

On Fibrewise τ – Paracompact Spaces

Moreover, $\overline{O_{m\alpha}}^{X_w} \subseteq \overline{V_{m\alpha}}^{X_w} \subseteq V_{(m+1)\alpha} \subseteq U_\alpha \cap X_w$, so $\{\overline{O_{m\alpha}}^{X_w} \mid \alpha \in \Delta, m \in N\}$ is a refinement of $\{U_\alpha \cap X_w \mid \alpha \in \Delta\}$.

Thus by theorem 2.4, X is fibrewise τ – paracompact.

Remark 2.10: in the proof of (2) \rightarrow (1) of the last theorem we show that $\{O_{m\alpha} \mid \alpha \in \Delta\}$ is directed for each $m \in N$, hence a fibrewise topological space X over B , where X_w is normal for every open subset W of B , is fibrewise τ – paracompact if and only if for every $b \in B$ and every directed open (in X_w) cover $\mathcal{U} = \{U_\alpha \mid \alpha \in \Delta\}$ of X there exists a nbhd W of b and a σ – discrete open (in X) cover \mathcal{V} of X_w in X_w such that X_w covered by \mathcal{U} and $\{\overline{V}^{X_w} \mid V \in \mathcal{V}\}$ is a refinement of $\{U_\alpha \cap X_w \mid \alpha \in \Delta\}$.

Also we have the following theorem.

Theorem 2.11: Let X be a fibrewise topological space over B such that X_w is normal for every open subset W of B . then the following are equivalent:

- 1) X is fibrewise τ – paracompact.
- 2) For every $b \in B$ and every monotone increasing open (in X) cover $\{U_\alpha \mid \alpha \in \Delta\}$ of X_b with cardinality $\leq \tau$, there exists a nbhd W of b and a σ – discrete open (in X) cover \mathcal{V} of X_w in X_w such that X_w is covered by and $\{\overline{V}^{X_w} \mid V \in \mathcal{V}\}$ is a refinement of $\{U_\alpha \cap X_w \mid \alpha \in \Delta\}$.
- 3) For every $b \in B$ and every open cover $\mathcal{U} = \{U_\alpha \mid \alpha \in \Delta\}$ of X_b with cardinality $\leq \tau$, there exists a nbhd W of b and a σ –discrete open (in X) cover \mathcal{V} of X_w in X_w such that X_w is covered by \mathcal{U} and $\{\overline{V}^{X_w} \mid V \in \mathcal{V}\}$ is refinement of $\{U_\alpha \cap X_w \mid \alpha \in \Delta\}$.

Proof:

(3) \rightarrow (1) Clear.

(2) \rightarrow (1) From Theorem 2.9, see remark 2.10.

(1) \rightarrow (3) Let $b \in B$ and $\mathcal{U} = \{ U_\alpha \mid \alpha \in \Delta \}$ be an open (in X) cover X_b with cardinality $\leq \tau$. Then there exists a nbhd W of b such that X_w is covered by \mathcal{U} and $\{ U_\alpha \cap X_w \mid \alpha \in \Delta \}$ has a locally finite open refinement $\mathcal{V} = \{ V_\alpha \mid \alpha \in \Delta \}$ in X_w with $V_\alpha \subseteq U_\alpha \cap X_w$ for each $\alpha \in \Delta$. Since X_w is normal and \mathcal{V} is locally finite then there exists a closed cover $\{ F_\alpha \mid \alpha \in \Delta \}$ of X_w with $F_\alpha \subseteq V_\alpha$ for any $\alpha \in \Delta$. Also since X_w is normal then there exists a sequence $\{ M_m \alpha \mid \alpha \in \Delta, m \in \mathbb{N} \}$ of open (in X) collections of X_w that covers X_w such that $F_\alpha \subseteq M_m \alpha \subseteq \overline{M_m \alpha}^{X_w} \subseteq M_{(m+1)} \alpha \subseteq V_\alpha$ for any $\alpha \in \Delta$. For each $m \in \mathbb{N}$ and each $\alpha \in \Delta$ let $O_m \alpha = M_m \alpha \setminus \overline{\{ M_{(m+1)\beta} \mid \beta < \alpha \}}^{X_w}$. Then $\mathcal{O} = \{ O_m \alpha \mid \alpha \in \Delta, m \in \mathbb{N} \}$ is an open cover of X_w . also $\overline{O_m \alpha}^{X_w} \subseteq \overline{M_m \alpha}^{X_w} \subseteq V_\alpha \subseteq U_\alpha \cap X_w$ for any $\alpha \in \Delta, m \in \mathbb{N}$.

Now, let $x \in X_w$ and α be the first of $\{ \beta \in \Delta \mid x \in M_{(m+1)} \beta \}$. Then for each $\beta > \alpha$ we have that $M_{(m+1)} \alpha \cap O_m \beta = \emptyset$ because $\{ O_m \beta \cap \overline{\{ M_{(m+1)\beta} \mid \alpha < \beta \}}^{X_w} = \emptyset$ and for each $\beta < \alpha$ we have $(X_w \setminus \overline{\{ M_{m\gamma} \mid \gamma < \alpha \}}^{X_w}) \cap O_m \beta = \emptyset$ because $O_m \beta \subseteq M_m \alpha \subseteq \bigcup \{ M_{m\gamma} \mid \gamma < \alpha \}$ since $\beta < \alpha$. Therefore $M_{(m+1)} \alpha \cap (X_w \setminus \overline{\{ M_{m\beta} \mid \beta < \alpha \}}^{X_w})$ is nbhd of x (because $x \notin \overline{M_{m\beta}}^{X_w}$ for all $\beta < \alpha$ since $x \notin M_{(m+1)} \beta$ and $\overline{M_{m\beta}}^{X_w} \subseteq M_{(m+1)} \beta$ for all $\beta < \alpha$ by the choice of α) which intersects at most one member $O_m \alpha$ of $\{ O_m \alpha \mid \alpha \in \Delta \}$, so $\{ O_m \alpha \mid \alpha \in \Delta \}$ is discrete in X_w for each $m \in \mathbb{N}$.

Thus $\mathcal{O} = \bigcup \{O_m \alpha \mid m \in \mathbb{N}, \alpha \in \Delta\}$ is a σ -discrete open cover of X_w with $\{\overline{O_{m\alpha}}^{X_w} \mid m \in \mathbb{N}, \alpha \in \Delta\}$ is a refinement of $\{U_\alpha \cap X_w \mid \alpha \in \Delta\}$.

Theorem 2.12: Let X be fibrewise topological over B . then the following are equivalent:

- 1) X is fibrewise τ -paracompact.
- 2) For every $b \in B$ and every monotone increasing open (in X) cover $\mathcal{U} = \{U_\alpha \mid \alpha \in \Delta\}$ of X_b with cardinality $\leq \tau$, there are a nbhd W of b and monotone increasing and finitely closure-preserving open (in X) cover $\{V_\alpha \mid \alpha \in \Delta\}$ of X_w in X_w such that X_w is covered by \mathcal{U} and $\overline{V_\alpha}^{X_w} \subseteq U_\alpha \cap X_w$ for any $\alpha \in \Delta$.

Proof:

(1) \rightarrow (2) Clear from the note below definition 1.11 and corollary 2.7.

(2) \rightarrow (1) Let $b \in B$ and $\mathcal{U} = \{U_\alpha \mid \alpha \in \Delta\}$ be a monotone increasing open (in X) cover of X_b with cardinality $\leq \tau$. Then there are a nbhd W of b and monotone increasing and finitely closure-preserving (in X) open (in X) cover $\mathcal{V} = \{V_\alpha \mid \alpha \in \Delta\}$ such that X_w is covered by \mathcal{U} and $\overline{V_\alpha}^{X_w} \subseteq U_\alpha \cap X_w$ for any $\alpha \in \Delta$. For each $\alpha \in \Delta$, let $F_\alpha = \overline{V_\alpha}^{X_w} \setminus \bigcup \{\overline{V_\beta}^{X_w} \mid \beta < \alpha\}$, and $\zeta = \{F_\alpha \mid \alpha \in \Delta\}$. Let $x \in X_w$. Then if $x \in \overline{V_1}^{X_w}$, then $x \in F_1$. Suppose $x \in \overline{V_1}^{X_w}$ and let α_0 be the largest of $\{\alpha \in \Delta \mid x \notin \overline{V_\alpha}^{X_w}\}$. Then $x \in \overline{V_{\alpha_0+1}}^{X_w} \setminus (\bigcup \{\overline{V_\beta}^{X_w} \mid \beta \leq \alpha_0\}) = F_{\alpha_0+1}$, hence ζ is a cover of X_w such that $\overline{F_\alpha}^{X_w} \subseteq U_\alpha \cap X_w$ for any $\alpha \in \Delta$.

Now, let $x \in X_w$ and α_0 be the first of $\{\alpha \in \Delta \mid x \in V_\alpha\}$ and $H_0 = V_{\alpha_0}$. Then H_0 is a nbhd of x in X_w and $H_0 \cap F_\lambda = \emptyset$ for any $\lambda > \alpha_0$. By lemma 1.12 there are a nbhd H_1 of x (in X) and $\alpha_1 < \alpha_0$ such that $H_1 \cap (\bigcup \{\overline{V_\beta}^{X_w} \mid \beta \leq \alpha_0\}) \subseteq \overline{V_{\alpha_1}}^{X_w}$. For any β

with $\alpha_1 < \beta < \alpha_0$, we have $H_1 \cap V_\beta \subseteq H_1 \cap \overline{V_{\alpha_1}}^{X_w} \subseteq H_1 \cap \overline{(\cup \{V_\lambda \mid \lambda < \beta\})}^{X_w}$, because $V_{\alpha_1} \subseteq (\{V_\lambda \mid \lambda < \beta\})$, so $H_1 \cap (\overline{V_\beta}^{X_w} \setminus \cup \{\overline{V_\lambda}^{X_w} \mid \lambda < \beta\}) = \phi$, hence $H_1 \cap F_\beta = \phi$ for any β with $\alpha_1 < \beta < \alpha_0$

By repeated use of lemma 1.12 there are a nbhds $\{H_n \mid n \in N\}$ of x and a sequence $\{\alpha_n \mid n \in N\}$ such that $\alpha_1 > \alpha_2 > \dots$. And $H_n \cap F_\beta = \phi$ for any β with $\alpha_n < \beta < \alpha_{n-1}$. Therefore $\alpha_n = 0$ for some n . Let $H = \cap \{H_t \mid t \leq n\}$. Then H is a nbhd of x in X_w which does not meet the elements of $\zeta \setminus \{F_{\alpha_i} \mid i = 0, 1, 2, \dots, n\}$. Hence ζ is a locally finite in X_w . Thus $\zeta' = \{\overline{F_\alpha}^{X_w} \mid \alpha \in \Delta\}$ is a closed locally finite refinement of $\{U_\alpha \cap X_w \mid \alpha \in \Delta\}$ in X_w . Therefore, by theorem 2.5, X is fibrewise τ – paracompact over B .

Theorem 2.14: Let X be a fibrewise topological space over B . then the following are equivalent:

- 1) X is fibrewise τ – paracompact.
- 2) For every $b \in B$ and every interior – preserving direct open (in X) cover $\mathcal{Z} = \{U_\alpha \mid \alpha \in \Delta\}$ of X_b , with cardinality $\leq \tau$, there a nbhd W of b such that X_w is covered by \mathcal{Z} and $\{U_\alpha \cap X_w \mid \alpha \in \Delta\}$ has an interior – preserving open (in X) local star – refinement X_w .
- 3) For every $b \in B$ and every directed open cover $\mathcal{Z} = \{U_\alpha \mid \alpha \in \Delta\}$ of X_b , there exists a nbhd W of b such that X_w is covered by \mathcal{Z} and $\{U_\alpha \cap X_w \mid \alpha \in \Delta\}$ has a σ -closure preserving closed (countable union of closure preserving closed collections) refinement ζ in X_w such that $\{Int(F) \mid F \in \zeta\}$ covers X_w .

Proof :

(1) \rightarrow (3) clear from corollary 2.7 since locally finite collection is closure- preserving.

(3) \rightarrow (2) First we show that X is fibrewise countably paracompact. Let $b \in B$ and $\mathcal{U} = \{U_n \mid n \in N\}$ be an increasing open cover of X_b . since a monotone increasing open cover is interior- preserving and directed then there exists a nbhd W of b such that X_w is covered by \mathcal{U} and $\{X_w \cap U_n \mid n \in N\}$ has a σ - closure preserving closed refinement ζ in X_w such that $\{Int(F) \mid F \in \zeta\}$ covers X_w . Let $\zeta_n = \{F_{nm} \mid n \in N\}$ such that $F_{n,m} \subseteq U_m \cap X_w$ for any m and $F_{n,1} \subseteq F_{n,2} \subseteq \dots$. $\zeta = \bigcup \{\zeta_n \mid n \in N\}$ and let $\zeta = \bigcup \{\zeta_n \mid n \in N\}$. Let $V_n = U_n \cap X_w \setminus \bigcup \{F_{i(n-1)} \mid i \leq n-1\}$, $\mathcal{V} = \{V_n \mid n \in N\}$ and let $x \in X_w$. Let n be the first of $\{k \in N \mid x \in U_k\}$. Then $x \in F_{i(n-1)}$ for all $i \leq n-1$, so $x \in U_n \cap X_w \setminus \bigcup \{F_{i(n-1)} \mid i \leq n-1\} = V_n$ hence \mathcal{V} is a cover of X_w .

Now, let $x \in X_w$, since $\{Int(F) \mid F \in \zeta\}$ covers X_w . Then $x \in Int(F_{nm})$ for some $n, m \in N$. Let $k > n, m$. then $V_k = U_k \cap X_w \setminus \bigcup \{F_{i(k-1)} \mid i \leq k-1\}$ has an empty intersection with $Int(F_{nm})$, so $Int(F_{nm}) \cap V_k = \emptyset$ for all $k > n, m$. Therefore \mathcal{V} is a locally finite open refinement of $\{U_n \cap X_w \mid n \in N\}$. Hence X is fibrewise countably paracompact.

Let $b \in B$ and $\mathcal{U} = \{U_\alpha \mid \alpha \in \Delta\}$ be a directed open (in X) cover of X_b with cardinality $\leq \tau$. Then there exists a nbhd W of b in B such that X_w is covered by \mathcal{U} and $\{U_\alpha \cap X_w \mid \alpha \in \Delta\}$ has a σ - closure preserving closed refinement ζ in X_w $\{int(F) \mid F \in \zeta\}$ covers X_w . Let $\zeta = \bigcup \{\zeta_n \mid n \in N\}$, where each ζ_n is closure- preserving.

For each $n \in N$, let $C_n = \bigcup \{Int(F) \mid F \in \zeta_n\}$. Then $\mathcal{C} = \{C_n \mid n \in N\}$, is a countable open cover of X_w , so there exists a nbhd $W' \subseteq W$ of b such that $X_{w'}$ is covered by \mathcal{C} and $\{C_n \cap X_{w'} \mid n \in N\}$ has a locally finite open refinement $\{\overline{V_n}^{X_{w'}} \mid n \in N\}$ in $X_{w'}$ with $V_n \subseteq C_n \cap X_{w'}$ for each $n \in N$.

Let $\mathcal{H}_n = \{\overline{V_n}^{X_{w'}} \cap F \mid F \in \zeta_n\}$. Then \mathcal{H}_n is a cover of V_n and is a closure-preserving (in X) collection, by lemma 1.14 and the fact that $\{\overline{V_n}^{X_{w'}} \mid n \in N\}$ is locally finite, it follows that $\bigcup \{\mathcal{H}_n \mid n \in N\}$ is a closure-preserving closed refinement of $\{U_\alpha \cap X_{w'} \mid \alpha \in \Delta\}$ in $X_{w'}$ such that $\{Int(H) \mid H \in \mathcal{H}_n, n \in N\}$ covers $X_{w'}$. Therefore, by lemma 1.16, $\{U_\alpha \cap X_{w'} \mid \alpha \in \Delta\}$ has an interior-preserving open local star-refinement.

(2) \rightarrow (1): Let $b \in B$ and $\mathcal{Z} = \{U_\alpha \mid \alpha \in \Delta\}$ be a directed open (in X) cover of X_b with cardinality $\leq \tau$. Then there exists a nbhd W of b in B such that X_w is covered by \mathcal{Z} and $\{U_\alpha \cap X_w \mid \alpha \in \Delta\}$ has an interior preserving open (in X) local star – refinement. Hence by lemma 1.16, $\{U_\alpha \cap X_w \mid \alpha \in \Delta\}$ has a closure-preserving closed refinement ζ with $\{int(F) \mid F \in \zeta\}$ covers X_w , so from the proof of (3 \rightarrow 2), X is fibrewise countably paracompact.

Let $b \in B$ and $\mathcal{Z} = \{U_\alpha \mid \alpha \in \Delta\}$ be a directed open (in X) cover of X_b with cardinality $\leq \tau$. Then there exists a nbhd W of b in B such that X_w is covered by \mathcal{Z} and $\{U_\alpha \cap X_w \mid \alpha \in \Delta\}$ has an interior-preserving open (in X) local star – refinement in X_w . Hence by lemma 1.15, $\{U_\alpha \cap X_w \mid \alpha \in \Delta\}$ has an interior-preserving open local W – refinement. Hence by lemma 1.15, the collection $\{U_\alpha \cap X_w \mid \alpha \in \Delta\}$ has a σ - locally finite open refinement.

Thus, by theorem 2.5, X is fibrewise τ – paracompact.

الفضاءات الليفيه شبه المتراصه

عبدالله المومني

ملخص

في [2] و [3] عرف بوهاجيار المؤثرات شبه المتراصه، المؤثرات شبه المتراصه الجزئيه، المؤثرات ماوراء المتراصه والمؤثرات التجميعيه الطبيعيه والتي تعتبر النظائر التوبولوجيه الليفيه للفضاءات شبه المتراصه، شبه المتراصه الجزئيه ، ماوراء المتراصه والتجميعيه الطبيعيه. في هذا البحث سنقوم بتقديم بعض التوصيفات المكافئه للفضاءات التوبولوجيه الليفيه من النوع شبه المتراص من النمط τ .

References:

- [1] AL- Zoabi K., Countably Paracompact Mappings, Q& A *General Topology*, 21(2003) 41-51.
- [2] Buhagiar D., Paracompact maps, Q & A *General Topology*, 15(1997)203-223 .
- [3] Buhagiar D. and Miwa T., covering properties f maps,, Q & A *General Topology*, 16(1998)53-66.
- [4] Bark D.E., "covering properties", Hand book set-theoretic topology, North-Holland, (1984).
- [5] James I. M., spaces, *Bull. London Math. Soc.* 18 (1986) 529-559.
- [6] James I. M., "Fibrewise Topology". Cambridge Univ. press, Cambridge, (1989).
- [7] Yasui Y., "Generalized paracompactness". Topics in General topology. K. Morita and J. Nagata North Holland. Amsterdam. 1989. pp (161-202).

Radon Measurements in Caves and Houses in Umm- Qais, Jordan

Khitam Khasawinah and Khalid Abumurad *

Received on May 14, 2006

Accepted for publication on Sep. 14, 2006

Abstract

Radon (^{222}Rn) levels were determined in caves and houses in Umm Qais (ancient Jadara) north of Jordan using passive diffusion dosimeters consisting of nuclear track detectors CR-39. The average radon concentrations are reported for different periods of times. The overall radon average is comparable to radon levels in other locations in Jordan and within the internationally acceptable values. Domestic caves are reported to have higher average concentrations than houses and field caves.

Keywords: Radon, Umm-Qais, Jadara, CR-39, Caves.

Introduction:

Raised radon levels are known to exist in mines and show caves. For indoor radon, the main sources are soil, building materials and water supplies. The outdoor radon concentration is typically low and less than average indoor levels, it may therefore be neglected as a contributor to radon exposures of radiological health significance. In most countries, the source of indoor radon is in the soil or rock subjacent to the house

The earth and its rock grains contain uranium ^{238}U and thorium ^{232}Th . ^{222}Rn and ^{220}Rn are produced as a result of ^{238}U and ^{232}Th decay. ^{222}Rn has a half life of 3.82 days. ^{220}Rn has a half life of 55 seconds. Because of its short half life, ^{220}Rn disappears rather quickly after its production and therefore has little consequences in terms of radiological health. The term radon will then refer to ^{222}Rn exclusively unless otherwise stated. Radon is produced within rock grains that contain uranium. Its immediate parent is ^{226}Ra . For a given radium concentration in various rock specimens the amount of radon that escapes is different depending on various parameters such as grain size, thermal history, etc.

Radon and its daughter products are identified as a radiation hazard causing health problems such as lung cancer for those exposed to high levels of radiation such as underground miners [1-5].

It has not been clear if radon poses a similar risk of causing lung cancer in humans exposed to generally lower levels found in homes and caves. However for people who

live near caves or visit caves, the presence of this heavy radioactive gas is a point of concern.

Radon levels in the air of caves vary with underlying geology, structure of the soil (porosity, and permeability), weather conditions and ventilation. Many researchers have studied radon levels in caves [6-12]. For example, Solomon [6] found radon concentration in Australian caves ranged from 20 Bqm⁻³ up to 9000 Bqm⁻³. The summer season was marked with the highest value. Jovanovic [13] in Slovenia found radon levels in caves ranged from several 100 Bqm⁻³ up to 27 kBqm⁻³. Higher values were measured in summer time. Gillmore [8] reported high radon levels for caves and mines in Devon and Cornwall, England.

This study is an attempt to evaluate and gather fresh data related to radon concentration in dwellings and both domestic and field caves at Umm-Qais area. In addition, the collected data could be of interest for world pooling on caves and to characterize dwellings and caves with radon levels in excess of 1000 Bqm⁻³ as an action level. Also, the collected data will be used to estimate the absorbed dose by people who use these caves as dwellings and/or storage for house hold things.

Experimental Procedure

Study Area Discription

The study area, Umm-Qais (Jadara), is one of the Decapolis cities located about 100 km North of Amman. It lies on a mountain of 600 m elevation and it looks down west onto the Jordan River. Most of the dwellings under consideration consist of one story house, built of black cement and lime stone rock materials. As a rustic area, the ventilation habit during hot seasons is opening widows and doors with or without fans. Similarly, most studied caves are internally connected, horizontally extended with two or more entrances which provide good air exchange. These caves were engraved in limestone rocks with relatively small chamber volume ranging from 500 to 1500 m³. Most of the caves under investigation are internally plastered so radon exhalation is minimized. In the past, these caves were used as dwellings or storage for house hold things, cattle and their food stuff.

Dosimeters and Calibration

Passive integrated closed can technique was used to measure radon concentration in the dwellings and caves of Umm-Qais. The dosimeters consist of pieces (1.5 x 1.5 cm²) of nuclear track detectors (CR-39) mounted in the bottom of a cylindrical cup which is described elsewhere [14]. The prepared dosimeters were distributed in 31 houses and in the caves belonging to those houses (domestic caves) and in some caves in the fields far away from the houses (field caves). Two dosimeters were placed inside each cave and one dosimeter was placed inside each house one meter below the ceiling in the bedrooms.

The study period started in the beginning of October 2002 and it lasted for one month for caves and three months for dwellings. This period is characterized of being meteorologically moderate (temperature, humidity and pressure were about the average)

Radon Measurements in Caves and Houses in Umm- Qais, Jordan

in the study area. The study was repeated one year later (October 2003) for places showed high radon concentration in the first study. The dosimeters in caves and houses in the second experiment were left for three months.

Detector Treatment and Analysis

The retrieved detectors were chemically etched using 30% KOH solution for 9 hours in a temperature controlled water bath fixed at 70°C. An optical microscope was used to count the alpha track density, ρ (tracks cm^{-2}), on the exposed detectors. This type of dosimeters was previously calibrated in the school of physics and space research at Birmingham University, UK, using a chamber of standard radon concentration ($C_0 = 90 \text{ kBq m}^{-3}$) and the irradiation period, t_0 , was 48 hrs. These dosimeters were treated as those exposed in the study area.

Results and Discussion

To calculate ^{222}Rn concentration, the radon activity density was determined by measuring the tracks densities on the detector according to the following relation

$$C = \frac{C_0 t_0 \rho}{\rho_0 t} \dots\dots\dots (1)$$

Where C_0 , t_0 were defined earlier and ρ_0 is the average surface density of tracks on the calibrated detector ($3.302 \times 10^4 \text{ tracks cm}^{-2}$), ρ is the average surface density of tracks on the exposed detectors, and t is the exposure time.

Samples collected from domestic caves after two weeks have radon concentration level ranged between 26 and 114 Bq m^{-3} with an average of $65 \pm 12 \text{ Bq m}^{-3}$ and the estimated dose 1.78 mSv. The samples collected from field caves after two weeks have radon concentration levels ranged between 9 and 54 Bq m^{-3} with an average of $33 \pm 8 \text{ Bq m}^{-3}$ and the corresponding dose was 0.75 mSv.

Samples collected from domestic caves after four weeks have radon concentration ranged between 43 and 260 Bq m^{-3} with an average of $130 \pm 16 \text{ Bq m}^{-3}$ and the related dose was 2.95 mSv. The samples collected from field caves after four weeks have radon concentration ranged between 39 and 172 Bq m^{-3} with an average of $101 \pm 10 \text{ Bq m}^{-3}$ and the estimated dose was 2.3 mSv. Samples collected from houses after three months have radon concentration levels ranged between 40 and 109 Bq m^{-3} with an average of $63 \pm 14 \text{ Bq m}^{-3}$ and the related dose was 1.43 mSv. Values of average concentrations are summarized in Table 1.

Table1: Average concentration (Bqm^{-3}) in dwellings' caves for different periods during 2002. Numbers between brackets are doses in mSv.

<i>location</i>	<i>2 weeks</i>	<i>4 weeks</i>	<i>3 months</i>
houses	-	-	63 (1.43)
Domestic caves	65 (1.48)	130 (2.95)	-
Field caves	33 (0.75)	101 (2.30)	-

It is important to know that domestic caves are taken care of. The caves are provided with doors which are locked for the safety of stored goods or animals so they are poorly ventilated, while the field caves (caves outside the village of Umm Qais) are always wide open and better ventilated. This fact explains the lower concentration of radon in the field caves.

Similarly when comparing concentration in houses to the respective domestic caves, one finds that even after three months the concentration in houses ($63 Bqm^{-3}$) almost equal to the concentration of domestic caves ($65 Bqm^{-3}$) in two weeks. Houses are definitely better ventilated, beside that houses are full of furniture rather than rocks and soil, the potential host of radon.

Table 2 shows the results radon concentration in some houses and their respective caves having in mind that this table does not show results for caves where detectors were lost along with their respective houses.

Table 2: Average radon concentration in houses and their respective domestic caves (Bqm^{-3}) for different periods.

<i>Location</i>	<i>Radon Concentration (Bqm^{-3})</i>									
Houses (3 months)	64	62	57	40	60	40	54	109	60	51
Domestic Caves (2 weeks)	46	40	20	30	114	45	32	82	80	52
Domestic Caves (4 weeks)	160	94	43	85	260	94	80	225	168	125

Table 3 shows the results of a second experiment carried out on ten houses and their caves during 2003. These houses were selected from areas, in Umm-Qais, showed high radon concentration in the first study. It is clear that the concentration level in the second observation of the same order except in very few cases, which means that radon level can vary from day to day and from one location to another depending on many factors such as temperature, humidity, pressure, elevation, etc.... However, the average concentration of radon in these houses was about $162 \pm 30 Bqm^{-3}$ and for the caves was about $192 \pm 35 Bqm^{-3}$. These areas, including the caves in it, are characterized by thin exposed phosphatic limestone layer, which is considered a potential source of ^{238}U , the grandfather of radon.

Table 3: Average radon concentration (Bqm^{-3}) in houses and their respective caves.

Radon Measurements in Caves and Houses in Umm- Qais, Jordan

Location	Concentration									
Houses (3 months)	160	165	155	168	153	225	130	160	148	160
Caves (3 months)	180	168	160	180	160	240	230	220	200	190

It is important to note that houses with higher concentration are constructed according to modern style which is interconnected rooms with corridors, contrary to the other houses with less concentration which are constructed according to the old style; houses are consist of a row of rooms open to the atmosphere usually facing due south for a better sun exposure. The latter mentioned houses are obviously better ventilated.

Conclusion

Most of the studied caves and houses show in general low radon levels. Results were highly correlated with the degree of ventilation. Houses built according to modern style having interconnected rooms (poorly ventilated) have higher radon levels than those built according to old style having rooms arranged in rows. Domestic caves (caves in the village) with doors have higher radon levels than field caves (outside the village) of wide open entrances. So if a cave is well ventilated, there will be a little to worry about unless one stays in the cave for a long period of time. Two or four weeks as an exposure time for CR-39 in the dwellings and caves is not enough to judge radon concentration in these places. However, the average radon levels measured in houses and in both kinds of caves are within the internationally acceptable values.

قياسات الرادون في كهوف و منازل من أم قيس- الاردن.

ختام خصاونة و خالد موسى أبو مراد

ملخص

لقد حُددت مستويات غاز الرادون (^{222}Rn) في كهوف و منازل في قرية أم قيس (جدارا القديمة) الواقعة في شمال الاردن، وذلك باستخدام مجراعات الانتشار السلبية والتي تتألف من كواشف الاثر النووي (CR-39). لقد قيست معدلات تركيز غاز الرادون خلال فترات زمنية مختلفة. كان معدل تركيز غاز الرادون في أم قيس قريباً من معدلاته في مناطق اخرى من الاردن، ويقع ضمن التراكمات الدولية المقبولة. إن معدل تركيز غاز الرادون في الكهوف المجاورة للمنازل أعلى من تركيزه في البيوت و في الكهوف البعيدة عن المنازل.

كلمات مفتاحية: الرادون ، أم قيس ، جدارا ، CR-39 ، كهوف.

References

- [1] ICRP, International Commission on Radiological Protection. 'Limits on Inhalation of Radon Daughters by Workers', *Publication 32*, Pergamon Press, Oxford. (1981).
- [2] Vaupotic I. and Kbol I., 'Radon doses based on alpha spectrometry', *Acta chim.slov.*, 51 (2004)159-168.
- [3] Lubin J. H., Boice J. D. and Edling C., 'Lung cancer in radon-exposed miners and estimation of risk from indoor exposure', *J Natl Cancer Inst.*, 87(1995) 817-827.
- [4] Darby S., Whitley E. and Howe G. R., 'Radon exposure and cancers other than lung cancer in underground miners; a collaborative analysis of 11 studies', *J. Natl. Cancer Ins.*, 87(1995) 378-384.
- [5] Denman A. R., Eatough J. P., Gillmore G. and Phillips P. S., 'Assessment of health risks to skin and lung of elevated radon levels in abandoned mines', *Health Phys.*, 85(6)(2003) 733-739.
- [6] Solomon S. B., Langroo R. and Peggie J. R., 'Occupational exposure to radon in Australian tourist cave-an Australia-wide study of radon levels', *ARL/TR* 119 (1996).
- [7] Papachristodoulou C. A., Ioannides K. G., Stamoulis K. C., Patiris, D. L. and Pavlides S. B., 'Radon activity levels and effective doses in the Perama Cave, Greece', *Health Phys.*, 86(6)(2004) 619-624.
- [8] Gillmore G. K., Phillips P, Denman A, Sperrin M and Pearce G., 'Radon levels in abandoned metalliferous mines, Devon, southwest England', *Ecotoxicol Environ Saf.*, 49 (3)(2001a) 281-292.
- [9] Gillmore G. K., Sperrin M., Phillips P. and Denman A., 'Radon hazards, geology, and exposure of cave users: a case study and some theoretical perspectives' *Ecotoxicol Environ Saf.*, 46(3)(2000) 279-288.
- [10] Szerbin, P., 'Radon concentrations and exposure levels in Hungarian Caves' *Health Phys.* 71(3). (1996) 362-369.
- [11] Gillmore G. K., Phillips P. S., Denman A. R. and Gilbertson D. D., 'Radon in the creswell crags Permian limestone caves', *J Environmental Radioactivity*, 62 (2)(2002)165-179.
- [12] Sperrin M., Gillmore G. and Denman T., Radon concentration variations in a Mendip cave cluster', *Environmental Management and Health*, 12(5)(2001)467-482.
- [13] Jovanovic P., 'Radon measurements in the cave Vilencia', *IRPA9, Vienna*, Vol. 2-25. (1989).

Radon Measurements in Caves and Houses in Umm- Qais, Jordan

- [14] Abumurad K. M., Kullab M. K., Al-Bataina B. A., Ismail A. M and Lehlooh, A.D., 'Estimation of radon concentration inside houses in Jordanian regions', *Mutah J.Res.Stud.*, 9(1994) 9-21.

Critical Current Enhancement by Iron Doping in $Y_1Ba_2Cu_3O_{7-\delta}$ Superconducting System

Abdul Raouf El Ali (Al-Dairy) and Khitam Khasawinah *

Received on Jan. 1, 2006

Accepted for publication on Aug. 10, 2006

Abstract

$Y_1Ba_2Cu_3O_{7-\delta}$ superconducting system doped in percentage ratio with Fe have been studied. X-ray diffraction patterns indicated a slight shift in intensity peaks in the doped samples proportional to iron content while the critical temperature was slightly suppressed. I-V characteristic curves were obtained for the samples at various temperatures below T_c and with different applied magnetic fields. Critical currents were evaluated and their behavior versus temperature and applied field was studied for different iron content. The critical currents were found to increase with increasing iron content at temperature below T_c .

Keywords: Doping, Y-Superconductor, I-V Characteristics, Critical current enhancement, Magnetic field.

Introduction

Y-based superconductors are the most widely studied systems and are classified as type II superconductors. Superconductors can carry high currents in the presence of external magnetic fields. However, there is an upper limit for currents and magnetic fields before superconductivity is completely removed. The enhancement of critical currents is important to some applications in electrical devices. There are many reported results [1-6] on techniques to improve the critical current density, J_c . The magnitude of the critical current is greatly affected by the existence of impurities, grain boundaries, voids, and structural defects. All these can act as pinning centers which prevent vortex movement.

In the superconducting state, the vortices do not move easily because they are pinned at some pinning centers and a very small force is needed to remove a vortex from its pinning center. The critical current, I_c , can be used as a measure of the pinning force [7]. It is well known that single crystals can carry much higher critical currents than polycrystalline samples. It is well known that grinding, compressing, and annealing have major effects on I_c . These can help in improving contacts and in optimizing O_2 content leading superconductors to have high critical current density. There are different ways to find J_c . The current density can be determined from measurements of transport current or

can be calculated from magnetization currents deduced from hysteretic loops. However, J_c has smaller values when calculated from transport currents [8,9,10].

The effect of iron addition on Y-based systems was previously studied and an increase in vortex pinning that results in high J_c was reported [4,6]. In this work, we have prepared Y-based samples and Fe was added in different weight percentages. The effect of iron addition on I-V characteristics will be reported and discussed. The critical currents are evaluated from the I-V curves for various temperatures, applied fields, and for different iron contents. In addition, the flow resistance will be calculated and discussed under different temperatures and applied fields.

Experimental Procedure

The samples were prepared by the solid-state reaction method using Y_2O_3 , $BaCO_3$, CuO , and Fe_3O_4 high purity powder oxides as starting materials. First, we prepared $YBa_2Cu_3O_{7-\delta}$ superconducting system (Y123) from Y_2O_3 , $BaCO_3$, CuO high purity oxides. We divided the material into four samples. Iron in the form of Fe_3O_4 was added to three samples of Y123 as a weight ratio of 1%, 2%, and 4%. Each sample was ground separately and mixed thoroughly for two hours and then pressed into a pellet under pressure of 10 tons. Each pellet has a diameter of about ~10mm and ~1mm thickness. The pellets with iron were then heat treated at 840°C for 20 hours and allowed to cool to 450°C and held at that temperature for 6 hours under flow of O_2 and then cooled to room temperature.

A small amount of each sample was ground into powder for X-ray diffraction and a diffraction pattern was obtained using $Cu K_\alpha$ x-ray radiation. For I-V measurements a small slab from each sample of a rectangular shape with dimensions $5 \times 3 \times 1 \text{ mm}^3$ was used. The I-V characteristics were measured using the standard dc four-probe method with the magnetic field applied parallel to the surface of the sample. Every sample was first cooled in zero field to 50K. We obtained I-V curves for all samples at various temperatures below T_c for different applied fields. Scanning electron microscope (SEM) micrographs were taken for the samples containing iron (1%, 2%, 4%) and are shown in figure 1.

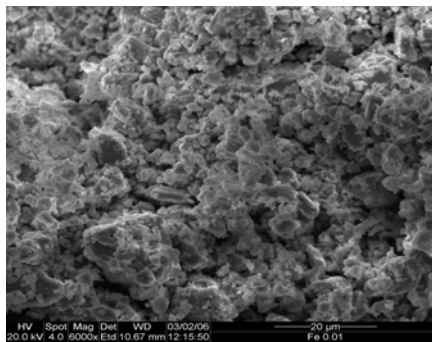


Figure 1a: SEM scan for powdered part from the sample with 1% Fe.

Critical Current Enhancement by Iron Doping in $Y_1Ba_2Cu_3O_{7.5}$ Superconducting System

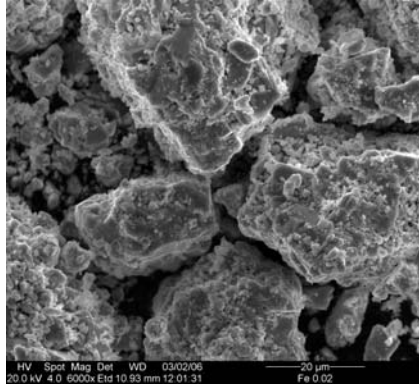


Figure 1b: SEM scan for powdered part from the sample with 2% Fe.

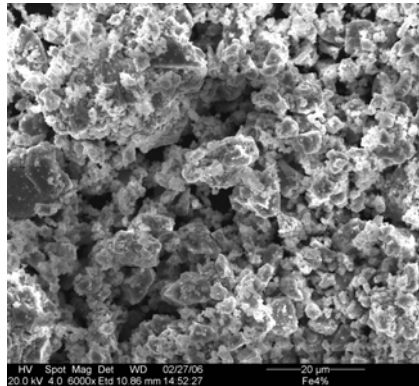


Figure 1c: SEM scan for powdered part from the sample with 4% Fe.

Results

X-ray diffraction measurements revealed the existence of the Y123 superconducting phase with a very slight shift in the peak positions for samples containing iron and the amount of shift was increasing with increasing iron content. The values for T_c are listed in Table 1.

Table 1: List of critical temperatures for the samples

% of Fe in sample	0%	1%	2%	4%
T_c	92K	91.2K	89.5K	91.8K

After analyzing the SEM micrographs it was clear that the 4% Fe sample micrograph contains agglomerates of iron that did not substitute for copper. However, from the analysis of the 1% Fe and 2% Fe samples micrographs the iron atoms seem to substitute for copper, with larger grains in the case of the 2% Fe sample. The values of T_c indicate that it decreases with iron content up to 2%, but for 4% iron content the iron aggregates in islands leaving Y123 phase and this was confirmed by scanning electron microscope EDAXS analysis of different spots on the surface of each sample.

Figure 2 shows the I-V characteristics for the sample with 1% Fe for various temperatures. Similar graphs have been obtained for various samples at different temperatures and different applied fields. These curves have been used to calculate I_c and flow resistance.

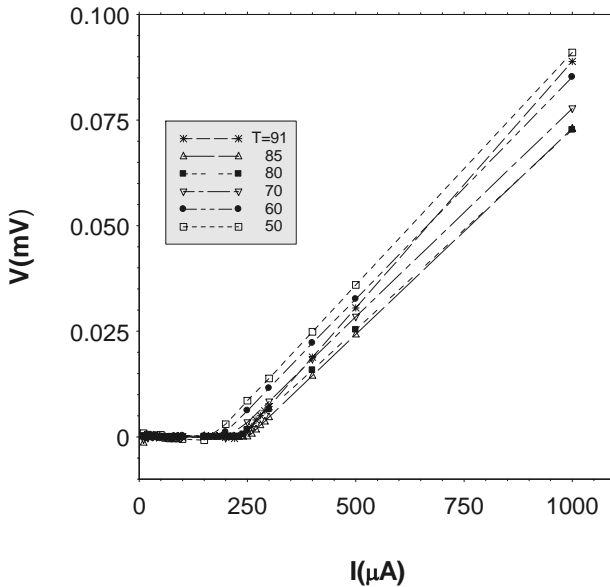


Figure 2: I-V characteristics for the sample with 1% Fe .

The critical currents calculated for various samples with zero applied field were evaluated and are shown in Figure 3. It is clear from Figure 3 that the sample with 1% Fe has nearly the optimum iron content to have maximum critical current. The figure shows also that iron content enhances the critical current as temperature is increased compared to reduction in I_c for the sample with no Iron added. Figure 4 represents the critical currents versus temperature for the sample with 4% Fe with different applied fields, it shows slow decrease in I_c up to 85K , and a fast increase when approaching the critical temperature.

Critical Current Enhancement by Iron Doping in $Y_1Ba_2Cu_3O_{7.5}$ Superconducting System

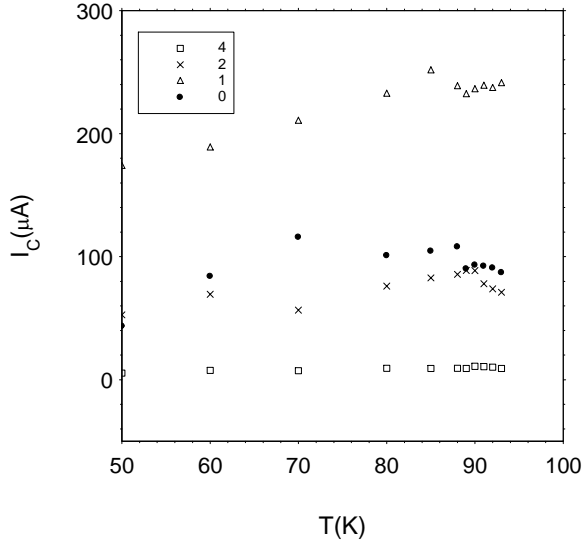


Figure 3: Critical currents versus temperature for various samples with $B=0$

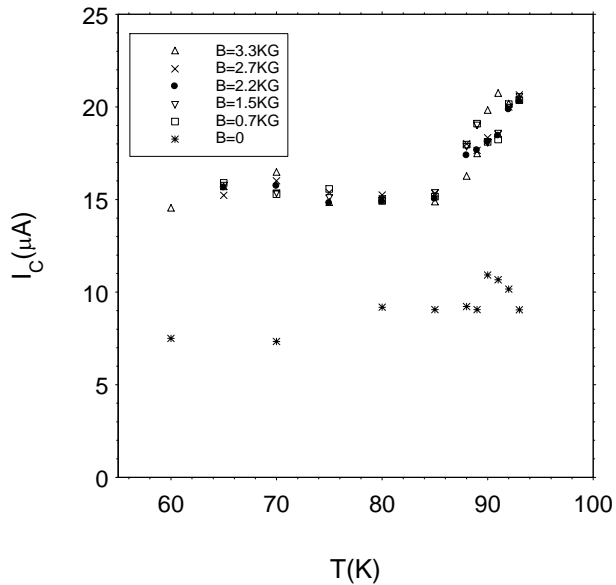


Figure 4: Critical currents versus temperature with different applied fields for 4% Fe.

Figure 5 shows the critical currents versus the applied field for various temperatures for the sample with 4% Fe. It is clear from that graph that I_c behaves independent of the field for all temperatures, with higher values near the critical temperature. Figure 6 shows the flow resistance R in units of ohms calculated for the samples against

temperature for applied fields having the values $B=0$ and $B=3.3\text{kG}$. It shows very clearly that the resistance drops with increasing temperature for the sample with 4% Fe.

Figure 5: Critical currents versus applied field at various temperatures for 4% sample.

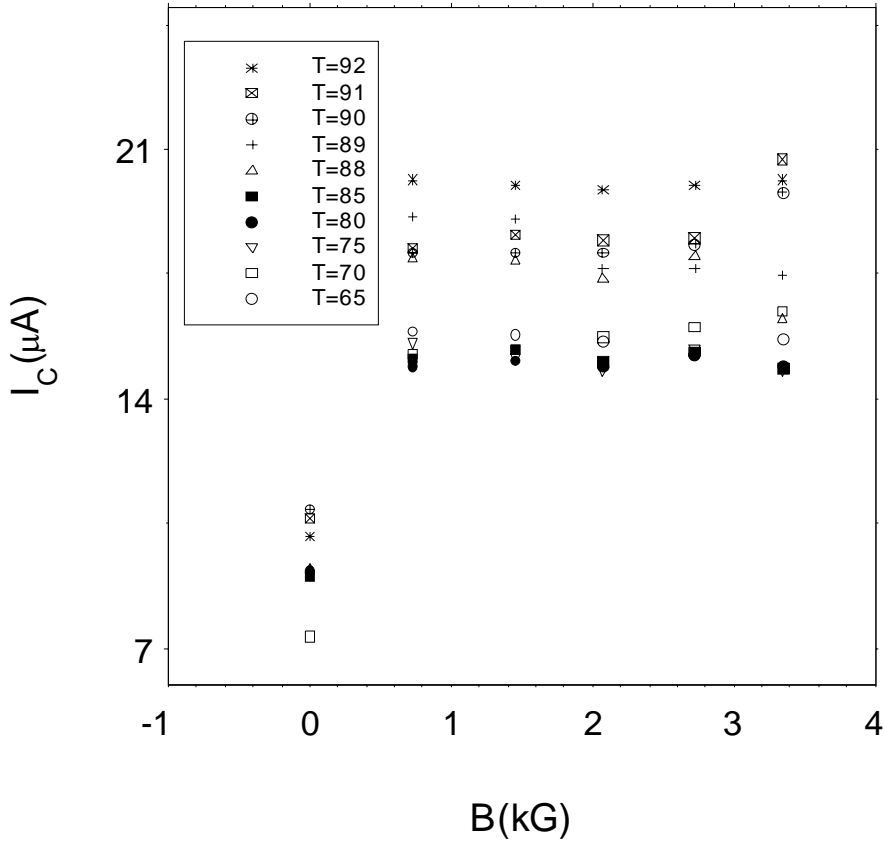


Figure 5: Critical currents versus applied field at various temperatures for 4% sample.

Critical Current Enhancement by Iron Doping in $Y_1Ba_2Cu_3O_{7.5}$ Superconducting System

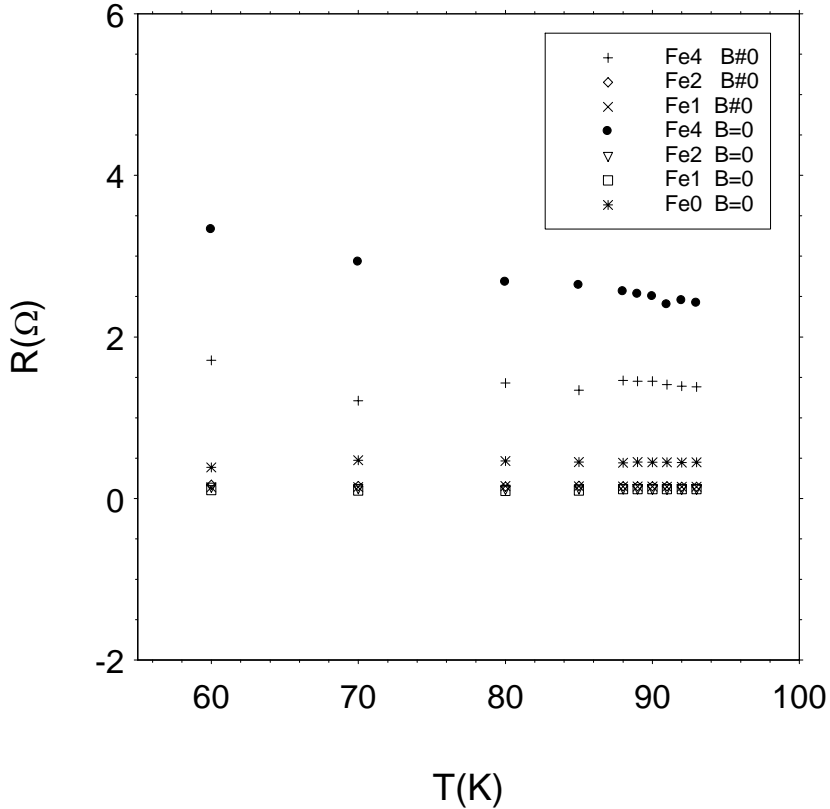


Figure 6: Flow resistance R in ohms versus different temperature at $B=0$ and $B=3.3$ kG.

Discussion

The iron addition to the Y-based compounds enhances the critical currents if the optimum iron content is added as can be seen from Figure 2. The sample with 1% Fe has the highest I_c for all temperatures while for samples with 2% and 4% Fe, the addition of iron suppresses I_c . In the sample with 1% Fe, the pinning force was the strongest and this results in a high critical current. However, for the sample with 4% Fe, the iron aggregates together and do not substitute for Cu and this was verified by the SEM measurements. The large grains seen in the sample with 2% Fe were behind the decrease observed in both T_c and I_c since these can reduce pinning forces.

The critical current was observed to increase in sample with 4% Fe with the applied field, and a drastic increase was observed for temperatures just below T_c (85K – 92K).

While the value of I_c is independent of the applied field, it seems that the pinning forces build up and strengthen for that temperature range when applying an external field. When plotting I_c versus applied field as shown in Figure 5, a similar behavior was observed. The critical currents are independent of applied fields, with a noticeable increase above 85K. Figure 6 shows almost a constant flow resistance for the samples except the sample with 4%. A very slight increase in R with B for the pure sample with no significant change in R with temperature and field for the samples with 1% and 2% Fe. For the sample with 4% Fe, its flow resistance decreases slightly with temperature with no applied field but it decreases more with temperature when a field is applied ($B=3.3kG$) and this should result in a higher critical current.

Conclusion

The critical currents for Y-based superconductors doped with Fe were studied. The iron enhanced the critical currents. It was found that the 1% Fe substitution gave the higher critical currents. Higher amounts of iron results in a separate aggregates of Fe from the Y123 phase and that can suppress the critical currents. A further study is needed to find the optimum amount of iron to be added that can enhance greatly the critical current without any further suppression of T_c .

Acknowledgments

We would like to thank Wajeeh Yousef for helping with the SEM micrographs.

إثراء التيار الحرج بإضافة الحديد إلى نظام مفرط الموصلية $Y_1Ba_2Cu_3O_{7-\delta}$

عبدالرؤوف العلي (الديري) و ختام خصاونه

ملخص

تمت دراسة نظام مفرط الموصلية $Y_1Ba_2Cu_3O_{7-\delta}$ المطعم بالحديد بنسب مئوية مختلفة. تبين من دراسة العينات بواسطة حيود الأشعة السينية أن هناك إزاحة طفيفة في مواقع قمم العينات المطعمة بالحديد مقارنة مع العينات غير المطعمة، كما لاحظنا نقصاناً في درجة الحرارة الحرجة T_c . تم إيجاد منحنيات التيار - الجهد عند درجات حرارة أقل من T_c وتحت تأثير مجالات مغناطيسية مختلفة. ومن منحنيات التيار والجهد تم حساب التيارات الحرجة I_c ، ودراسة سلوكها عند درجات حرارة ومجالات مغناطيسية مختلفة. وقد وجد من النتائج أن التيارات الحرجة تثرى بإضافة الحديد.

References

- [1] Zhao Y. E., He Z. H., Lou Y. Y. and Gawalek W., 'The structure and superconductivity of $Y_{1-x}Ca_xBa_2Cu_3O_{7-\delta}$ coatings on YSZ single crystal substrate', *Physica C*, 415(2004) 197-202.
- [2] McBrien H. B., Burnell G., Tarte E. J., Schulz R. R., Schneider C. W., Schmehl A., Bielefeldt H., Hilgenkamp H. and Mannhart J., 'Capacitance Measurements on Grain Boundaries in $YBa_2Cu_3O_{7-\delta}$ ', *Phys Rev B*, 70(2004) 104502-104513.
- [3] Upreti U. C. and Narlikar A. V., 'Exploring the site occupancy effects of equal low concentrations of Zn and Fe dopants on order parameter fluctuations in Y123 bulk samples: A preliminary investigation', *Indian Journal of Pure & Applied Physics*, 40(2002) 801-815.
- [4] Ciurcha D., Pop A. V., Cozar O., Ilonca G., Pop V. and Konopko L. A., 'Statistical representation of the excess conductivity in Bi-Sr-Ca-Cu-O superconductor' *Supercond Sci Technol*, 9(1996) 88-92.
- [5] Lal R., Awan V. B.S. Pandey S. P., Yadav V. S., Varandani D., Narlikar A. V., Chhikara, A., and Gmelin, E. 'Tc degradation in cuprate superconductors from the resistivity of $YBa_2(Cu_{1-x}M_x)_4O_8$ for M=Fe and Ni', *Phys Rev B*, 51(1995) 539-546.
- [6] Ilonca G., Pop A. V., Corega C., Geru I. I., Gauter V. G., Konopko L. A., Min Y. and Deltour R., 'Superconducting, magnetic and normal state properties in Bulk $(Bi_{1.6}Pb_{0.4})(Sr_{1.8}Ba_{0.2})Ca_2(Cu_{1-x}Cr_x)_8O_y$ ', *Physica C* 235-240(1994) 1391-1392.
- [7] Buckel W. and Kleiner R., "Superconductivity Fundamentals and Applications, Revised and enlarged edition", Wily-VCH Verlag, Berlin, Germany. (2004) 149-302.
- [8] Bean C. P., 'Magnetization of High-Field Superconductors', *Phys. Rev. Mod.*, 36 (1964) 31-39.
- [9] Bean C. P., 'Magnetization of Hard Superconductors', *Phys. Rev. Lett.*, 8 (1962) 250-253.

- [10] Hampshire D. P., Cai X., Seuntjens J. and Larbalester D. C., 'Improved critical current characteristics in 1-2-3 oxide superconductors : weak flux pinning and percolative aspects', *Supercon. Sci. Technol* ,1 (1988) 12-19.
- [11] Terrel Vandrah A.(Editor), *Chemistry of superconductor material preparation, chemistry ,characterization and theory*, Noys Publications, Park Ridge ,N. J., USA. (1992) 469-571.

Introducing English-Arabic Dictionary-Based Cross Language Information Retrieval

Awni Hammouri *

Received on Feb. 12, 2008

Accepted for publication on July 30, 2008

Abstract

Cross-language information retrieval (CLIR) is a rapidly growing area of research in the information retrieval (IR) field. There is an increasing interest in the ability to enter queries in one language and retrieve documents in a different language. There are several existing approaches to cross language information retrieval; however in this research; one particular approach based on bilingual dictionaries of Arabic and English languages has been discussed, implemented, and evaluated. The retrieval performance of the above approach has been studied in two situations: when the query consists of full words and when the query words are in base (root) form. The query is selected in the source language (English) to retrieve documents in Arabic and English languages. The experiment results show that the retrieval performance in Arabic and English languages is improved when querying is done based on the root of the query words

Keywords: Cross-language, Information retrieval, Bilingual dictionary.

Introduction:

Much research work has been done in the information retrieval field, in order to develop systems that are able to provide efficient access to the enormous amount of information available in various languages on the internet. Since this information has risen noticeably and considerably the importance of the cross language information retrieval is increased. In general, people are able to read more languages than they are able to formulate queries in. So that the main advantages of the CLIR is that it is useful for people who can read a foreign language well enough to understand the document contents and judge its relevance, although they can't speak it well.

CLIR is defined as the retrieval of relevant documents based on queries expressed by a human in a given natural language against a collection on which the documents are expressed in another language [5]. English-Arabic CLIR, therefore focuses on the retrieval of documents based on queries formulated by a user in the English language and the documents are in the Arabic language. Any retrieval method based matching the query in one language against documents in a different language would fail when there

are no cognates between this language pair [4]. So that both the documents and queries need to be expressed in one language.

In cross-language information retrieval, either the documents translated into the query language, or the queries are translated into the documents language, or translate both the documents and queries into a third language. Since the document translation is computationally expensive, most efforts focus on accurate translation of the query. When the query is translated, the translated amount will be less in comparison with the document collection. In addition to that, there is no need to carry out analysis for the syntactic and linguistic rules since the query is a set of words. If we perform an efficient translation for the query or the document collection into the target language, the problems in cross-language information retrieval system will be reduced to the problems of monolingual information retrieval.

There are three main general approaches to CLIR. First, Machine Translation (MT) is translating query from one language into another depending on the context. This way of using machine translation systems as a method to translate the query is inappropriate and inefficient in the CLIR system for many reasons [5]:

1. Wasting of time and effort in an attempt to produce a correct syntactical and linguistic sentence, although these efforts do not have any effect on information retrieval system.
2. The language problems and the inclusion of the query to certain words that have more than one meaning and sentences of complicated linguistic structure and the inability to distinguish the references of the pronouns.
3. The machine translation select one translation for the word and this process is very difficult and most often the result of the selection is incorrect translation of the word which will cause a loss to many documents related to the subject although it contains other translations to this word.

The second approach is know as Comparable or Parallel Corpus. In this approach, some probabilistic and statistical methods applied on the parallel text. Which includes pairs of comparable documents but they are written in different languages. To identify and specify the translation of a word this method gives high efficiency, but it suffers from some problems like the relation between pairs of parallel words existing in the text is of specific domain. Consequently the relation with the synonyms for the words will be less outside this domain. The other problem is the unavailability of parallel text for different language pair [5, 12].

The third approach is the Dictionary-based CLIR which translates the source language query terms via a bilingual dictionary and generate the target language query by considering one or all of the translations [1, 5, 6]. The basic idea in this approach is to replace each term in the source language query with an appropriate term or set of terms in the target language by using a bilingual dictionary. A common method to handle the untranslatable words is to pass them as such to the final target language query.

Introducing English-Arabic Dictionary-Based Cross Language Information Retrieval

Two factors limit the performance of the dictionary-based CLIR approach. The first is that many words have several translations in the dictionary, and these translations may have very different meanings. In this case there are three methods that can be used:

- ❑ First match method (FM): In this method only the first match translation from the dictionary for each query term is retained [1, 5].
- ❑ Every match method: In this method every possible translation for the query term is retained. (i.e., using all the listed translations) [5].
- ❑ Two phase method: The assumption used is that Inverse-Function ($\text{Function}(x) = x$), which means that: the original term should be the result of the translation of the translated term. (i.e., when the query in the source language (S) is translated using every match method into a query in the target language (T), then T is translated using every match method into (S'), after that compare S with S' . If the assumption is satisfied, the translation is valid.) This method reduces the ambiguity of every match method [5].

The second factor that limits the performance of a dictionary-based approach is that the dictionary may lack some terms that may be the main search keys in the query. This may occur either because the user has entered some form of abbreviation or slang which is not included in the dictionary or because the query deals with the following cases [6, 7]:

- ❑ Special terms or technical topic which is outside the scope of the general dictionary: These terms that are used in a specific domain. In many cases these are main search keys in the query, so the domain specific dictionary is used to solve this problem when translate the query words.
- ❑ Inflecting words: This can be solved by using the rooting.
- ❑ Compound word: A word consists of a number of words that are written together. So, in order to solve the problem, the compound word is split into its components, and each component is translated separately.
- ❑ Cross-lingual spelling variants: In the case of spelling variants the source language form does not match the variant form in the database index and this causing loss of retrieval effectiveness. This problem can be solved by using the N-gram matching.

As dictionaries specifically designed for query translation are developed, the effect of this limitation may be reduced. But it is unlikely to be eliminated completely because language use is a creative activity, with new terms entering the lexicon all the time [2].

The focus of this paper is on developing an English-Arabic dictionary-based cross language information retrieval by translating the queries to the documents language. That is, the English queries are translated into queries in Arabic language using domain specific dictionary. In order to reduce the effect of the factors that limit the performance of the dictionary-based CLIR a domain specific dictionary has been used that is designed manually to translate the query words.

Hammouri

This paper is organized as follows. The next section gives an overview of the Arabic Language. Literature review and previous work are presented in section 3. Sections 4 presents the experiments and their results. Finally, the conclusion is given in section 5.

The Arabic Language

The Arabic language belongs to the Semitic family of languages. It is written from right to left and has 28 letters. This language is structured on precise grammar and word derivation. The grammar of written Arabic is based essentially on the traditional three parts of speech: the noun, the verb, and the particle. There are two types of sentences. The sentence that begins with a noun. ("Nominal Sentence") and the sentence that begins with a verb ("Verbal Sentence").

The vocabulary in the Arabic language are derived through the derivation mechanism " الاشتقاق ", in which the words formation is done by derivation from roots, these roots are paradigms to which the prefixes or suffixes are added to form the words. For example, The root "علم" (Science) may produce the following derivations:

- تعليم : education.
- معلومات : information.
- علماء : scientists.

Similarly, several nouns may also be derived from the same root.

The basic order of the word in the Arabic structure is (فاعل) verb, followed by (مفعول به) subject, then (مفعول به) object. For example:

كتب الطالب الدرس

The student wrote the lesson.

The other variations of the word order, which are allowed in the Arabic language, can be derived from the basic order by shifting the subject or object. For instance the noun (subject) can be fronted to precede its verb.

For example:

الطالب كتب الدرس

The student wrote the lesson.

A good knowledge of grammar and usage are required if one is to avoid misreading an item.

Introducing English-Arabic Dictionary-Based Cross Language Information Retrieval

Previous work

There are several contributions in the information retrieval field concerning the cross language information retrieval system. Aljlal, *et. al.* [5] evaluated the performance when using machine translation as an approach to translate the query from Arabic language to the English language in the Arabic-English CLIR system. This system tries to analyze the phrases in the text and consequently building meaningful relations which leads to establish a text in the English language. By using this system the query is translated from Arabic language to the English language, and then the query is indexed after removing the stop words. They empirically evaluated the effectiveness of machine translation as away to translate the query using the TREC-7 and TREC-9 topics and collections.

They also investigated the effect of query length on the performance of the machine translation. The experiment is done on queries with different lengths (title, description, narrative). By applying the MT on the query and the documents in TREC-7, the system achieved 61.7% for title, 64.7% for description, and 60.2% for the narrative. From the results they concluded that the query using description achieves the best results.

Hasnah and Evens [12] carried out Arabic-English CLIR based on bilingual dictionaries as an approach to translate the query from the source language to the target language. This system allows the user to submit a query in Arabic language or in the English language and retrieve documents in both languages. The goal is to compute the effectiveness of using the bilingual dictionaries as a way to translate the query in the Arabic-English CLIR system, and to compare the performance of bilingual retrieval with the performance of monolingual retrieval. The system is based on the vector model which computes the similarity between the document vector and the query vector.

The experiments are done to retrieve documents in Arabic language using Arabic language query, and retrieve documents in English language using English language query, these experiments are considered the base to measure the performance of retrieving documents in both languages. The Arabic-English retrieval system gives 33.1% which is approximately 70% of monolingual retrieval system for the Arabic language. While the English-Arabic retrieval system gives 42.4% which is approximately 82% of monolingual retrieval system for the English language.

Ballesteros and Croft [1] apply the CLIR system on English-Spanish by using the bilingual dictionary as a way to translate the query. They present experiments which analyze the factors that affect dictionary based method for cross language information retrieval. They apply the process "local feed back" that reduces the errors. They define the relevance feedback as a method by which the query can be modified using the information from the documents whose relevance is known to this query. When they apply a pre-translation feedback, they found that this creates a stronger base query for translation. But in case of post-translation feedback the result is a reduction in the effects of irrelevant query terms "by adding more context specific terms".

Andriani and Croft [10] study the effectiveness of using the bilingual dictionary in the CLIR system and they make their study on both languages English and Indonesian.

They use the local feed back technique to expand the query. This technique is applied before translation, after translation, and before and after the translation. Their experiment indicates that, the local feed back is efficient in English- Indonesian and Indonesian – English.

Chen, *et. al.* [4] described the English-Chinese cross-language information retrieval experiments, by translating the queries into document language by dictionary look-up. They present a simple and effective Chinese word segmentation method and compared the cross-language retrieval performance of two bilingual dictionaries for query translation. They performed three English-Chinese cross language information retrieval runs, one manual and two automatic. They reach the conclusion that the performance of the best automatic English-Chinese cross-language retrieval performance is only about 57% of the monolingual retrieval performance. They found that the main performance limiting factor is the limited coverage of the dictionary used in query translation, where some of the key concepts were either not translated or improperly translated.

Experiments and Results

This paper discusses a particular approach to CLIR, which is based on using bilingual dictionaries. We will show how the queries can be translated from a source language to a target language using a bilingual dictionary and retrieve documents in both languages. The system is designed that allows the user to select either retrieving documents based on full word query or retrieving documents based on query in base form.

In Arabic and English languages, where the words are separated by a blank, it is easy to index the documents by the words occurring in the text after eliminating the stop-words. Two indexes have been generated, one consists of full words as index terms and the other consists of the roots of the words as index terms. The test collection used consist of 242 Arabic documents from the proceedings of the Saudi Arabian National Conference and 170 English documents from different locations on the internet with 59 queries in both languages. The relevant documents for each query have been found manually by a group of participants. Each subgroup takes part of these documents and the 59 queries in order to determine the relevancy.

The system has been implemented using Visual Basic 6.0. The implementation process has gone through the following steps:

Step1: Remove stop words from the Arabic and English documents.

Step2: Build the inverted file for each of the Arabic and English documents where the index terms are full word.

Step3: Build the inverted file for Arabic documents where index terms are roots. In this step the Arabic root program is used [14]. Then, build the inverted file for English documents after rooting the index terms. In this step the porter algorithm is used [15].

Step4: Build a bilingual dictionary English-Arabic dictionary. The English-Arabic bilingual dictionary used is designed manually, and it is a domain specific dictionary. The using of domain specific dictionary reduces the ambiguity translation, and gives one

Introducing English-Arabic Dictionary-Based Cross Language Information Retrieval

or two equivalent words to a source language word, whereas the general dictionary gives many equivalent words.

Step5: The construction of the target query: after the user selects his choice to execute the query based on either full word or on the roots of the query words, the user can select the desired query from the source language query list. This query is then segmented into words that are translated by means of a bilingual dictionary to produce the target Arabic query.

Step6: In this step one of the following processes is executed depending on the choice selected by the user:

First, if the user selects "Full word", the search is beginning for the documents in both languages that are hopefully to be relevant to the selected query based on full word. In this case we take the full words from the English query to retrieve documents in English language, and the full words from the translated target Arabic query to retrieve documents in Arabic language. The search for query words is done in the inverted file for the full words. This file has the following information:

- The document number.
- The index terms in each document.
- The frequency of each index term in the corresponding document.
- Number of documents in which the index term appears.
- The maximum frequency that is computed over all index terms mentioned in the document.
- The weight of each index term in the document is calculated according to the following formula [13]:

$$w_{ij} = (\text{freq}_{ij} / (\max_l \text{freq}_{lj})) * \log (N/n_i).$$

Where, W_{ij} is the weight of term k_i in document d_j ,

N is the total number of documents in the system,

n_i is the number of documents in which the term k_i appears,

freq_{ij} is the frequency of term k_i in the document d_j ,

$\max_l \text{freq}_{lj}$ is the maximum computed over all terms in document d_j .

Second, if the user selects "Root", the querying is done after rooting the translated target Arabic query and the source English query to retrieve documents in the corresponding language. This is done by performing the following operations:

- Find the root for each word in the English query (using porter's algorithm).
- Find the root for each word in the Arabic query (using Arabic root algorithm).
- Use the root of the English query to retrieve documents in English language, and the root form from the translated target Arabic query to retrieve documents in Arabic

Hammouri

language. The search for query words is done in the corresponding inverted file for the root.

Step7: Use Cosine formula [14] in order to determine the similarity between the query and the retrieved documents.

$$sim(d_j, q) = \frac{\sum_{i=1}^t w_{ij} \times w_{iq}}{\sqrt{\sum_{i=1}^t w_{ij}^2} \times \sqrt{\sum_{j=1}^t w_{iq}^2}}$$

The query term weights are calculated according to the following formula [13]:

$$w_{iq} = (0.5 + [0.5 * freq_{ij}] / \max_i freq_{ij}) * \log (N/n_i).$$

After that the retrieved documents in both languages (Arabic and English languages) appear, each with it's similarity to the selected query.

Step 8: After that we compare the retrieval performance in both cases (full word and root) for Arabic language and for English language.

The evaluation of the retrieval system plays an important role in judging the efficiency and effectiveness of the retrieval process. Several evaluation criteria were used in different experiments, among them, *recall* and *precision*. Recall measure is defined as the fraction of relevant documents that have been retrieved and is calculated by dividing the number of retrieved relevant documents by the total number of relevant documents. Precision is defined as the fraction of retrieved documents that are relevant and is calculated by dividing the number of retrieved relevant documents by the total number of retrieved documents [13]. The program has been run several times. Each time one query has been chosen, the translated query appears immediately after the query is selected. As a result of the execution, the retrieved documents in Arabic and English languages are displayed with their similarity to that query. Expert users, whose judgments regarding the relevance of each document to each query were taken into consideration. The performance measures, recall and precision, are calculated for each query. This produces a sequence of recall-precision pairs that can be plotted as a curve. In such a graph, for each recall point there is a corresponding precision value.

To evaluate the retrieval performance of the system over all test queries (59 queries), we average the precision values at each recall level as follows:

$$P_{avg} = \sum_{i=1}^{N_q} \frac{P_i(r)}{N_q} \quad \text{Where } P_{avg} \text{ is the average precision at the recall level } r, N_q \text{ is the number of queries used, and } P_i(r) \text{ is the precision at recall level } r \text{ for the } i\text{-th query [13].}$$

The average precision values at 10 recall points for all Arabic queries using full word and root query terms are shown in figure 1. The summaries provided by the

Introducing English-Arabic Dictionary-Based Cross Language Information Retrieval

average recall-precision values suggest that the root retrieval method of the individual query words outperforms the full word retrieval method.

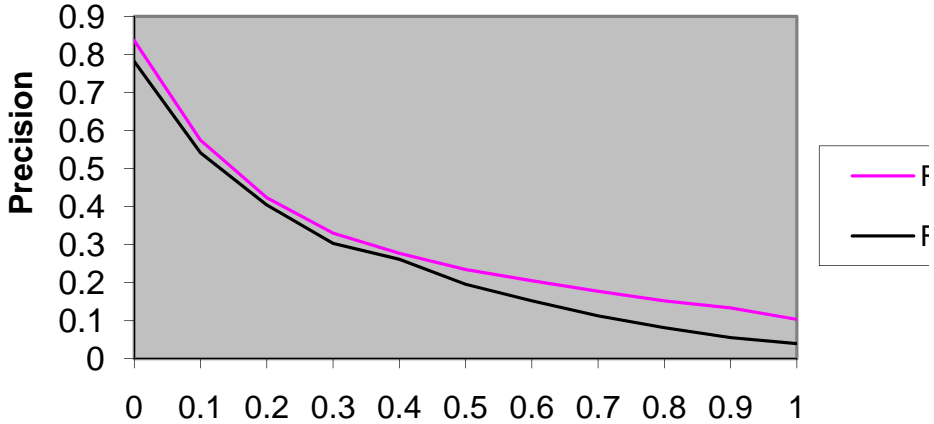


Figure 1: Average recall-precision full word and root Arabic query terms.

The average precision values at 10 recall points for all English queries using full word and root query terms are shown in figure 2. The summaries provided by the average recall-precision values suggest that the root retrieval method of the individual query words outperforms the full word retrieval method.

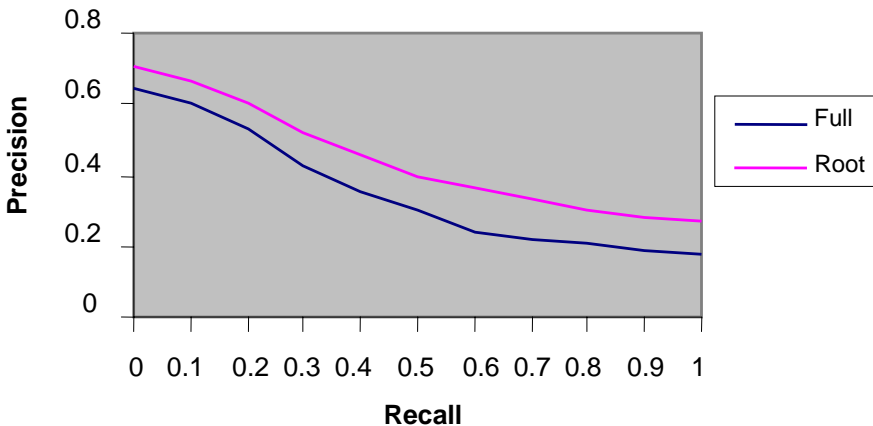


Figure 2: Average recall-precision full word and root English query terms.

Conclusion

An effective method to deal with the derivationally related keys is to remove affixes and prefixes from word form, and the output is a common root. When this method is used the document index terms, the source language and the target language query words have to be rooted. Although the Arabic root program was not perfectly accurate, the retrieval performance had an acceptable improvement.

The recall improved due to rooting since a larger number of relevant documents are retrieved. Also for Arabic and English languages the rooting improves the precision. These results were similar to the results that appeared in [6]. The experiment shows that a better retrieval results were achieved using the root in English language compared to rooting method used in the Arabic language. In summary, when the query words are rooted in both languages the retrieval performance is significantly improved.

An English-Arabic Dictionary-Based CLIR system has been designed, implemented, and evaluated. The system uses 242 Arabic documents, 170 English documents, 59 queries, and domain specific dictionary. From this experiment we can conclude that, in dictionary-based cross-language information retrieval, rooting of words to base forms is necessary to be able to match the query with the best relevant documents. Therefore, the root retrieval method was significantly better than the word retrieval method in both languages. When the query words are rooted, more documents will be retrieved because each document may contain more words that have the same root. Additionally, the results show that the rooting of English query words gives better retrieval results than rooting the Arabic query words.

تقييم نظم إسترجاع المعلومات باستخدام المعاجم الثنائية على اللغة العربية

عوني الحموري

ملخص

ان استعادة معلومات فيما بين اللغات المختلفة هي من مجالات البحث التي تنمو وتتسع باستمرار في ميدان استعادة المعلومات .

وهناك اهتمام متزايد في المقدرة على ادخال الاسئلة بلغة ما واستعادة المستندات بلغة اخرى، وتتوافر طرق مختلفة لاستعادة المعلومات اللغوية عبر اللغات المختلفة، الا ان هذه الدراسة تبحث في طريقة تقوم على المعاجم الثنائية الانجليزية العربية والعربية الانجليزية. وقد تمت دراسة عملية الاستعادة القائمة على هذه الطريقة في حالتين: الاولى عندما يتألف السؤال من كلمات تامة والثانية عندما يتألف السؤال من جذور الكلمات.

Introducing English-Arabic Dictionary-Based Cross Language Information Retrieval

ويتم اختيار الاسئلة باللغة الاصل (الانجليزية) ثم تستعاد المستندات باللغتين العربية والانجليزية. وقد خلصت هذه الدراسة الى ان عملية الاستعادة بين اللغتين الانجليزية والعربية تتحسن عندما تستخدم جذور الكلمات في صياغة الاسئلة المراد استعادة المعلومات الخاصة بها .

References

- [1] Ballesteros L. and Croft W. B., 'Dictionary method for cross-lingual information retrieval', In *Proceedings of the 7th International Conference on Database and Expert Systems Applications*, (1996) 791-801.
- [2] Oard D. W., *Alternative approach for cross-language text retrieval – free text retrieval*-(1997).
- [3] Larkey L. S. and Connell M. E., 'Arabic information retrieval at UMass in TREC-10', In *The Tenth Text Retrieval Conference, (TREC2001)*, (2001) 562-570.
- [4] Chen A., Jiang H. and Gey F., 'English-chinese cross-language IR using bilingual dictionaries', In *The Ninth Text Retrieval Conference (TREC-9)*, (2000) 517-522.
- [5] Aljlal M., Frieder O. and Grossman D., 'On arabic-english cross language information retrieval: A machine translation approach', In *Proceedings of the International Conference on Information Technology: Coding and Computing*, (2002) 2-7.
- [6] Pirkola A., Hedlund T., Keskustalo H. and Jarvelin K., 'Dictionary-based cross language information retrieval :problems, methods, and research findings', *Information Retrieval*, 4(3-4) (2001) 209-230.
- [7] Pirkola A., Keskustalo H., Leppanen E., Kansala A. P. and Jarvelin K., 'Targeted s-gram matching: a novel n-gram matching technique for cross-and mono-lingual word form variants', *Information Research*, 7(2) (2002).
- [8] Nie J. Y., Isabelle P., Plamondon P. and Foster G., 'Using a probabilistic translation model for cross-language information retrieval', In *The Sixth Workshop on Very Large Corpora*, (1998) 8-27.
- [9] Buitelaar P., Netter K. and Xu F., 'Integrating different strategies in cross-language information retrieval in the MIETTA project', In *Proceedings of the 14th Twente Workshop on Language Technology (TWLT14). Language Technology in Multimedia Information Retrieval*, (1998) 9-17.
- [10] Adriani M. and Croft W. B., 'The effectiveness of a dictionary-based technique for indonesian-english cross-language text retrieval. CLIR technical report IR-170', (1997).
- [11] Hasan M. M. and Matsumoto Y., 'Chinese-Japanese cross language information retrieval: A han character based approach', In *proceedings of the ACL-2000 Workshop on Word Senses and Multi-Linguality*, 8 (2000) 19-26.

Hammouri

- [12] Hasnah A. and Evens M., 'Arabic/English cross language information retrieval using a bilingual dictionary', In *Arabic NLP Workshop at ACL/EACL 2001: Arabic Language Processing Status and Prospects*, (2001).
- [13] Baeza-Yates R. and Ribeiro-Neto B., *Modern Information Retrieval*. Addison Wesley, (1999).
- [14] Al-Shalabi R., Kanaan G. and Muaidi H., 'New approach for extracting Arabic roots', In *proceedings of the International Arab Conference on Information Technology*. Alexandria, Egypt, (2003).
- [15] Porter M. F., 'An algorithm for suffix stripping', *Program*, 14(3) (1980) 130–137.
- [16] Gey F., Kando N. and Peters C., 'Cross-Language information retrieval: the way ahead,' *Information Processing & Management*. 41(3) (2005) 415-431.
- [17] Levow G., Oard D.W. and Resnik P., 'Dictionary-Based techniques for cross-language information retrieval, ' *Information Processing & Management*. 41(3) (2005) 523-547.

Parallel Graph Colouring Based on Saturated Degree Ordering

Ahmad Sharieh and Khair Eddin Sabri *

Received on Nov. 5, 2006

Accepted for publication on June 10, 2007

Abstract

The use of graph colouring is essential to many applications such as the estimation of sparse Jacobins, scheduling and registering allocation. There are many existing sequential and parallel algorithms used in graph colouring. A parallel graph colouring algorithm usually requires communication between processors or re-colouring conflict nodes. As the communication between processors increases the time efficiency decreases. Also, when the number of conflict nodes increases the time efficiency decreases and the total number of colours increases. In this paper, we introduce a new parallel graph colouring based on saturated degree ordering (SDO). This algorithm and the one introduced by Gebremedhin and Manne (GM), both based on SDO, were implemented on a single processor and simulated a parallel processing using multiple threads. The algorithms were tested on graphs of different sizes, densities and number of processors. The time required for colouring and the number of colours were measured. Both algorithms decrease their running time as the number of threads increases. In case of sparse graphs, the results indicate that the introduced algorithm is more efficient than the GM algorithm. Also, it was found that the proposed algorithm used less number of colours for the tested samples.

Keywords: Graph algorithms, Heuristic parallel graph colouring, Threads.

Introduction

Colouring of a graph is one of the most useful models in graph theory. This model has been used to solve problems such as school timetabling, computer register allocation, electronic bandwidth allocation, numerical computation, and optimization [5].

Assume you have a graph $G = (V, E)$, where V is the set of all nodes and E is the set of all edges in G . The colouring of a graph G is a mapping $C(V): G \rightarrow S$, where S is a finite set of "colours", such that if (v, w) is an edge in G , that is if $(v, w) \in E$, then $C(v) \neq C(w)$. In other words, adjacent vertices are not assigned the same colour [4]. This leads to the question: can we colour a graph where no adjacent vertices have the same colour by using the fewest number of colours?

Sometimes it is necessary to perform the colouring of a graph on multiple processors system. This will speed up the process of colouring and manipulate graphs

with large number of vertices. The system can be multi-computers (loosely coupled distributed processing elements) or multiprocessors (tightly coupled with shared memory)[8]. Colouring graphs in parallel introduces problems regarding communication, synchronization, or re-colouring conflict nodes. In this paper, we introduce a new algorithm to colour a graph in parallel, where the processors can run concurrency without having conflict nodes to be coloured.

In Section 2, several graph colouring algorithms are reviewed. In Section 3, the proposed algorithm is introduced. In Section 4, experiments and results are presented. Section 5 concludes this work.

Review

Graph coloring algorithms are implemented to color a graph sequentially or concurrency. There are many heuristic sequential techniques for coloring a graph. One of them is greedy graph colouring [5]. The greedy colouring is heuristic and concentrates on carefully picking the next vertex to be colored. In the heuristic technique, once a vertex is colored its color never changes.

The *First Fit (FF) algorithm* assigns, sequentially, each vertex the lowest legal colour. It is the easiest and fastest of all heuristic greedy colouring algorithms. This algorithm has the advantages of being very simple and fast [2].

The *Degree-Based Ordering (DBO)* algorithm uses a certain selection criterion for choosing the vertex to be coloured. It picks up a vertex from an arbitrary order. It is a better strategy than the FF to colour a graph. Many strategies for selecting the next vertex to be colored have been proposed. Some of the strategies are: Largest Degree Ordering (LDO), Saturation Degree Ordering (SDO), and Incidence Degree Ordering (IDO).

The LDO chooses a vertex with the highest number of neighbors. Intuitively, the LDO provides a better colouring than the FF technique. This heuristic technique can be implemented to run in $O(|E|)$, which is bounded by $O(n^2)$, in terms of worst case complexity running time, where n is the number of nodes in the graph [2].

The saturation degree of a vertex is defined as the number of its adjacent vertices of different colors. The SDO is heuristic approach provides a better colouring than LDO. This approach can be implemented to run in $O(|E|)$ [2].

A modification of the SDO heuristic is the incidence degree ordering algorithm. The incidence degree of a vertex is defined as the number of its adjacent coloured vertices. This heuristic can be implemented to run in $O(n^2)$, in worst case nodes [2]

There are two types of parallel graph colouring based on *graph partitioning approach* and *block partitioning approach* [7]. The graph partitioning approach assumes that the vertices of a graph $G = (V, E)$ are partitioned into p sets as $\{V_1, \dots, V_p\}$. The set of shared edges E^S is defined as the set of edges $E^S \subseteq E$, where $(v, w) \in E^S$ and $P(v) \neq P(w)$. Let the set of shared vertices be the set V^S , where a vertex is in this set if and only if it is an endpoint for some edge in E^S . Let the set of local vertices in a processing

Parallel Graph Colouring Based on Saturated Degree Ordering

element, denoted by V^L , be the set $V - V^S$. The V^L vertices can be coloured, sequentially, using one of the local graph colouring.

The problem is in the V^S vertices, where there are adjacent vertices located on different processors. So, we need here synchronization between them. There are many heuristic parallel graph coloring algorithms to resolve this problem such as: *Jones-Plassmann (JP)*, *Largest Degree First (LDF)*, and *Smallest Degree First (SDF)* algorithms. The JP is an asynchronous heuristic parallel and is proposed for distributed memory parallel systems. The proposed heuristic is based on a message-passing model [3]. Jones & Plassman first partition the vertices of the input graph across p processors in a distributed memory parallel computer. Then, they apply a coloring approach which consists of two phases [3]:

- 1) An initial parallel phase, which resolves the problem of adjacent vertices on different processors
- 2) Local phase that uses some good heuristic sequential colouring technique to colour the local vertices of each processor.

At the beginning of the algorithm, each vertex is assigned a random number, and then coloring is performed in parallel depending on the random numbers.

The LDF algorithm is basically similar to the JP algorithm. The only difference is that instead of using random weights to create the independent sets, each weight is chosen to be the degree of the vertex in the graph induced by the uncolored vertices. Random numbers are only used to resolve conflicts between neighbouring vertices having the same degree. Vertices are thus not colored in random order, but rather in order of decreasing degree. The LDF aims to use fewer colors than the JP algorithm [1].

The SDO algorithm tries to improve the LDF algorithm by using a more sophisticated system of weights. In order to achieve this, the algorithm operates in two phases: a weighting phase and a coloring phase. The weighting phase begins by finding all vertices with degree equal to the smallest degree d , presently in the graph. These vertices are assigned the current weight and removed from the graph, thus changing the degree of their neighbours. When there are no vertices of degree d left, the algorithm looks for vertices of degree $d+1$. This process continues until all vertices are assigned weights [1].

The *Block Partitioning Approach* strategy is to solve the original problem in two phases. In the first phase, the input vertex set is divided into p blocks of equal sizes. The vertices in each block are colored in parallel using p processors, where they operate in a synchronous manner. In doing so, two processors may simultaneously attempt to color adjacent vertices leading to an invalid coloring. In the second phase, the vertex set is block partitioned as in the first phase and each processor checks whether or not its vertices are legally colored. If a conflict is discovered, one of the endpoints of the edge, in conflict, is stored in a table. Finally the vertices in this table are colored sequentially [2].

Another strategy of three phases was introduced in [6]. In the first phase, the input vertex set V of the graph G is partitioned into p blocks (of V/p vertices each). The

vertices in each block are then colored in parallel using p processors. The parallel coloring comprises of $k = p$ parallel steps with synchronization barriers at the end of each step. When coloring a vertex, all its previously colored neighbors, both local ones and those found on other blocks, are taken into account. In doing so, two processors may simultaneously attempt to color vertices that are adjacent to each other. If these vertices are given the same color, the resulting coloring becomes invalid and called a pseudo coloring. In the second phase, each processor p_i checks whether vertices in V_i are assigned valid colors by comparing the color of each vertex against all its neighbors that were colored at the same parallel step in the first phase. This checking step is also done in parallel. If a conflict is discovered, one of the endpoints of the edge in conflict is stored in a table. Finally, in the third phase, the vertices stored in this table are colored sequentially.

The Proposed Algorithm

The disadvantage of the graph partitioning algorithms is that it takes more time in colouring the V^S vertices (first phase), as some processors become idle for a long time, waiting for other processors to color their vertices. Another disadvantage of the block partitioning algorithms is that it recolors conflict vertices sequentially, so it will take more time to recolor a large number of such vertices. However, in the algorithm proposed by Gebremedhin and Manne (GM) [6], the number of conflict nodes is minimized. Therefore, the time used to recolor the nodes is minimized.

Our proposed algorithm uses the SDO algorithm to colour the nodes. It has a technique based on block partitioning that aims at deleting the conflict nodes, so there is no need to recolor them. Therefore, the total number of colors and the time used in coloring should be minimized.

The proposed algorithm works as shown in Figure 1. The total number of processors are p . Each P_i , $i = 1, 2, \dots, (p-1)$, chooses the next node to be colored and P_c colors the selected nodes for coloring. The main steps in the proposed algorithm are shown in Figure 2. The example in Figure 3 shows a snapshots of colouring a graph.

Parallel Graph Colouring Based on Saturated Degree Ordering

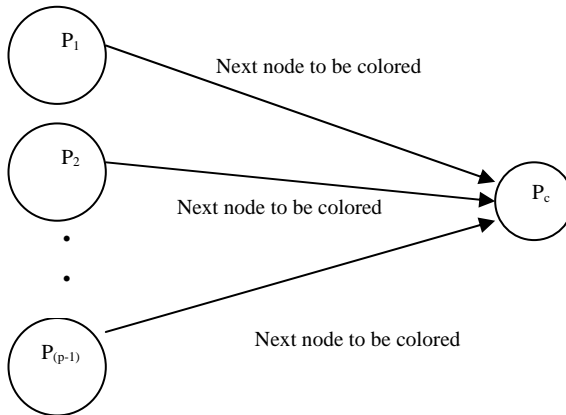


Figure 1: Diagram of the proposed algorithm

1. Partition the graph $G=(V,E)$ into $(p-1)$ blocks and assign each block to a processor.
2. For each P_i (Search-Processor), do in parallel:
 - 2.1 Call SDO algorithm to select the next node to be coloured.
 - 2.2 Flag the selected nodes for P_c to be coloured.
 - 2.3 P_c (Colouring-Processor) applies the colouring algorithm to colour the flagged nodes. This algorithm colours the selected nodes with the minimum possible colour which is different from the color of all adjacent nodes to this received node.
 - 2.4 Repeat the process in 2.1 to 2.3 until all nodes have been coloured
3. End.

Figure 2: The major steps in the proposed colouring algorithm corresponding to Figure 1.

To colour a graph in parallel, using p processor, $(p-1)$ processors are used to search for the next nodes to be coloured and one processor is used in colouring. The graph is partitioned into $(p-1)$ blocks. The sizes of the blocks are almost equal. Each block is assigned to a processor to colour the nodes in this block. The function of each processor holding a block is to search for the next node to be coloured. The colouring process for the selected nodes is performed by another processor P_c , specialized for colouring. Therefore, the colouring step is done in parallel with other processors that search for the best nodes to be coloured. The P_c has information kept in its site about the previously coloured nodes. It can use any sequential colouring algorithm such as: LDO, SDO, and IDO. In this research, the P_c employees the SDO algorithm. It needs only to colour new nodes from other processors, thus conflicts is removed.

The worst case run time of the SDO algorithm is bounded by $O(n^2)$, where n is the total number of nodes. Most of the time is needed in searching for the best nodes to be coloured. The colouring steps take no more than $O(n*c)$, where c is the total number of colours.

The run time cost of the proposed algorithm consists of: time in step 1, time in steps 2.1 and 2.2 for the first round, time in steps 2.1, 2.2 and 2.3 in round two to last round minus 1, and time to colour nodes in the last round by P_c . The run time in performing

step 2.1 and 2.2 is the cost of searching for the candidate to be coloured in each block, using the SDO. This time is bounded by $O(\frac{n^2}{(p-1)} + (p-1))$ of computation (searching and assigning flags) time. The cost in step 2.3 is bounded by $O(k*(p-1))$, where k is the maximum number of colours needed to colour the $p-1$ flagged nodes in a round. The colouring process in step 2.3 is performed concurrently with that in step 2.1 and 2.2. The total run time can be approximated by $O(\frac{n^2}{(p-1)} + O(p-1) + O(k*(p-1)))$. This is in the worst case. The run time complexity is dominated by $O(\frac{n^2}{(p-1)})$. Note that the first round will take the longest time to colour first set of nodes. Then, the number of nodes to select a candidate from and the number of nodes to colour are decreased at the end of each round. This will speed up the process of colouring the graph.

Parallel Graph Colouring Based on Saturated Degree Ordering

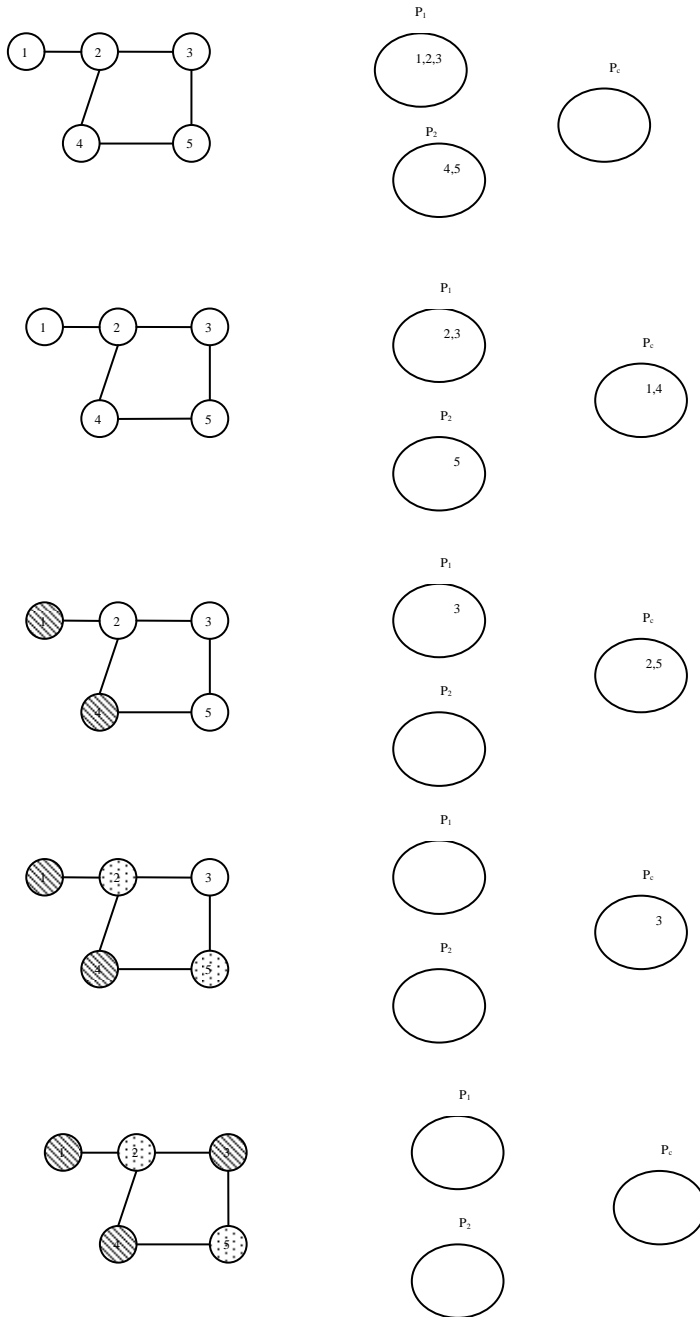


Figure 3: Snapshots of colouring a graph.

The complexity of the sequential algorithm (SDO) is bounded by $O(n^2 + c*n)$, where n is the total number of nodes and c the total number of colours. The worst case is when the graph is fully connected, so we have $c=n$. Therefore, the worst case is $O(2*n^2)$. The SDO in step 2.1 can be replaced by a more efficient algorithm if there is one.

For a system with shared memory, the blocks will be loaded once and the time for communication is replaced by the time for synchronization. The searching-processors work on their blocks independently. The synchronization is between each of the searching-processors and the colouring-processor P_c . Thus, the algorithm will perform better in case of using multi-processors system. This is what we investigated in this work.

Result and Analysis

The proposed algorithm has been implemented using Java programming language and tested on a single processor computer (PC). Threads were used to represent processors. A similar implementation and testing of the previous algorithm due to Gebremedhin and Manne [6] was provided. The experimental results from the GM and the proposed algorithm are reported. Both implementations were based on the SDO. Different graphs, generated randomly, have been used.

The two algorithms were tested on different graphs, using more than one processor and different densities. Samples of the results are shown in Table 1. Three different sets of graphs with 500, 1000, 1500 nodes are presented here. Three different densities 10%, 50%, and 90% are used. The algorithms were tested by using different number of threads: 1 to 9 threads. The same experiments were repeated ten times and the average were taken. This is to smoothen out the effects of the random numbers. The following results were obtained:

Table 1: Time and Number of colors for coloring different graphs with different densities by the proposed algorithm and the GM algorithm.

Line	no of processors	Connection Density %	no of nodes	Proposed Algorithm		Gebremedhin & Manne Alg.	
				Time	No. Of colors	Time	No. Of colors
1	1	10	500	139	16	139	16
2	2	10	500	141	16	50	18
3	3	10	500	43	18	34	19
4	4	10	500	28	19	28	19
5	5	10	500	25	19	26	19
6	6	10	500	19	19	28	19
7	7	10	500	20	19	27	19
8	8	10	500	26	19	28	19
9	9	10	500	23	19	30	19
11	1	50	500	1128	68	1128	68

Parallel Graph Colouring Based on Saturated Degree Ordering

12	2	50	500	1128	68	331	70
13	3	50	500	326	70	159	72
14	4	50	500	165	71	123	72
15	5	50	500	114	72	97	72
16	6	50	500	87	71	83	72
17	7	50	500	75	72	78	72
18	8	50	500	69	72	75	72
19	9	50	500	67	72	69	72
21	1	90	500	1345	167	1345	167
22	2	90	500	1346	167	428	174
23	3	90	500	439	174	212	176
24	4	90	500	203	176	145	177
25	5	90	500	144	176	113	176
26	6	90	500	115	176	94	175
27	7	90	500	100	176	84	177
28	8	90	500	91	175	82	178
29	9	90	500	81	177	73	176
31	1	10	1000	957	30	957	30
32	2	10	1000	962	30	311	30
33	3	10	1000	308	30	175	31
34	4	10	1000	172	30	135	31
35	5	10	1000	119	31	118	31
36	6	10	1000	101	31	103	31
37	7	10	1000	84	31	95	31
38	8	10	1000	78	31	92	31
39	9	10	1000	75	31	94	31
41	1	50	1000	8351	116	8351	116
42	2	50	1000	8584	116	2392	124
43	3	50	1000	2431	125	1261	126
44	4	50	1000	1258	125	819	126
45	5	50	1000	823	125	637	126
46	6	50	1000	629	126	514	127
47	7	50	1000	505	126	459	127
48	8	50	1000	433	125	430	126
49	9	50	1000	377	126	384	126
51	1	90	1000	10383	304	10383	304
52	2	90	1000	10187	304	3136	317

Sharieh and Sabri

53	3	90	1000	3126	319	1723	320
54	4	90	1000	1679	317	1158	321
55	5	90	1000	1164	318	830	319
56	6	90	1000	878	319	659	321
57	7	90	1000	732	319	570	320
58	8	90	1000	645	319	495	320
59	9	90	1000	590	319	450	321
61	1	10	1500	2991	40	2991	40
62	2	10	1500	3086	40	931	41
63	3	10	1500	937	41	530	42
64	4	10	1500	550	41	384	42
65	5	10	1500	348	41	323	42
66	6	10	1500	273	41	278	42
67	7	10	1500	234	41	262	42
68	8	10	1500	206	41	241	42
69	9	10	1500	197	41	237	42
71	1	50	1500	27917	163	27917	163
72	2	50	1500	28922	164	7810	174
73	3	50	1500	7958	174	4086	176
74	4	50	1500	4012	175	2678	176
75	5	50	1500	2649	175	2039	176
76	6	50	1500	1964	175	1570	177
77	7	50	1500	1587	175	1339	176
78	8	50	1500	1386	175	1183	176
79	9	50	1500	1191	175	1119	176
81	1	90	1500	34606	433	34606	433
82	2	90	1500	34660	433	10230	452
83	3	90	1500	10250	452	5358	452
84	4	90	1500	5328	452	3592	455
85	5	90	1500	3598	452	2733	457
86	6	90	1500	2939	452	2130	456
87	7	90	1500	2428	454	1830	455
88	8	90	1500	2103	452	1522	455
89	9	90	1500	1881	452	1353	454

Parallel Graph Colouring Based on Saturated Degree Ordering

1. When a small number of processors was used, the GM algorithm worked better than the proposed algorithm. This is because of unbalanced distribution of work that could happen in this case. The P_c has more load than the other processors. This can be shown clearly in line 2, 12, 22, etc. where the number of processors is two.
2. It was found that the proposed algorithm performs better than the GM algorithm if the graph is sparse and the number of processors is more than four, as shown, for example, in lines 4-9, 34-39, 64-69 in Table 1. This is due to the fact that in the proposed algorithm there is no conflict nodes need to be resolved, which usually takes time.
3. If the density of the graph is close to one, the GM algorithm performs better in some cases as shown, for example, in lines 21-29, 51-59, 89-89 in Table 1. This is because in a graph with high density, the load on colouring processor increases.
4. The proposed algorithm produced fewer number of colours than GM did, as shown, for example, in lines 2-9, 32-39, 64-69 in Table 1. This is because in the GM algorithm, the number of conflict nodes increases the number of colours.

We used timing of simulation to justify the proposed algorithm compared to the GM algorithm. The simulation results include the time spent for synchronization communication in both algorithms. The results verify the good quality of the proposed algorithm against the GM algorithm. See Figure 4. The proposed algorithm ended up with smaller chromatic number than the GM algorithm.

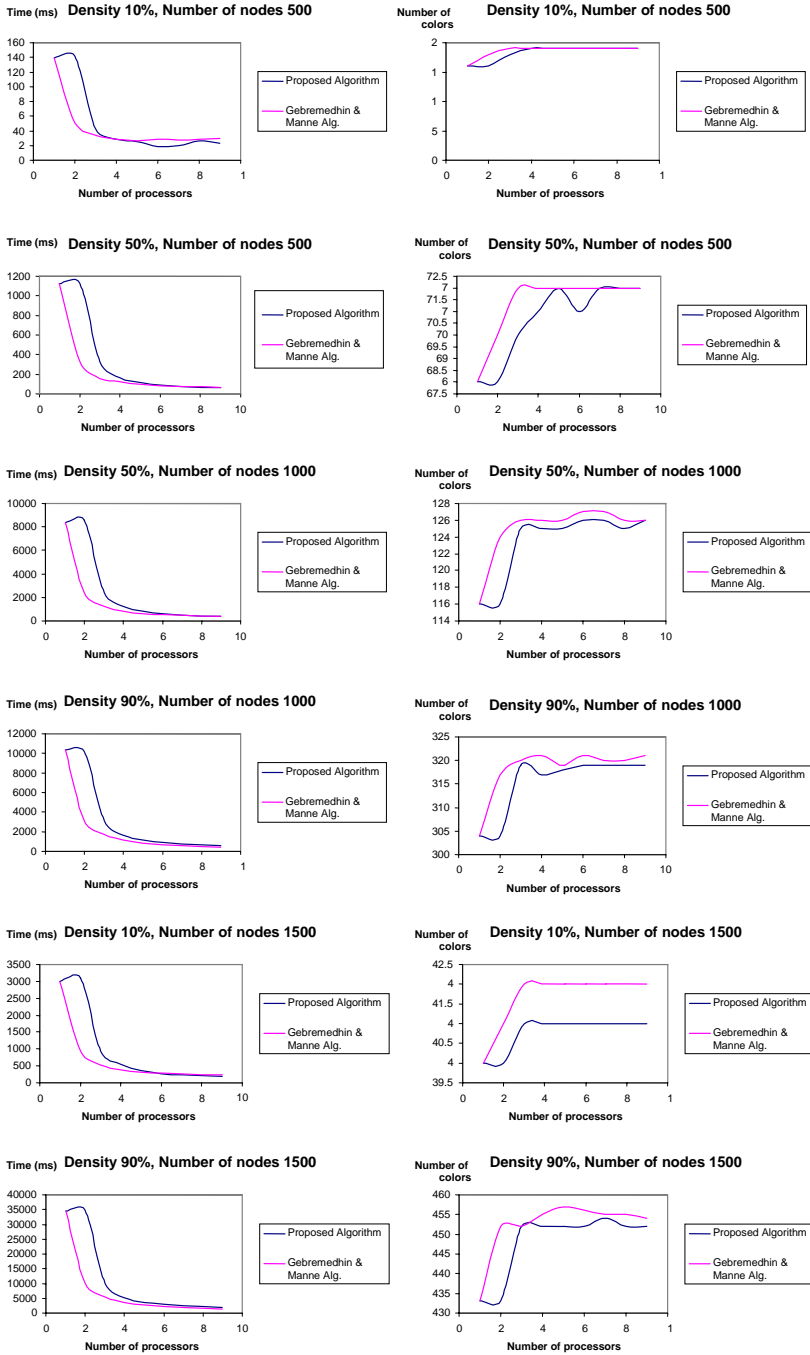


Figure 4: comparison between the proposed algorithm and the GM algorithm.

Conclusion

In this paper, we propose a new parallel algorithm for graph coloring. It aims at eliminating the conflict nodes. The main differences from the GM algorithm are: SDO was used instead of FF and one processor is dedicated to do the colouring to avoid conflict. It should be obvious that different degree-based ordering can be used with the block partitioning approach, so the first difference is not very novel. The second difference is the major contribution in this work.

The results have shown that

1. The proposed algorithm is faster than the GM when using more than four processors.
2. The number of colours produced by the proposed algorithm is less than of that produced by GM algorithm in most cases.
3. The proposed algorithm and the GM algorithms show good results in implementing them on one machine with multithreads.

This work can be extended by

1. Implementing and testing the proposed algorithm on real multi-processors machines.
2. Focusing on modifying the proposed algorithm to decrease the time needed to color the nodes, especially if the density of the graph is high. It is suggested that more than one processor is used to color nodes and make synchronization between them.
3. In the proposed algorithm, all the nodes are colored using P_c processor. Alternative work can be done by letting the P_c colour the shared nodes only and each processor colour its local nodes.

تلوين مخطط بناءً على الدرجة المشبعة للعقدة فيه

أحمد الشرايعه و خير الدين صبري

ملخص

عملية تلوين المخططات ضرورية لكثير من التطبيقات مثل الجدولة والحجز والتعامل مع مصفوفة جيكوب. والعملية تحتاج لوقت طويل لتنفيذها. ويوجد عدد من الخوارزميات المتسلسلة والمتوازية المستخدمة للتلوين، إلا أن الخوارزمية المتوازية تتطلب الاتصال بين المعالجات أو التزامن لتلوين عقد مشتركة، وكلما زاد زمن التواصل قلت الفعالية، ويزداد عدد الألوان كلما زادت التعارضات. وفي هذه الورقة تم تقديم خوارزمية متوازية جديدة للتلوين مبنية على أساس الدرجة المشبعة للعقدة. وتم تنفيذ الخوارزمية المقترحة وقورنت مع الخوارزمية المقدمة من جبرمدن ومين. وعلى شكل تسلسلي ومتوازي وباستخدام خطوط المهام المتعددة.

وتم اختبار الخوارزمية المقترحة لتلوين مخططات بعدد من العقد المختلفة وذات كثافة مختلفة وعلى عدد مختلف من المعالجات. وتم قياس الزمن اللازم لتلوين المخططات وعدد الألوان المستخدمة. ووجد أن الخوارزمية المقترحة أفضل في حال كان المخطط غير كثيف من حيث المدة اللازمة للتلوين وعدد الألوان ولجميع العينات التي تم اختبارها.

References

- [1] Allwright J. R., Bordawekar R., Coddington P. D., Dincer K. and Martin C. L. "A comparison of parallel graph coloring algorithms". *Technical Report Tech. Rep.*, Northeast Parallel Architecture Center, Syracuse University, (1995).
- [2] Gebremedhin A.H., *Parallel Graph Coloring*. Thesis University of Bergen Norway Spring, (1999).
- [3] Jones M.T. and Plassmann P.E., "A Parallel graph coloring heuristic", *SIAM journal of scientific computing*, 14(3) (1993) 654-669.
- [4] Sara B. and Gelder A.V., *Computer Algorithms: Introduction to Design and Analysis*, 3rd Edition, Pearson Education Pub, (1999).
- [5] Klotz W., "Graph coloring algorithms," Mathematics Report, Technical University Clausthal, May 2002, pp. 1-9
- [6] Gebremedhin A. and Manne F. "Scalable parallel graph coloring algorithms", *Concurrency: Practice and Experience*, 12(12) (2000) 1131-1146.

Parallel Graph Colouring Based on Saturated Degree Ordering

- [7] Wilkinson B. and Allen M., "Parallel Programming: Techniques and Applications Using Network Workstations and Parallel Computers", Prentice Hall, 1st edition, (1999).
- [8] V.Kumar A., Grama A., Gupta G. and Karypis, "Introduction to Parallel Computing: Design and Analysis of Algorithms, 2nd Edition, Addison-Welsey, (2003).

Automated Global Prayer Calls Using GPS

Zakaria Saleh *

Received on May 7, 2008

Accepted for publication on July 30, 2008

Abstract

This study uses GPS to provide the five daily prayer calls "Athans" for Muslims worldwide. The result of the study will serve millions of Muslims residing in Non-Muslim countries, where information on the most important Muslim daily practice (daily prayers) is provided by independent Islamic centers in the form of prayer time tables. While large numbers of civilian applications benefit from GPS signals, this study will extend the use of GPS to one more, and yet important civilian application

Keywords: GPS, GPS Application, NMEA 0183, Prayers Time.

Introduction:

Muslims living in Non-Muslim countries get information on the most important Muslim daily practice (daily prayers) from independent Islamic centers. Some use audio devices designed specifically for "Athan", while others use advanced mobile systems that are programmed with audio prayer calling capabilities. This study will develop an automated "Athan" system that will rely on the GPS signal to calculate the five daily Athans. The system will employ a standard GPS receiver to periodically determine the latitude, longitude and evaluate its location. Based on GPS time and the receiver's location, the system will calculate the upcoming prayer time, set the time for it, and call Athan when it's time for it.

The problem of relying on prayer time tables provided by Islamic Centers is not having a center in all towns worldwide to provide the time table. In addition, the table will not call for Athan. The audio household Athan calling devices are designed to be sold worldwide, and are not programmed for the time table based on any location, therefore, they require a manual daily setting for all five prayers. Besides being time consuming, and requiring continued human intervention to update the prayer times, users still have to have a time table. Computer "Athan" programs require installation of extensive software, a computer that is running all the time, and still only cover major cities worldwide. The advanced mobile systems, while work well, when going far out of town, their timing may not be accurate. In all cases, Athan's are based on personal clocks/watches that may or may not be accurate. Using GPS will not only provide accurate prayer time, but it will also eliminate the need for tables or human intervention.

© 2008 by Yarmouk University, Irbid, Jordan.

* Department of Management Information Systems, Faculty of Information Technology and computer, Yarmouk University, Irbid, Jordan.

Limitations

The system will be developed to provide Athan globally, regardless on its location. It will be programmed with an algorithm that will evaluate a GPS signal, determine location, and then calculate time for the upcoming prayer time. However, it will not be possible to test the system in different locations worldwide, therefore, testing will be limited to using a GPS simulator, which will provide the international standardized NMEA-0183 protocol for GPS data exchange to introduce fixes for major cities, and call for Athan based on the calculated Athan time. The system will also rely on GMT time, and will not calculate current time in any of the tested cities. In addition, the systems capable of determining if it's a 'Fajir" or other "standard" Athan will not be tested, since the objective of the study it mainly to deploy GPS data in determining Athan time based on location.

GPS Basics

The basis of the GPS technology is a set of 24 satellites that are continuously orbiting the earth [10]. These satellites are equipped with atomic clocks and send out radio signals of accurate GMT time and location. The radio signals from the satellites are picked up by the GPS receiver. Once the GPS receiver locks on to four or more of these satellites, it can triangulate its location from the known positions of the satellites [6].

A typical GPS receiver calculates its position using the signals from four or more GPS satellites, or Space Vehicles (SV). Orbiting at an altitude of approximately 20,200 kilometers (12,600 miles or 10,900 nautical miles; orbital radius of 26,600 km (16,500 mi or 14,400 NM)), each SV makes two complete orbits each sidereal day [1].

The GPS design originally called for 24 SVs, eight each, in three circular orbital planes [4] was then later modified to six planes with four satellites each. The orbital planes are centered on the Earth, not rotating with respect to the distant stars [5]. The orbits are arranged so that at least six satellites are always within line of sight from almost everywhere on Earth's surface [11].

Many civilian applications benefit from GPS signals, using one or more of three basic components of the GPS: absolute location, relative movement, and time transfer. The ability to determine the receiver's absolute location allows GPS receivers to perform as a surveying tool or as an aid to navigation. The capacity to determine relative movement enables a receiver to calculate local velocity and orientation, useful in vessels or observations of the Earth. Being able to synchronize clocks to exacting standards enables time transfer, which is critical in large communication and observation systems.

GPS Radio Signals

GPS satellites transmit two types of radio signals: Coarse Acquisition (C/A) and Encrypted Precision (P/Y). C/A-Code is known as the Standard Positioning Service (SPS) and is the type of signal that is allowed for civil GPS receivers. C/A-code is transmitted at a frequency of 1575.42 MHz. P-Code is known as the Precise Positioning Service (PPS), where the U.S. military is the primary user of P/Y -Code transmissions, which is an encrypted form of the data. The P-code signal is transmitted at 1227.6 MHz.

Automated Global Prayer Calls Using GPS

Accepted methods for generating the C/A-code and P-code were established by the satellite developer in 1991 [8].

The NMEA 0183 standard calls for data communication in the form of coded "sentences." Each sentence begins with the character "\$" and ends with a carriage return and line feed (<CR><LF>). Between the beginning and end of each sentence are "fields" of data, each field separated by a comma. There are many different sentences [7].

RMC GPS Fix Data message Structure

NMEA data is sent as comma-delimited "sentences" which contain information based on the first word of the sentence. There are over fifty kinds of sentences, yet an interpreter really only needs to handle a few to get the job done. The most common NMEA sentence is the "Recommended Minimum" sentence. It begins with "\$GPRMC" as indicated below [7]:

```
$GPRMC,<hhmmss>,<A|V>,<ddmm.mmmm>,<N|S>,<dddmm.mmmm>,<E|W>,<kkk.k>,<ddd.d>,<ddmmyy>,<ddd.d>,<E|W>*hhcrlf
$GPRMC,225446,A,4916.45,N,12311.12,W,000.5,054.7,191107,020.3,E*68
```

Where, 225446 (Time of fix 22:54:46 UTC), A (Navigation receiver warning A = OK), 4916.45,N (Latitude 49 deg. 16.45 min North), 12311.12,W (Longitude 123 deg. 11.12 min West), 000.5 (Speed over ground, Knots), 054.7(Course Made Good, True), 191107 (Date of fix 19 November 2007), 020.3,E (Magnetic variation 20.3 deg East), *68 mandatory checksum.

Prayer Time Algorithm

To calculate the prayer times the latitude (B), longitude (L), and the reference longitude (R) of the location are needed. B and L will be obtained from GPS and R is calculated by multiplying 15 by the difference between local time and GMT (Basic time zones are 15 Degrees of longitude apart: 360°/24H = 15 Degrees/H).

We also need to know two astronomical measures called the declination angle of the sun (□) and the real time-mean time difference, also known as the equation of time (T). The Earth is tilted by 23.45° and □ varies plus or minus this amount calculated by the equation [3 □

The equation of time is a correction to be added to the apparent solar time (as read on a sundial), to obtain a mean solar time, as commonly used [8]. This difference is a consequence of tilt of the Earth's orbit. The following equations are used to calculate the five daily prayer times [2]:

$$Z = 12 + \frac{(R - L)}{15} - \frac{T}{60} \dots\dots\dots 1$$

$$U = \frac{1}{15} * ArcCos \left[\frac{Sin[(-0.8333 - 0.0347 * Sin(H)^{0.5})] - Sin(\delta) * Sin(B)}{Cos(\delta) * Cos(B)} \right] \dots\dots\dots 2$$

$$V = \frac{1}{15} * ArcCos \left[\frac{-Sin(G) - Sin(\delta) * Sin(B)}{Cos(\delta) * Cos(B)} \right] \dots\dots\dots 3$$

$$W = \frac{1}{15} * ArcCos \left[\frac{Sin\{ArcCot(1 + Tan(B - \delta))\} - Sin(\delta) * Sin(B)}{Cos(\delta) * Cos(B)} \right] \dots\dots\dots 4$$

Where:

$$\delta = \frac{180}{\mu} * \{ 0.006918 * [0.399912 * Cos[\beta]]_+ [0.070257 * Sin[\beta]]_- [0.006758 * Cos[2 * \beta]]_+ [0.000907 * Sin[2 * \beta]]_- [0.002697 * Cos[3 * \beta]]_+ [0.001480 * Sin[3 * \beta]] \}$$

$$T = 229.18 * \{ 0.000075 * [0.001868 * Cos[\beta]]_- [0.032077 * Sin[\beta]]_- [0.014615 * Cos[2 * \beta]]_- [0.040849 * Sin[2 * \beta]] \}$$

$$\beta = \frac{J * 360}{365} \text{ , and J is the day of year (e.g. J=0 for Jan 01, and J=41 Feb 10)}$$

- B= latitude of place
- L= longitude of place
- R= reference longitude (i.e. TIME BAND x 15)
- H= height above sea level in meters
- δ = declination angle of sun from celestial equator
- T= equation of time
- G= twilight angle (=18 Degrees)
- FAJR = Z-V
- ZUHR= Z
- ASR = Z+W

Automated Global Prayer Calls Using GPS

MAGHRIB = Z+U

ISHA = Z+V

Approach

The GPS receiver should receive signals directly from the GPS satellites. The Athan system is capable of processing the data and making decision on when to call for Athan. It will also be capable of determining if it's a 'Fajr' or other "standard" Athan. The system is illustrated in figure 1.

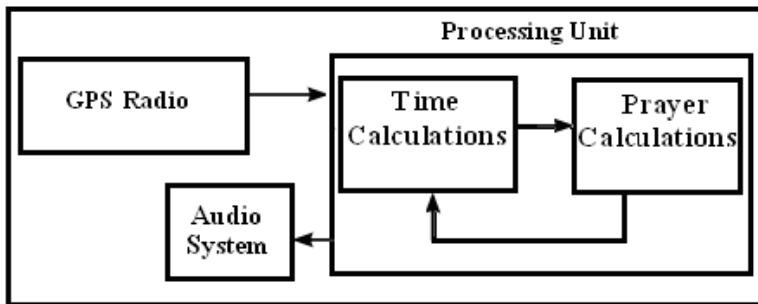


Figure 1: GPS Athan System

Once powered up, the system will receive signals directly from the GPS Satellites. A small sample of the GPS satellite signal is captured and stored in memory. Then later, the signal samples are uploaded to a PC, and processed by the Processing Unit to calculate the location where the signal was captured. The Processing Unit will then calculate time, and determine time for next Athan call. The process is illustrated in figure 2.

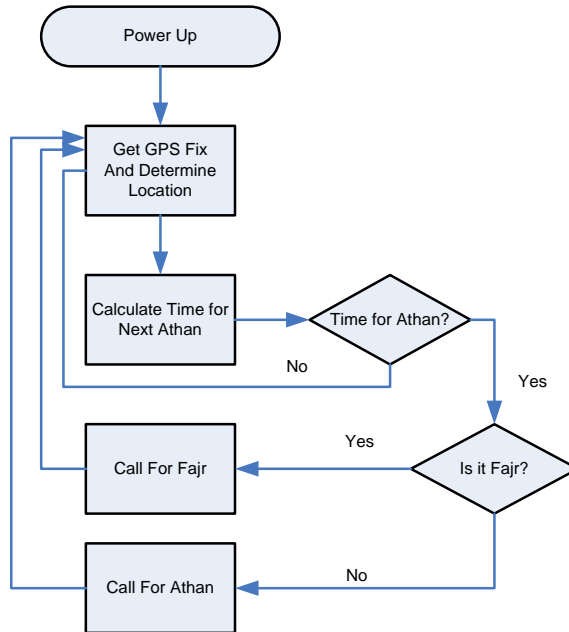


Figure 2: Athan Calculation and calling Algorithm

Hardware Simulation and Test Set-Up

To fully realize the potential of GPS acquisition and updating, in the absence of any operational GPS receiver, it is necessary to use a signal simulator to test and verify the research algorithms. Skylab GPS Simulator 2.0 is used. The Skylab GPS Simulator provides a complete suite for all GPS simulating needs. The Simulator uses the international standardized protocol NMEA-0183 for GPS data exchange. The Skylab GPS Simulator provides the simulation of a GPS receiver on several interfaces. Furthermore Skylab GPS Simulator provides several input methods for GPS data: Manual Input, Map Input, Logfile Playback, and Forwarded Input [9]. This research will apply the Map Input method (see figure 3).

Automated Global Prayer Calls Using GPS

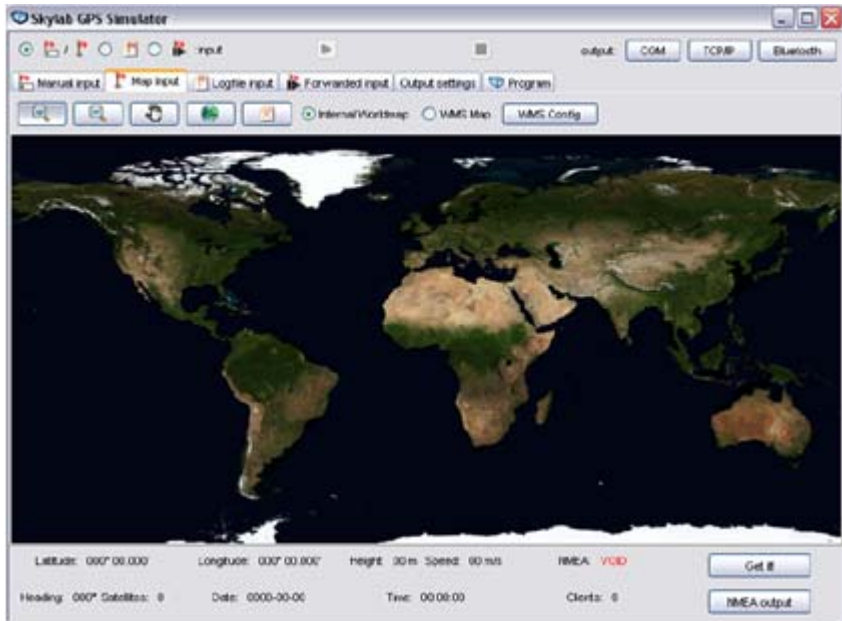


Figure 3: Skylab GPS Simulator Map Input

The map input method lets the user choose a position visually from a map, where a city will be selected and then the simulator will produce the NMEA sentence for the selected location (see figure 4).

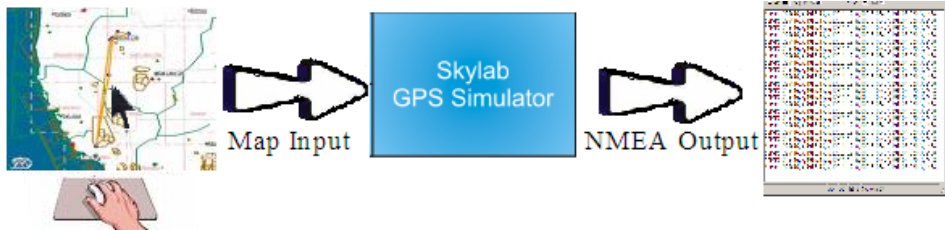


Figure 4: The NMEA Functions Overview

System Testing

When creating our location modeling system, the objective was to process as much data as possible without any a prior knowledge of the city under test.

The testing was run at 13:00 GMT. The objectives were to indicate the upcoming prayer time in selected major world cities. Table 1 illustrates a sample result for the several selected cities. Names for cities provided were manually entered based on knowledge of the locations of those cities on the world map, and while several GPS longitude latitude were used in the test for the same city, the table shows tests results of

Saleh

only one GPS sample from each tested city. Cities have ranges of GPS fixes. For example, the following data represents all samples of the Chicago area in the USA:

Latitude = 41.7938, Longitude = -87.6451

Latitude = 41.7785, Longitude = -87.7397

Latitude = 41.7487, Longitude = -87.7417

Latitude = 41.8435, Longitude = -87.6959

Latitude = 41.7939, Longitude = -87.6891

Latitude = 41.7765, Longitude = -87.8010

Latitude = 41.7627, Longitude = -87.6789

Latitude = 41.8526, Longitude = -87.6465

Latitude = 41.8790, Longitude = -87.6818

All of the above returns the same Athan time. Therefore, there is no need to list them all in the table. Nevertheless, the test results are encouraging, and by looking at the data from the study, it shows the proposed systems has the capability to employ GPS for one more civil application, and provides data with high accuracy to be used in calculating the prayer time for any location in the planet earth. To compare the results with known prayer time table published by Chicago Islamic Center for the month of September 2007 (see appendix A), the system was tested to produce prayer times for random days in the same month. The test results are shown in table 2.

Table 1: Calculated Next Prayer Time for several Cities World Wild

City , Country	Latitude	Longitude	Next Prayer	Next Prayer Time
Amman, Jordan	31.9394	35.9349	Maghrib	15:17
Lublin, Poland	33.5158	36.2939	Asr	2:17
Lubango, Angola	30.0571	31.2272	Asr	14:11
Moscow, Russia	36.1334	-95.9757	Maghrib	14:50
Venice, Italy	47.369	8.538	Asr	15:06
Chicago, USA	51.5002	-0.1262	Zuhr	17:39
Paris, France	48.8567	2.351	Asr	14:41
London, UK	41.8795	-87.6243	Asr	3:45
Fairbanks, Alaska	64.8351	-147.6465	Zuhr	21:38
Zurich, Switzerland	45.4343	12.3388	Asr	15:20
Tulsa, USA	55.7558	37.6176	Zuhr	16:11
Cairo, Egypt	-14.9181	13.5006	Asr	13:04

Automated Global Prayer Calls Using GPS

Table 2: Random Athan Calculations for September 2007

Date	Fajr	Zuhr	Asr	magrib	Isha
15	5:12	12:47	5:11	7:05	8:18
17	5:16	12:45	5:07	7:01	8:16
20	5:17	12:47	5:04	6:55	8:07
22	5:20	12:45	5:02	6:53	8:07
25	5:25	12:42	5:55	6:46	8:02
28	5:29	12:43	5:53	6:43	7:55
30	5:29	12:41	5:49	6:37	7:51

While the result were with minor to no errors in the calculations of the Athan time (within one to two minutes of error), the accuracy to be achieved when the system is deployed using an actual GPS receiver, will depend on the number of the GPS satellites from which signals are captured, position in the sky, signal strength, and environmental conditions. In worst cases, signals received by civilian GPS users can be accurate only to 100 meters. However, such accuracy does not have any effect on this study, because prayer times do not change for such small distance.

Conclusion and Future Study

As evident by the test results, the proposed system has shown its capability to employ GPS for one more civil application. GPS can be employed to calculate automated prayer time, from anyplace on the planet. While the result were with minor errors in the calculations of the Athan time (within one to two minutes of error) however, for an important month such as Ramadan, where Fajr and Magrib must be accurate, future work to reach such accuracy will be conducted. In addition, the study will be extend to provide calculations for prayer time while in motion to provide Athan time while traveling onboard an airplane and update the prayer time as the distance changes when traveling (with or against the sun movement), where the prayer time will change constantly moving in either direction.

النداء للأذان ذاتياً باستخدام نظام تحديد المواقع العالمي (GPS)

زكريا صالح

ملخص

إن نظام تحديد الموقع العالمي (GPS) كان قد صمم أصلاً للاستخدام العسكري ومن ثم تم تسخير هذا النظام للأغراض السلمية والتجارية وقد روي أنه بالإمكان استخدام هذا النظام أيضاً لتقديم خدمة أخرى يستفيد منها عدد كبير من المسلمين المقيمين في العالم وفي بلاد غير إسلامية بحيث تتم حسابات مواقيت الصلاة دون الحاجة للتدخل البشري أو أي نوع من البرمجة وإنما يقوم النظام بكل ذلك ذاتياً.

ويقوم هذا البحث بتقديم مشروع جهاز أذان باستخدام نظام تحديد الموقع العالمي (GPS) لمعرفة الموقع الموجود فيه جهاز الأذان عالمياً وبالتالي وبناءً على إحداثيات الموقع تتم عملية حساب مواقيت الصلاة لذلك المكان وبالتالي النداء للأذان عندما يحين الوقت.

References

- [1] Agnew D.C. and Larson K.M., "Finding the repeat times of the GPS constellation". *GPS Solutions* 11: 71--76. Springer, (2007).
- [2] Chen M. J. Soh W. J., Tan J. P. and Tahira B., *Islamic Astronomy*. National University of Singapore. Accessed March 10, 2007. From www.math.nus.edu.sg/aslaksen/gem-projects/hm/0203-1-37-islamic.pdf (2007).
- [3] Cooper P. I., The absorption of radiation in solar stills. *Solar Energy* 12(1969)333-346.
- [4] Daly P. , Navstar GPS and GLONASS: global satellite navigation systems. *IEEE*, 5(6)(1993).
- [5] Flandern T. V. , What the Global Positioning System Tells Us about Relativity. Accessed January 2, 2007 from <http://metaresearch.org/cosmology/gps-relativity.asp> (2007).
- [6] Kaplan E. D. and Hegarty C., *Understanding GPS: Principles and Applications*, 2nd Ed. Artech House, Norwood, MA, (2005).
- [7] Mihai A., NMEA-0183 Protocol Description, Version 2.20, (2004).
- [8] Rockwell International corporation. "GPS Interface Control". Document # ICD GPS-200, revision B. (1991)
- [9] Skylab Mobilesystems. *Skylab GPS Simulator User Manual*, Version 2.0, (2007).
- [10] Thompson D., How accurate is GPS. *Equal-I-Zer Newsletter*, 12 (1)(2008).

Automated Global Prayer Calls Using GPS

- [11] USCG Navcen . GPS Frequently Asked Questions. Accessed January 3, 2007, from <http://www.navcen.uscg.gov/faq/gpsfaq.htm> (2007).

Bayesian Prediction Interval from Grouped Data: Exponential Distribution

Moh'd Alodat, Khaled Aludaat and Tareq Alodat*

Received on Oct. 3, 2006

Accepted for publication on March 19, 2007

Abstract

In this paper, we find Bayesian prediction intervals for the first order statistic and the sample mean of a future sample taken from the exponential distribution when the given sample is grouped. The intervals that we have obtained require numerical calculations to find them. We apply our results to real data.

Keywords: Bayesian prediction, Grouped data, Posterior distribution.

Introduction:

Data for which true values are known only up to subsets of the sample space, such as rounding and interval censoring, are called grouped data. Real examples of grouped data are given and discussed in Wu and Perloff [1,2]. The disease relapse time and the time to failure of a product are two examples of grouped data, since they are observed only up to intervals. It is impossible to observe exactly the time to failure of a product, but it is possible to observe it up to an interval. Because of its wide application, the grouped data from exponential distribution will be considered, as follows, let X_1, X_2, \dots, X_n be a random sample from $\exp(\theta)$, the exponential distribution with parameter θ , and $I_j = ((j-1)\delta, j\delta)$; $j=1, 2, \dots, k$ and $I_{k+1} = (k\delta, \infty)$ be a partition of the interval $(0, \infty)$. Let N_j be the number of X_j 's that fall in I_j for $j=1, 2, \dots, k+1$. Then, the grouped frequency table $\{(I_1, N_1), (I_2, N_2), \dots, (I_{k+1}, N_{k+1})\}$ represents grouped data. We will use these grouped data to find Bayesian prediction intervals for $Y_{(1)}$, the first order statistic, $Y_{(1)}$, and \bar{Y} , the sample mean of a future sample Y_1, Y_2, \dots, Y_m from $\exp(\theta)$. The problem of finding Bayesian prediction intervals for $Y_{(1)}$ and \bar{Y} of a random sample from exponential distribution, when the given data are un-grouped, is considered by Lawless [3,4]. Such prediction intervals are missing from the literature when the given data are grouped. To fill this gap, we consider in this paper the problem of finding prediction intervals for $Y_{(1)}$ and \bar{Y} when the given data are grouped in frequency table. It is known that there is a loss in information due to grouping. This can be noted from comparing the two Fisher's information numbers about θ that have been obtained from grouped and unground samples. Schervish [5], page 114, shows the following

$$I_{\underline{X}}(\theta) = I_{\underline{n}}(\theta) + E_{\theta} \{I_{\underline{X}|\underline{n}}(\theta|\underline{n})\},$$

where $I_{\underline{X}}(\theta)$ and $I_{\underline{n}}(\theta)$ are the Fisher's information numbers obtained from ungrouped and grouped samples, respectively, and $E_{\theta} \{I_{\underline{X}|\underline{n}}(\theta|\underline{n})\}$ is the conditional score function. This implies that $I_{\underline{X}}(\theta) \geq I_{\underline{n}}(\theta)$ for all θ , i.e, there is a loss in the information due to grouping the data. Because of this loss in information, the prediction intervals, obtained using ungrouped, data are better than the prediction intervals obtained using grouped data. Using Bayesian approach we can add information about θ by using prior information about θ to reduce the loss in the information due to grouping.

In Sec. 2, we derive the posterior distribution of the parameter θ given the grouped data. In Sec. 3-4, we find the predictive densities of $Y_{(1)}$ and \bar{Y} given the grouped data. Our conclusions are stated in Sec. 5.

Posterior distribution of grouped data

Let X_1, X_2, \dots, X_n be a random sample from exponential distribution with parameter θ . Let N_j be the number of X_j 's that fall in the interval I_j , where $I_j = ((j-1)\delta, j\delta)$ for $j=1, 2, \dots, k$ and $I_{k+1} = (k\delta, \infty)$, $\delta > 0$. The set of pairs $\{(I_1, N_1), (I_2, N_2), \dots, (I_{k+1}, N_{k+1})\}$ is called grouped data. Let $\underline{n} = (n_1, n_2, \dots, n_{k+1})$. The joint distribution of $(N_1, N_2, \dots, N_{k+1})$ is *multinomial* (n, p_1, \dots, p_{k+1}) , where

$$\begin{aligned} p_j &= \int_0^{\infty} \theta^{-1} \exp(-x/\theta) dx, \\ &= \exp\left(-\frac{(j-1)\delta}{\theta}\right) - \exp\left(-\frac{j\delta}{\theta}\right), \quad \text{for } j = 1, 2, \dots, k, \end{aligned}$$

and

$$p_{k+1} = \exp\left(-\frac{k\delta}{\theta}\right).$$

The joint density of \underline{n} is given by

Bayesian Prediction Interval from Grouped Data: Exponential Distribution

$$\begin{aligned}
 f(\underline{n} | \theta) &= \frac{n! \left(\exp\left(-\frac{k\delta}{\theta}\right) \right)^{n_{k+1}}}{n_1! n_2! \dots n_{k+1}!} \prod_{j=1}^k \left(\exp\left(-\frac{(j-1)\delta}{\theta}\right) - \exp\left(-\frac{j\delta}{\theta}\right) \right)^{n_j}, \\
 &= c \prod_{j=1}^k \exp(-(j-1)\delta n_j) (1 - \exp(-\frac{\delta}{\theta}))^{n_j} \exp(-\frac{k\delta n_{k+1}}{\theta}), \\
 &= c \exp\left(-\frac{\delta}{\theta} \sum_{j=1}^{k+1} (j-1)n_j\right) \left(1 - \exp(-\frac{\delta}{\theta})\right)^{n-n_{k+1}}.
 \end{aligned}$$

The following conjugate prior distribution for $f(\underline{n} | \theta)$ is considered by Alodat and Al-saleh [6]

$$\pi(\theta) = c_1 \theta^{-r} \exp\left(-\frac{1}{\beta\theta}\right) \left(1 - \exp(-\frac{\delta}{\theta})\right)^\alpha, \alpha, \beta > 0, r \geq 0, \theta > 0. \quad (1)$$

Note that as $\beta \rightarrow \infty, r = 1, \alpha = 0, \pi(\theta) \rightarrow \frac{1}{\theta}$, the non-informative prior for θ from $\exp(\theta)$. The posterior distribution of θ given $\underline{n}=(n_1, n_2, \dots, n_{k+1})$ is given by

$$\begin{aligned}
 \pi(\theta | \underline{n}) &= \frac{f(\underline{n} | \theta)\pi(\theta)}{\int_0^\infty f(\underline{n} | \theta)\pi(\theta)}, \\
 &= \frac{f(\underline{n} | \theta)\pi(\theta)}{f(\underline{n})},
 \end{aligned}$$

where $f(\underline{n}) = \int_0^\infty f(\underline{n} | \theta)\pi(\theta)d\theta$ is the marginal density of \underline{n} . The marginal

$f(\underline{n})$ can be used to estimate the hyper parameters r, α and β . We can simplify $\pi(\theta | \underline{n})$ to

$$\pi(\theta | \underline{n}) = c^* \exp\left(-\frac{\delta}{\theta} \sum_{j=0}^{k+1} (j-1)n_j\right) \left(1 - \exp(-\frac{\delta}{\theta})\right)^{n-n_{k+1}} \times \theta^{-r} \exp(-\frac{1}{\beta\theta}) \left(1 - \exp(-\frac{\delta}{\theta})\right)^\alpha, \theta > 0,$$

where c^* is a normalizing constant. If $A = \sum_{j=1}^{k+1} (j-1)n_j, \rho = \alpha + n - n_{k+1}$ and

$D = A\delta + \beta^{-1}$, then

$$\pi(\theta | \underline{n}) = c^* \theta^{-r} \left(1 - \exp\left(-\frac{\delta}{\theta}\right)\right)^\rho \exp\left(-\frac{D}{\theta}\right), \quad \theta > 0. \quad (2)$$

Using the binomial series and the transformation $y = 1/\theta$, we simplify the reciprocal of the normalizing constant c^* to

$$\begin{aligned} c^{*-1} &= \int_0^\infty \theta^{-r} \left(1 - \exp\left(-\frac{\delta}{\theta}\right)\right)^\rho \exp\left(-\frac{D}{\theta}\right) d\theta, \\ &= \sum_{i=0}^\infty \binom{\rho}{i} (-1)^i \int_0^\infty \theta^{-r} \exp\left(-\frac{\delta i + D}{\theta}\right) d\theta, \\ &= \sum_{i=0}^\infty \binom{\rho}{i} (-1)^i \int_0^\infty y^{r-2} \exp(-(\delta i + D)y) dy, \\ &= \sum_{i=0}^\infty \binom{\rho}{i} (-1)^i \frac{\Gamma(r-1)}{(\delta i + D)^{r-1}}, \quad r > 1, \end{aligned} \quad (3)$$

where

$$\binom{\alpha}{k} = \frac{\alpha(\alpha-1)(\alpha-2)\dots(\alpha-k+1)}{k!}.$$

Using the equations (2) and (3) we simplify the posterior distribution of θ given \underline{n} to

$$\pi(\theta | \underline{n}) = \frac{\theta^{-r} \left(1 - \exp\left(-\frac{\delta}{\theta}\right)\right)^\rho \exp\left(-\frac{D}{\theta}\right)}{\sum_{i=0}^\infty \binom{\rho}{i} (-1)^i \frac{\Gamma(r-1)}{(\delta i + D)^{r-1}}}, \quad \text{for } \theta > 0.$$

Predictive density of first order statistic $Y_{(1)}$

Let Y_1, Y_2, \dots, Y_m be a future sample from $\exp(\theta)$. The density of $Z = \min \{ Y_1, \dots, Y_m \}$ is given by

$$f(z | \theta) = \frac{m}{\theta} \exp(-mz/\theta) \quad \text{for } z > 0.$$

The predictive density of Z given $\underline{n} = (n_1, n_2, \dots, n_{k+1})$ is

Bayesian Prediction Interval from Grouped Data: Exponential Distribution

$$f(z | \underline{n}) = \int_0^{\infty} f(z | \theta) \pi(\theta | \underline{n}) d\theta$$

Using the Binomial series we get

$$\begin{aligned} f(z | \underline{n}) &= mc^* \int_0^{\infty} \theta^{-r-1} \left(1 - \exp\left(-\frac{\delta}{\theta}\right)\right)^{\rho} \exp\left(-\frac{mz + D}{\theta}\right) d\theta, \\ &= mc^* \int_0^{\infty} \theta^{-r-1} \sum_{i=0}^{\infty} \binom{\rho}{i} \left(-\exp\left(-\frac{mz + D}{\theta}\right)\right)^i d\theta, \\ &= mc^* \sum_{i=0}^{\infty} \binom{\rho}{i} (-1)^i \int_0^{\infty} \theta^{-r-1} \exp\left(-\frac{-i\delta + mz + D}{\theta}\right) d\theta. \end{aligned}$$

Using the transformation $y = \theta^{-1}$ we get

$$\begin{aligned} f(z | \underline{n}) &= mc^* \sum_{i=0}^{\infty} \binom{\rho}{i} (-1)^i \int_0^{\infty} y^{r+1} \exp(-(i\delta + mz + D)y) y^{-2} dy, \\ &= mc^* \sum_{i=0}^{\infty} \binom{\rho}{i} (-1)^i \int_0^{\infty} y^{r-1} \exp(-(i\delta + mz + D)y) dy, \\ &= mc^* \sum_{i=0}^{\infty} \binom{\rho}{i} (-1)^i \frac{\Gamma(r)}{(i\delta + mz + D)^r}, \\ &= m\Gamma(r)c^* \sum_{i=0}^{\infty} \binom{\rho}{i} (-1)^i \frac{1}{(i\delta + mz + D)^r}, \quad r > 1. \end{aligned}$$

A $(1-\alpha)100\%$ prediction interval for Z is an interval $[L, U]$ for which $P\{Z \leq L | \underline{n}\} = \int_0^L f(z | \underline{n}) dz = \alpha / 2$ and

$P\{Z \leq U | \underline{n}\} = \int_0^U f(z | \underline{n}) dz = 1 - \alpha / 2$. To solve these equations for L and M numerical calculations are needed.

Predictive density of future sample mean

Let Y_1, Y_2, \dots, Y_m be a future sample of size m from $\exp(\theta)$. In this section, we are interested in a prediction interval of \bar{Y} , the sample mean of Y_1, Y_2, \dots, Y_m . To end this, let $S = Y_1 + \dots + Y_m$. Then S has a gamma distribution with parameters m and θ , i. e.,

$$f(s | \theta) = \frac{s^{m-1} \exp(-s / \theta)}{\Gamma(m)\theta^m}, \quad \text{for } s > 0.$$

The predictive density of S given \underline{n} is then

$$\begin{aligned} f(s | \theta) &= \int_0^\infty f(s | \theta)\pi(\theta | \underline{n})d\theta, \\ &= c^* \int_0^\infty s^{m-1} \theta^{-m} \exp(-\frac{s}{\theta}) \theta^{-r} \left(1 - \exp(-\frac{\delta}{\theta})\right)^\rho \exp(-\frac{D}{\theta}) d\theta, \\ &= \frac{c^* s^{m-1}}{\Gamma(m)} \int_0^\infty \frac{1}{\theta^{m+r}} \left(1 - \exp(-\frac{\delta}{\theta})\right)^\rho \exp(-\frac{D+s}{\theta}) d\theta. \end{aligned}$$

Using the Binomial series we get

$$\begin{aligned} f(s | \theta) &= \frac{c^* s^{m-1}}{\Gamma(m)} \int_0^\infty \frac{1}{\theta^{m+r}} \left(1 - \exp(-\frac{\delta}{\theta})\right)^\rho \exp(-\frac{D+s}{\theta}) d\theta, \\ &= \frac{c^* s^{m-1}}{\Gamma(m)} \int_0^\infty \theta^{-m-r} \sum_{i=0}^\infty \binom{\rho}{i} (-1)^i \exp(-\frac{\delta i}{\theta}) \exp(-\frac{D+s}{\theta}) d\theta, \\ &= \frac{c^* s^{m-1}}{\Gamma(m)} \sum_{i=0}^\infty (-1)^i \binom{\rho}{i} \int_0^\infty \theta^{-m-r} \exp(-\frac{\delta i + D + s}{\theta}) d\theta. \end{aligned}$$

Using the substitution $y = \theta^{-1}$ we get

$$\begin{aligned} f(s | \underline{n}) &= \frac{c^* s^{m-1}}{\Gamma(m)} \sum_{i=0}^\infty \binom{\rho}{i} (-1)^i \int_0^\infty y^{m+r} \exp(-(i\delta + D + s)y) y^{-2} dy, \\ &= \frac{c^* s^{m-1}}{\Gamma(m)} \sum_{i=0}^\infty \binom{\rho}{i} (-1)^i \int_0^\infty y^{m+r-2} \exp(-(i\delta + D + s)y) dy, \\ &= \frac{c^* s^{m-1}}{\Gamma(m)} \sum_{i=0}^\infty \binom{\rho}{i} (-1)^i \frac{\Gamma(r + m - 1)}{(i\delta + m\zeta + D)^{r+m-1}}. \end{aligned}$$

To find the predictive density of \bar{Y} given \underline{n} we need to use the transformation $\bar{Y} = S / m$. So

Bayesian Prediction Interval from Grouped Data: Exponential Distribution

$$f(s | \underline{n}) = \frac{c^* m^m \bar{y}^{m-1} \Gamma(r + m - 1)}{\Gamma(m)} \sum_{i=0}^{\infty} (-1)^i \binom{\rho}{i} \frac{1}{(\delta i + D + m \bar{y})^{r+m-1}}.$$

To find a $(1 - \alpha)100\%$ prediction interval for \bar{Y} , we need go find L and U such $P\{\bar{Y} \leq L | \underline{n}\} = \int_0^L f(\bar{y} | \underline{n}) d\bar{y} = \alpha / 2$ and $P\{\bar{Y} \leq U | \underline{n}\} = \int_0^U f(\bar{y} | \underline{n}) d\bar{y} = 1 - \alpha / 2$. To find a $(1 - \alpha)100\%$ prediction interval for one future observation from $\exp(\theta)$, we need only to consider the special case $m=1$.

Application to numerical data

In this section, we apply the results to real data. The data consist of life times of 500 batteries measured in hours taken from Cox [7]. The data are given as grouped frequency table in Table 1. It is well-known that the life time data are well fitted by the exponential distribution. The number of intervals of is 7 and $\delta = 50$. So $D=34700$, $A=694$ and $\rho = 485$. By choosing the values $r=1$, $\alpha = 2$, $m=500$ and $\beta = 500$ and then using the Mathematica Software, we obtain the 95% prediction intervals $[.0001, 1.512]$ and $[91.23, 96.87]$ for $Y_{(1)}$ and \bar{Y} , respectively. To support our results, we generated a sample of size 500 from the

Table 1: Life times of 500 batteries

Interval	I_i	n_i
1	[0-50]	208
2	[50-100]	112
3	[100-150]	75
4	[150-200]	40
5	[200-250]	30
6	[250-300]	18
7	[300- ∞]	17

exponential distribution. The sample produced the values $Y_{(1)}=0.0682$ and $\bar{Y}=93.8660$. We see that the prediction intervals contain these values.

Conclusion

In this paper, we found prediction intervals for first order statistic and the sample mean of a future sample from exponential distribution when the given sample is

grouped. The prediction intervals have no closed forms so numerical calculations are needed to obtain them.

Acknowledgements

The authors thank the two referees for their comments which helped us to improve the manuscript.

فترات تنبؤ بيزية من بيانات مجمعة للتوزيع الأسّي

محمد العودات ، خالد العودات و طارق العودات

ملخص

في هذا البحث نجد فترات تنبؤ بيزية لكل من الوسط الحسابي والاحصاء المرتب الاول لعينه مستقبلية مجمعة

أخذت من التوزيع الأسّي عندما تكون البيانات المتوفرة مجمعة. استخدمنا الطرق العددية للحصول على هذه الفترات وقد طبقنا النتائج على بيانات حقيقية.

References

- [1] Wu X. and Perloff J., 'Calculation of Maximum Entropy Densities with [7] Application to Income Distributions', *Journal of Econometrics*, 115(2003)347-354.
- [2] Wu X. and Perloff J., 'Chinas Income Distributions: 1985-2001', *Review of Economic and Statistics*, 87(2005)763-775.
- [3] Lawless J. F., 'A prediction problem concerning samples from the exponential distribution with applications in life testing'. *Technometrics*, 13(1971)725-730.
- [4] Lawless J. F., 'On prediction intervals for samples from the exponential distribution prediction limits for system survival'. *Sankhya, Ser B*, 34(1972)1-12.
- [5] Schervish M. J., theory of Statistics. Springer-Verlag, New York, Inc., (1995).
- [6] Alodat M. T. and Al-Saleh M. F., 'Bayesian estimation using grouped data with application to the exponential distribution.' *Soochow J. Mathematics*, 26(2000)342-357.
- [7] Cox D. R., 'Regression Models and life tables (with discussion)'. *J. R. Statist. Soc. B*, 34(1972)187-220.

Up-Crossing Rates of Particular Non-Gaussian Processes

Moh'd Alodat and Khaled Aludaat *

Received on Oct. 1, 2006

Accepted for publication on March 19, 2007

Abstract

We derived explicit formulas for the rates of up-crossings of some particular smooth non Gaussian processes. We also gave a general formula to find the rate of up-crossings of the output process when the derivative of the input process satisfies some condition.

Keywords: Memoryless, Non-Gaussian process, Up-crossing, Rice Formula

Introduction:

Gaussian random processes are widely used in the literature to model many random responses such as sea elevation level, weather temperature [1]. The distribution of the extreme values of such responses is very important for reliability analysis. For example, the distribution of the largest sea elevation allows us to determine the chance of complete damage of a ship during long-term exploration [2]. However, many random responses in real life are not Gaussian [3]. So non-Gaussian random processes are needed to model such responses [4]. For a high threshold, the extreme value distribution of a process is approximated by the expected number of up-crossings. We define an up-crossing of the threshold x_0 by a differentiable process $X(t)$ as follows. Let $X(t), t \in [0, A]$, be a stationary and differentiable random process with derivative $\dot{X}(t)$. The process $X(t)$ is said to have an up-crossing of the level x_0 at $t_0 \in [0, A]$ if $X(t_0) = x_0$ and $\dot{X}(t_0) > 0$. If $N_{x_0}(A)$ denotes the number of up-crossings of x_0 by $X(t)$ in $[0, A]$, then, for large threshold x_0 , the following approximation is accurate [5]:

$$P\{\sup_{t \in [0, A]} X(t) > x_0\} \approx EN_{x_0}(A),$$

where the mean value of $N_{x_0}(A)$ is given by the following well-known theorem [6]:

Theorem 1 (Rice Formula)

Let $X(t), t \in [0, A]$, be a differentiable stationary process with derivative $\dot{X}(t)$. If $f_{X(0)}(x)$ denotes the density of $X(t)$, then

$$E\{N_{x_0}(A)\} = Af_{X(0)}(x_0)E\{\dot{X}(0)^+ | X(0) = x_0\},$$

where $X^+ = \max\{0, X\}$.

The rate of up-crossings of processes is more interest in many applications of engineering to analysis of systems. For a smooth Gaussian process, the rate of up-crossings has an explicit form. Worsley [7] derived an asymptotic formulas for the expected number of local maxima of χ^2 , T_n and F processes as the crossing level goes to ∞ . It known that the rate of up-crossing of a high level of a process can be approximated by the rate of local maxima above that level. In this paper, we will derive explicit formulas for the rates of up-crossings of the above processes.

The rest of the paper is organized as follows: In Section 2, we give a general formula to derive the up-crossing rate for non-Gaussian processes. In Sections 3, 4, 5 and 6 derived the up-crossing rates for particular non-Gaussian processes. Our conclusions are stated in Section 7.

Through this paper, we will use the following notations: χ_n^2 , t_n and $F_{n, m}$ denote the chi square random variable with n degrees of freedom, the student random variable with n degrees of freedom and the Fisher random variable with n and m degrees of freedom, respectively. For a random variable W , the density function is denoted by $f_W(w)$. The notation $N(a, b)$ means a normal distribution with mean a and variance b . By the notation $W \sim f_W(w)$ we mean that W is a random variable distributed according to the density $f_W(w)$. The rate of up-crossings of a level x by a process $X(t)$ is denoted by $\mu_x^+(x)$. The following result will be used through the next sections:

Theorem 2. If M is a Gaussian random variable with mean μ and variance σ^2 , then

$$E\{M^+\} = \mu \left[1 - \Phi\left(-\frac{\mu}{\sigma}\right) \right] + \frac{\sigma}{\sqrt{2\pi}} \exp\left(-\frac{\mu^2}{2\sigma^2}\right).$$

General Formula

Let $H(t), t \in [0, T]$, be a differentiable and stationary random process and $g: \mathbb{R} \rightarrow \mathbb{R}$ be a

differentiable function with derivative $\dot{g}(x) > 0$ for each x . Consider the process $Q(t) = g(H(t))$. The Jacobian of the transformation $q = g(h)$ is $1/\dot{g}(g^{-1}(q))$. So the density

function of $Q(t)$ is

$$f_{Q(0)}(q) = \frac{f_{H(0)}(g^{-1}(q))}{\dot{g}(g^{-1}(q))}.$$

Assume that, for some function R , $\dot{H}(t)$ can be expressed as follows:

$$\dot{H}(t) = R(H(t), V(t))Z(t),$$

where $H(t) \sim f_{H(0)}(h)$, $V(t) \sim f_{V(0)}(v)$, $Z(t) \sim N(0, \sigma_{Z(0)}^2)$ and all are independent. Note that

$$\dot{Q}(t) | Q(t) = q, V(t) \sim N(0, \dot{g}(g^{-1}(q))^2 R(g^{-1}(q), V(t))^2 \sigma_{Z(0)}^2).$$

The rate of up-crossings of q by $Q(t)$ in $[0, T]$ is given by

$$\begin{aligned} \mu_q^+(q) &= T f_{Q(0)}(q) E\{\dot{Q}(0)^+ | Q(0) = q\}, \\ &= T f_{Q(0)}(q) E\{E\{\dot{Q}(0)^+ | Q(0) = q, V(0)\}\}, \\ &= T f_{Q(0)}(q) \sigma_{Z(0)} \dot{g}(g^{-1}(q)) E\{R(g^{-1}(q), V(0))\}. \end{aligned}$$

Memoryless Process

Let $X(t)$, $t \in [0, T]$ be a stationary and differentiable random process and $g: \mathbb{R} \rightarrow \mathbb{R}$ be a

differentiable function with derivative $\dot{g}(x) > 0$ for each x . The process $Y(t) = g(X(t))$, $t \in [0, T]$ is called a *memoryless* process. In engineering, the process $Y(t)$ is used as the output of a system with an input process $X(t)$. If $X(t)$ is a Gaussian process, then

$$Y(t) = \dot{g}(X(t))\dot{X}(t), \text{ and } \dot{Y}(t) | Y(t) = y \sim N(0, \dot{g}^2(g^{-1}(y))\lambda),$$

where $\lambda = \text{Var}\{\dot{X}(0)\}$. The density function of $Y(t)$ is given by

$$f_{Y(0)}(y) = \frac{\phi(g^{-1}(y))}{\dot{g}(g^{-1}(y))}, \quad g(-\infty) < y < g(\infty),$$

where $\phi(\cdot)$ is the density function of the standard Gaussian random variable. The rate of up-crossings of the level y_0 by $Y(t)$ in $[0, T]$ is given by Rice formula as follows

$$\mu_{Y(0)}^+(y_0) = T f_{Y(0)}(y_0) E\{\dot{Y}(0)^+ | Y(0) = y_0\}.$$

Since the conditional distribution of $\dot{Y}(0)$ given

$Y(0) = y_0$ is $N(0, \dot{g}^2(g^{-1}(y_0))\lambda)$, then using Theorem 2, we simplify the conditional expectation in the last expression to get

$$\begin{aligned} \mu_{Y(0)}^+(y_0) &= T f_{Y(0)}(y_0) \frac{\lambda^{\frac{1}{2}} \dot{g}(g^{-1}(y_0))}{\sqrt{2\pi}}, \\ &= T \frac{\lambda^{\frac{1}{2}} \phi(g^{-1}(y_0))}{\sqrt{2\pi}}, \end{aligned}$$

$$= T\mu_X^\dagger(\varrho^{-1}(y_0)).$$

χ^2 Process

The χ^2 process is defined in Adler [5] as follows: Let $X_i(t)$, $i = 1, 2, \dots, n$, be independent, stationary and differentiable Gaussian processes with zero mean and unit variance. Let $\lambda = Var\{X_1(0)\}$. The process $U(t) = X_1^2(t) + \dots + X_n^2(t)$ is called a *chisquare* process with n degrees of freedom. This implies that $U(0) \sim f_{U(0)}(u)$, where

$$f_{U(0)}(u) = \frac{u^{\frac{n}{2}-1} \exp(-\frac{u}{2})}{\Gamma(\frac{n}{2}) 2^{n/2}}, \text{ for } u > 0.$$

Worsley [7] writes $\dot{U}(t) = 2U^{1/2}(t)Z(t)$, where $Z(t) \sim N(0, \lambda)$, and $Z(t)$ is independent of $U(t)$. It is easy to check that $\dot{U}(t)|U(t) = u_0 \sim N(0, 4u_0\lambda)$. So the rate of up-crossings for the process $U(t)$ is

$$\begin{aligned} \mu_{\dot{U}(0)}^\dagger(u_0) &= T f_{U(0)}(u_0) E\{\dot{U}^+(0)|U(0) = u_0\}, \\ &= T \frac{u_0^{n/2-1} \exp(-\frac{u_0}{2}) 2u_0\lambda^{1/2}}{\Gamma(\frac{n}{2}) 2^{n/2} \sqrt{2\pi}}, \\ &= T \frac{\lambda^{1/2} u_0^{n/2} \exp(-u_0/2)}{\Gamma(\frac{n}{2}) 2^{\frac{n-1}{2}} \sqrt{\pi}}. \end{aligned}$$

T_n Process

Worsley [7] defines the T_n process as follows: Let $X(t), X_i(t), i = 1, 2, \dots, n$, be independent, stationary and differentiable Gaussian processes with zero mean and unit variance. Let $\lambda = Var\{X_1(0)\}$. The T_n process with n degrees of freedom is a process $T_n(t)$ defined by

$$T_n(t) = \frac{X(t)}{\sqrt{(X_1^2(t) + \dots + X_n^2(t))/n}}$$

Note that $T_n(t) \sim t_n$ for each t and

$$f_{T_n(0)}(t) = \frac{\Gamma(\frac{n+1}{2})}{(n\pi)^{1/2} \Gamma(\frac{n}{2})} \frac{1}{\left(1 + \frac{t^2}{n}\right)^{\frac{n+1}{2}}}, \text{ for } -\infty < t < \infty.$$

Worsley [7] writes the derivative of $T_n(t)$ as

$$\hat{T}_n(t) = n^{\frac{1}{2}}(1 + T_n^2(t))S^{-\frac{1}{2}}(t)Z(t),$$

where $S(t) \sim \chi_{(n+1)}^2, Z(t) \sim N(0, 1)$ and $T_n(t) \sim t_n$ all independently. It can be noted that $\hat{T}_n(t)|T_n(t), S(t) \sim N(0, n(1 + T_n^2(t))^2 S^{-1}(t)\lambda)$. So the rate of up-crossings of t_0 by $T_n(t)$ is

$$\mu_{T_n(t_0)}^+ = Tf_{T_n(t_0)}(t_0)E\{\hat{T}_n(0)^+ | T_n(0) = t_0\}.$$

Since $T(t)$ and $S(t)$ are independent, we use the law of iterated expectation, i.e., $E\{Y\} = E\{E\{Y|X\}\}$, to find the expectation $E\{\hat{T}_n(0)^+ | T_n(0) = t_0\}$. So

$$\mu_{T_n(t_0)}^+ = Tf_{T_n(t_0)}(t_0)E\left\{E\{\hat{T}_n(0)^+ | T_n(0) = t_0, S(0)\}\right\}.$$

Using Theorem 2 and the fact that

$$\hat{T}_n(t)|T_n(t), S(t) \sim N(0, n(1 + T_n^2(t))^2 S^{-1}(t)\lambda), \text{ we get}$$

$$\begin{aligned} \mu_{T_n(t_0)}^+ &= Tf_{T_n(t_0)}(t_0)E\left\{\frac{n^{\frac{1}{2}}\left(1 + \frac{t_0^2}{n}\right)S^{-1/2}(0)\lambda^{1/2}}{\sqrt{2\pi}}\right\}, \\ &= Tf_{T_n(t_0)}(t_0)\frac{n^{1/2}\lambda^{1/2}(1 + t_0^2/n)}{\sqrt{2\pi}}E\left\{S^{-\frac{1}{2}}(0)\right\}, \\ &= Tf_{T_n(t_0)}(t_0)\frac{n^{1/2}\lambda^{1/2}(1 + t_0^2/n)}{\sqrt{2\pi}}\frac{\Gamma\left(\frac{n}{2}\right)}{\sqrt{2}\Gamma\left(\frac{n+1}{2}\right)}. \end{aligned}$$

F process

Worsley [7] defines the SF\$ process as follows:

$X_i(t), Y_j(t), i = 1, 2, \dots, n, j = 1, 2, \dots, m$ be independent, stationary and differentiable Gaussian processes with zero mean and unit variance. Let $\lambda = Var(\{\dot{X}(0)\}) = Var(\{\dot{Y}_j(0)\})$. The *F* process is defined by

$$F(t) = \frac{\frac{1}{n}\sum_{i=1}^n X_i^2(t)}{\frac{1}{m}\sum_{j=1}^m Y_j^2(t)}.$$

Note that $F(t) \sim F_{n, m}$ for each t and

$$f_{F(0)}(f) = \frac{\Gamma\left(\frac{n+m}{2}\right)}{\Gamma\left(\frac{n}{2}\right)\Gamma\left(\frac{m}{2}\right)}\left(\frac{n}{m}\right)^{n/2}\frac{f^{\frac{n}{2}-1}}{\left(1 + \frac{n}{m}f\right)^{\frac{n+m}{2}}}$$
 for $f > 0$.

Worsley [7] expresses the derivative of $F(t)$ as follows:

$$\dot{F}(t) = 2 \sqrt{\frac{m}{n}} F(t)^{\frac{1}{2}} \left(1 + \frac{n}{m} F(t)\right) W^{-\frac{1}{2}}(t) Z(t),$$

Where $F(t) \sim F_{n,m}, W(t) \sim \chi_{n+m}^2, Z(t) \sim N(0, \lambda)$ and all are independent. Using the formula (3) and conditioning on $F(t) = f_0, Z(t), W(t)$, we reach to the following

$$\dot{F}(t)|F(t) = f_0, Z(t), W(t) \sim N\left(0, \frac{4m}{n} f_0 \left(1 + \frac{n}{m} f_0\right)^2 W^{-1} \lambda\right).$$

The expected number of up-crossings f_0 by $F(t)$ in $\{0, T\}$ is

$$\begin{aligned} \mu_F^+(f_0) &= T f_{F(0)}(f_0) E\{\dot{F}(t)^+ | F(0) = f_0\}, \\ &= T f_{F(0)}(f_0) E\{E\{\dot{F}(0)^+ | F(0) = f_0, W(0)\}\}, \\ &= T f_{F(0)}(f_0) E\left\{2 \sqrt{\frac{m}{n}} f_0^{\frac{1}{2}} \left(1 + \frac{n}{m} f_0\right) W(0)^{-1/2} \lambda\right\}, \\ &= T f_{F(0)}(f_0) 2 \sqrt{\frac{m}{n}} f_0^{\frac{1}{2}} \left(1 + \frac{n}{m} f_0\right) \lambda E\{W(0)^{-\frac{1}{2}}\}, \\ &= T f_{F(0)}(f_0) 2 \sqrt{\frac{m}{n}} f_0^{\frac{1}{2}} \left(1 + \frac{n}{m} f_0\right) \lambda \frac{\Gamma(\frac{n+m-1}{2})}{\Gamma(\frac{n+m}{2})}. \end{aligned}$$

Conclusion

In this paper, we derived the rates of up-crossing for the Memoryless χ^2, T_n and F processes in closed forms. These formulas give the exact rates for any value of the crossing level, while the expected numbers of local maxima given in Worsley [7] apply only for high levels. The result given in formula 2 is general for all process satisfying the required condition on the derivative of the input process. So the

formula 2 can be applied for any process of the form $Q(t) = g(H(t))$, where g is a differentiable function with $g'(x) > 0$ for each x and $H(t)$ is a χ^2, T_n or F process.

Acknowledgements:

The authors thank the two referees for their comments which improved the manuscript.

معدلات العبور لبعض العمليات غير الجاوسية الخاصة.

محمد العودات و خالد العودات

ملخص

قمنا باشتقاق صيغ واضحة لمعدلات نقاط العبور لبعض العمليات الغير جاوسيه الخاصة. وكذلك اعطينا صيغة عامة لمعدل العبور لعملية المخرجات عندما تحقق المشتقة بعض الشروط.

References:

- [1] Cherneva Z., Petrova P., Andreeva C. and Soares C. G. , ' Probability distribution of peaks, troughs and height of wind waves measured in the black sea coastal zone'. *Coastal Engineering*, 52(2005)599-615.
- [2] Rychlik I. , 'On the narrow-band approximation for expected fatigue damage'. *Probabilistic Engineering Mechanics*, 8(1993)1-4.
- [3] Grigoiu, M., 'Applied non-Gaussian processes'. Englewood Cliffs, NJ:prentice Hall, (1995).
- [4] Leira B. J., 'Extremes of Gaussian and non-Gaussian vector processes: a geometric Approach'. *Structural Safety*, 25(2003)401-422.
- [5] Adler R., 'The geometry of Random fields'. John Wiley and Sons, New York, (1981).
- [6] Leadbetter M. R. and Spanilo G. V., 'On statistics at level crossings by a stationary Process'. *Statistica Neerlandica*, 56(2002)152-164.
- [7] Worsley K. J., 'Local maxima and the expected Euler characterstic of excursion sets $X^{\geq u}$, $f^{\geq u}$, and \mathbb{E} fields'. *Advances in Applied Probability*, 26(1994)13-42.

Analysis of Rainfall in Southern Area of Jordan

Suleiman Tashtoush *

Received on Aug. 6, 2007

Accepted for publication on Oct. 8, 2008

Abstract

There are several methods to estimate rainfall which interpolation is important in many natural resources and agricultural studies. In this research, three Time Series models were used to estimate monthly rainfall in the southern area of Jordan. Regression, Box-Jenkins (ARIMA), and exponential smoothing models. The result of the study shows that exponential smoothing models perform better than Regression models. Investigation for accuracy and efficiency of various forecasting models used to forecast the rainfall in the studied area.

Keywords: Rainfall, Forecasting, Trend, Time series, Box-Jenkins models, Regression models, Exponential smoothing, Durbin-Watson statistics.

Introduction

The investigated area is considered a very arid to semi arid area. It is a Mediterranean type of climate. The rainfall over the study area starts in October or November and lasts till May. The bulk of annual rainfall is concentrated in the winter months from December to March is higher in the northern and central regions of the country (about 80%) than it is in the south and eastern regions when the contribution of Kamasin depressions to the annual rainfall becomes considerable. Early rainfall forms more than 13% of annual rainfall in the northern and central regions, and ranges between 14-19% in the south and east. Late rainfall forms more than 5% of annual rainfall in the northern and central regions, but ranges between 6-13% in the southern and eastern regions, with no precipitation occurring from June to September [1]. The average annual rainfall along the highlands is about 300 mm/year, while it is less than 50 mm/year in the desert region. The mean number of snowy days is 10 days per year in the highlands with maximum-recorded amount of snow of 75cm. The average maximum temperature is between 27.2°C to 34°C, and the minimum ranges between -1.2°C to 3.9°C, the yearly evaporation in the study area is the highest in Maan and the lowest in Shoubak area. The relative humidity ranges between 38% to 76%. The semi-arid areas are represented by Hasa area (900m a.s.l) with average sunshine of 9.9 hrs/day, towards the highland areas, Shoubak area (1365m.a.s.l) with an average sunshine of 9 hrs/day [2]. Rainfall is an important task for geographers, meteorologists, hydrologists and agricultural meteorologists who are interested in improving the analysis of water resources and knowing aerial distribution of rainfall amount over the region. Table (1) shows the

Tashtoush

period of study, mean, standard deviation, coefficient of determination, and Durbin-Watson test of independence for each station.

Table (1) Descriptive statistics for winter months, each station for the study period

Station	From	To	Elevation	Min	Max	Mean	Std	R ²	R ² -adj	Durbin-Watson
Mutah	Oct 1985	May 2001	1175	0	277	40.5487	52.2123	.452	.418	1.717
Rabba	Oct 1978	May 2001	920	0	246	44.0766	51.6732	.466	.443	1.864
Hasa	Oct 1979	May 2000	900	0	56	10.8148	11.6155	.461	.438	2.070
Maan	Oct 1978	May 2000	Desert	0	67.6	6.5636	11.037	.146	.110	1.901
Shoubak	Oct 1978	May 2001	1365	0	279.6	35.7489	46.0648	.423	.399	1.850
Tafilah	Oct 1978	May 2001	1200	0	174.6	26.8647	35.0445	.424	.400	1.925

Time series analysis and modeling commonly used in water resources. In this study an attempt has been made to investigate the appropriateness of various classes of forecasting model regression and time series analysis applied to monthly rainfall records in six stations of the south area of Jordan.

Researchers have used this approach for many different scientific and technical applications. Mc Kerchar and Delleur [3] used an ARIMA process to achieve stochastic modeling of monthly flows. McLeod *et al.* [4] applied the ARIMA approach to average annual stream flows, annual sunspot number series and monthly airline passenger data and suggested a different ARIMA model for each data set. Fernando and Jayawardena [5] used various ARIMA models in forecasting monthly rainfall records. Venama *et al.* [6] investigated climate change in the Senegal River basin via this approach. Chaloulakou *et al.* [7] forecasted daily maximum 1-h ozone concentrations, whereas Ahmad *et al.* [8] analyzed water quality data using an ARIMA model. Yurekli *et al.* [9] analyzed the residuals from the ARIMA models fitted to monthly streamflow data for three gauging stations located on Çekerek stream watershed by alternatives methods, while Sadhuram and Ramana Murthy [10] used simple multiple regression model with two parameters for long range forecasting of Indian summer Monsoon rainfall.

Forecasting Models

Regression

Regression models utilize a regression equation to establish a casual relationship between the dependent variables and independent variable(s). There are disadvantages in using regression models. Geurts and Kelly [20] noticed that, first, the future values of the casual variables have to be predicted. Second, even when a lagged causal variable in prediction for one period ahead, the reported value is often preliminary figure that is later revised. Both of these factors can cause data to be an accurate and the model to be weak in its ability to forecast. Third, the continual need to gather data which makes these models expensive. Farther more, the relationships can change over time. Lastly, the relationship between the dependent and independent variables may be a spurious one, so it is necessary to update and redesign the model. Since a trend was detected in the data; a

Analysis of Rainfall in Southern Area of Jordan

simple regression model is fitted to the data with eleven dummy variables. These dummy variables are used to capture the seasonality of individual months.

The fitted regression model is shown in figure (1) with this model the R squared, the Adj. R squared and the Durbin-Watson Statistics is shown in Table (1), Table (2) contains the coefficients of the regression models and Table (3) contains the ANOVA table of the regression model.

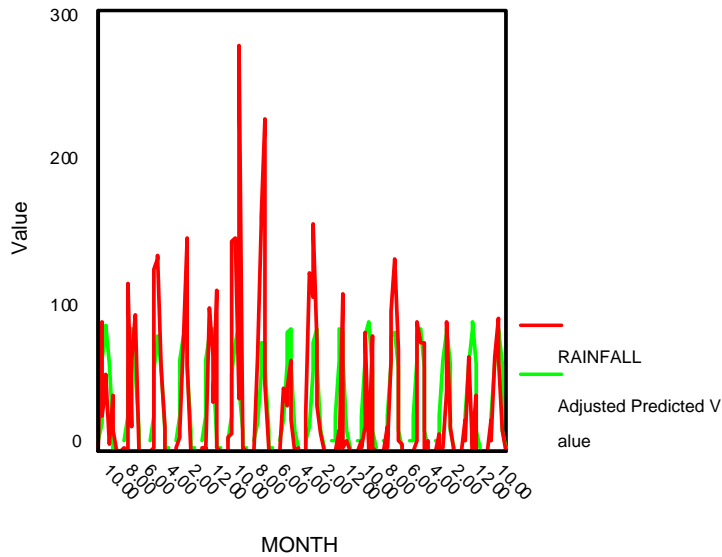


Figure 1. 1: Mutah station

Tashtoush

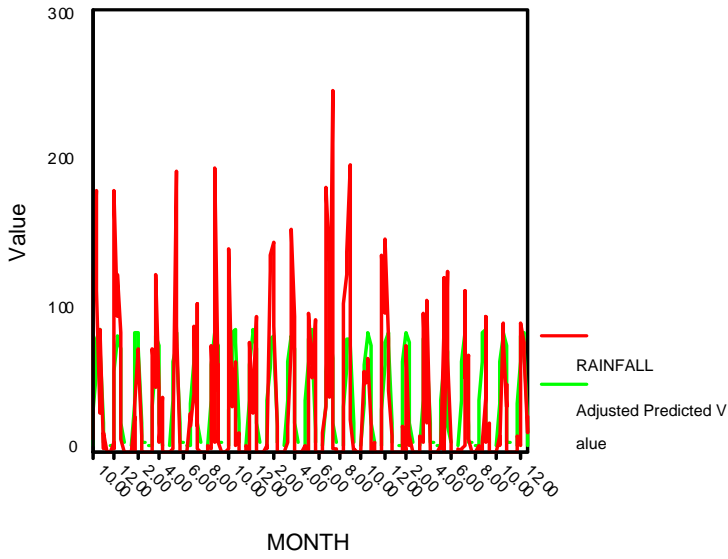


Figure 1.2: Rabba station

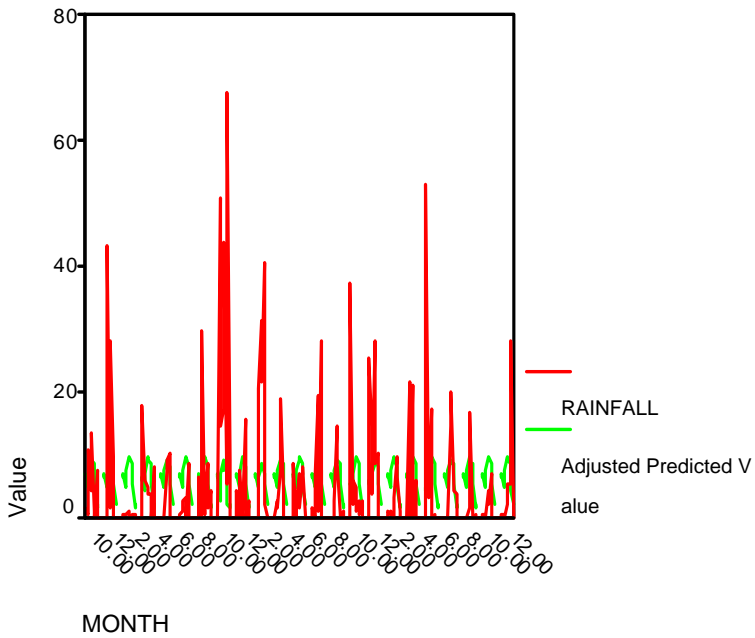


Figure 1.3: Hasa station

Analysis of Rainfall in Southern Area of Jordan

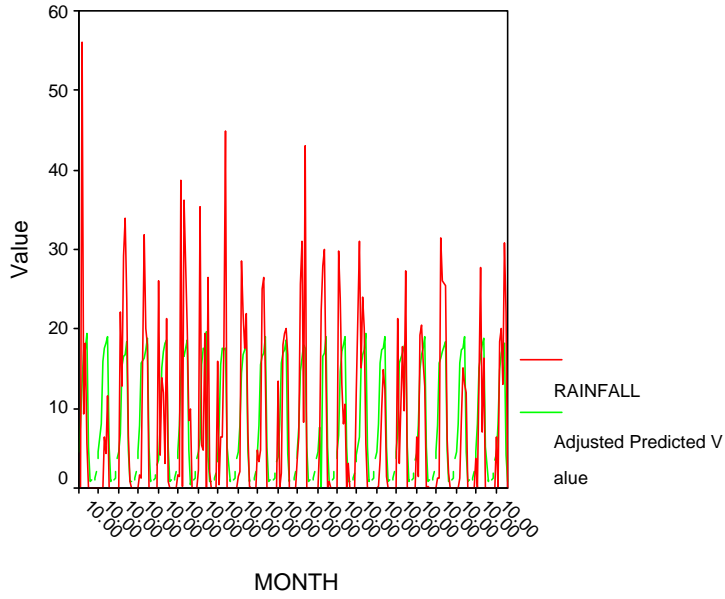


Figure 1. 4: Maan station

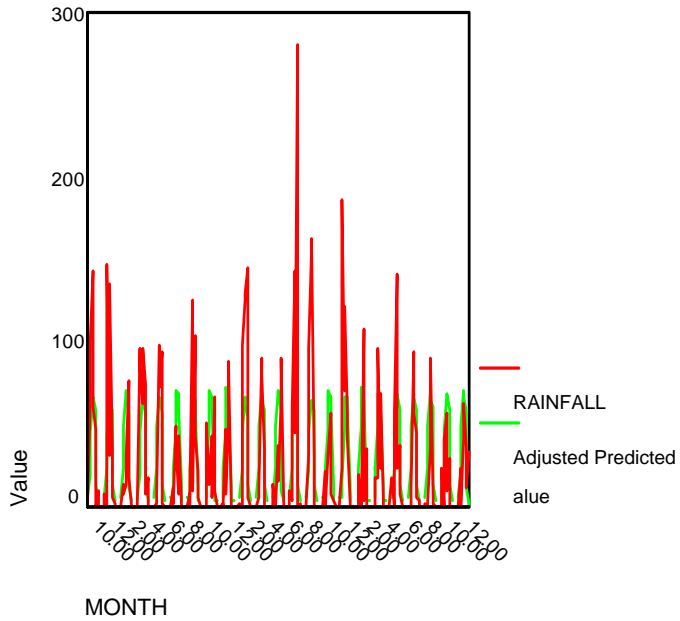


Figure 1. 5: Shoubak station

Tashtoush

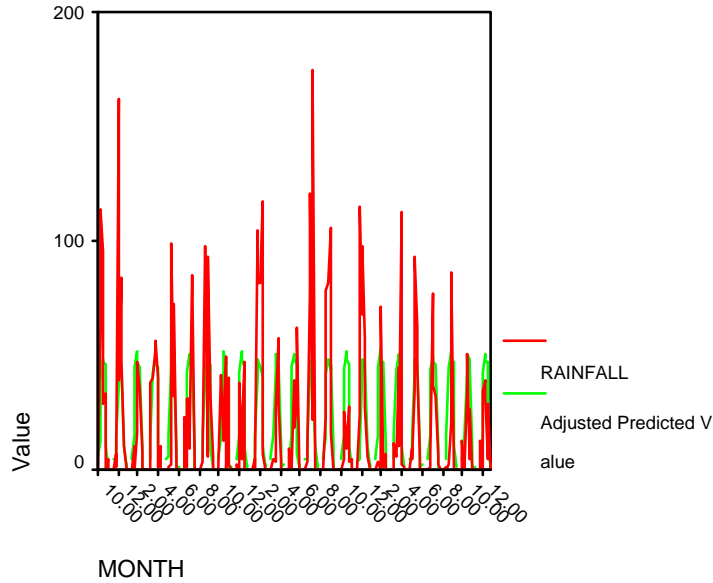


Figure 1. 6: Tafilah station

Table (2) Regression Model

Mutah					Rabba				
Variables	Coefficient	Std Error	t- Stat	Sig	Variables	Coefficient	Std Error	t- Stat	Sig
Constant	78.844	8.967	8.793	.000	Constant	78.161	7.347	10.638	.000
Q1	-20.669	12.681	-1.583	.115	Q1	-18.553	16.390	-1.786	.075
Q2	-56.350	12.681	-4.444	.000	Q2	-45.326	10.390	-4.362	.000
Q3	-71.256	12.891	-6.090	.000	Q3	-73.117	10.390	-7.037	.000
Q4	-78.844	12.891	-6.116	.000	Q4	-78.161	10.508	-7.438	.000
Q5	-78.844	12.891	-6.116	.000	Q5	-78.161	10.508	-7.438	.000
Q6	-78.844	12.891	-6.116	.000	Q6	-78.161	10.508	-7.438	.000
Q7	-78.844	12.891	-6.116	.000	Q7	-78.161	10.508	-7.438	.000
Q8	-77.031	12.681	-6.074	.000	Q8	-71.983	10.390	-5.928	.000
Q9	-64.525	12.681	-5.088	.000	Q9	-59.248	10.390	-5.702	.000
Q10	-21.612	12.861	-1.704	.090	Q10	-7.561	10.390	-.728	.467
Q11	4.244	12.861	-0.335	.738	Q11	3.117	10.390	.300	.764

Analysis of Rainfall in Southern Area of Jordan

Hasa					Maan				
Variables	Coefficient	Std Error	t- Stat	Sig	Variables	Coefficient	Std Error	t- Stat	Sig
Constant	17.006	1.693	10.042	.000	Constant	9.326	1.884	4.951	.000
Q1	-20.669	2.370	-.794	.428	Q1	-2.183	2.664	-.819	.418
Q2	-56.350	2.420	-3.880	.000	Q2	-4.770	2.664	-1.790	.075
Q3	-71.256	2.420	-5.190	.000	Q3	-2.400	2.664	-.980	.368
Q4	-78.844	2.449	-6.940	.000	Q4	-9.326	2.694	-3.460	.001
Q5	-78.844	2.370	-6.710	.000	Q5	-9.326	2.694	-3.460	.001
Q6	-78.844	2.449	-6.940	.000	Q6	-9.326	2.694	-3.460	.001
Q7	-78.844	2.449	-6.940	.000	Q7	-9.326	2.694	-3.460	.001
Q8	-77.031	2.420	-6.670	.000	Q8	-7.513	2.664	-2.820	.005
Q9	-64.525	2.420	-5.000	.000	Q9	-4.135	2.664	-1.550	.122
Q10	-21.612	2.420	.719	.473	Q10	-0.961	2.664	-.360	.719
Q11	4.244	2.420	.198	.846	Q11	-0.139	2.664	-.052	.958

Shoubak					Tafilah				
Variables	Coefficient	Std Error	t- Stat	Sig	Variables	Coefficient	Std Error	t- Stat	Sig
Constant	68.943	6.693	10.301	.000	Constant	50.083	5.077	9.866	.000
Q1	-21.796	9.465	-2.307	.022	Q1	-7.609	7.179	-1.060	.290
Q2	-46.543	9.465	-4.913	.000	Q2	-56.350	7.179	-4.942	.000
Q3	-62.439	9.465	-6.597	.000	Q3	-35.478	7.179	-6.277	.000
Q4	-68.943	9.572	-7.203	.000	Q4	-45.065	7.179	-6.898	.000
Q5	-68.943	9.572	-7.203	.000	Q5	-50.083	7.260	-6.898	.000
Q6	-68.943	9.572	-7.203	.000	Q6	-50.083	7.260	-6.898	.000
Q7	-68.943	9.572	-7.203	.000	Q7	-50.083	7.260	-6.898	.000
Q8	-64.987	9.465	-6.866	.000	Q8	-50.083	7.179	-6.791	.000
Q9	-56.252	9.465	-5.943	.000	Q9	-48.752	7.179	-5.609	.000
Q10	-10.839	9.465	-1.450	.253	Q10	-40.265	7.179	-7.12	.477
Q11	-2.700	9.465	-0.285	.776	Q11	-3.461	7.179	-0.482	.638

Tashtoush

Table (3) Analysis of Variance Regression Model

Station	SS -Reg	df	SS-Error	df	MS-Reg	MS-Error	F	Sig
Mutah	186867.8	11	226424.3	176	16987.978	1286.502	13.205	.00
Rabba	281475.1	11	322807.3	260	25588.643	1241.567	20.610	.00
Hasa	13965.534	11	16295.994	248	1269.594	65.710	19.321	.00
Maan	3638.809	11	21217.864	260	330.801	81.607	4.054	.00
Shoubak	196536.6	11	267861	260	17866.967	1030.236	17.343	.00
Tafilah	113597.8	11	154110.3	260	10327.07	592.732	17.423	.00

Durbin-Watson statistics shows a positive autocorrelation which means that the regression model violating the regression assumptions of independency of error terms, since it is correlated over the time.

Time Series Analysis

Autoregressive integrated moving average (ARIMA)

One of the most important and highly popularized time series models is the Box-Jenkins approach, commonly known as autoregressive integrated moving average (ARIMA) processes for modeling time series.

In order to analyze the monthly time series from the 6 stations, an ARIMA modeling approach was used in this study. A seasonal ARIMA model denoted as ARIMA (p,d,q)*(P,D,Q) that is a combination of past values and past residuals can be written as follows [8,11,12].

$$\emptyset(B)\Phi F(Bs)(w_i - \mu) = C + \theta(B)\Theta(Bs) a_i \tag{1}$$

$$w_i = (1 - B)^d(1 - B^s)^D x_i \tag{2}$$

$$\emptyset(B) = 1 - \emptyset_1 B - \emptyset_2 B^2 - \dots - \emptyset_p B^p \tag{3}$$

$$\theta(B) = 1 - \theta_1 B - \theta_2 B^2 - \dots - \theta_q B^q \tag{4}$$

$$\Phi(B^s) = 1 - \Phi_1 B^s - \Phi_2 B^{2s} - \dots - \Phi_P B^{Ps} \tag{5}$$

$$\Theta(B^s) = 1 - \Theta_1 B^s - \Theta_2 B^{2s} - \dots - \Theta_Q B^{Qs} \tag{6}$$

There are three stages for fitting a seasonal ARIMA model to a given time series [13,14]:

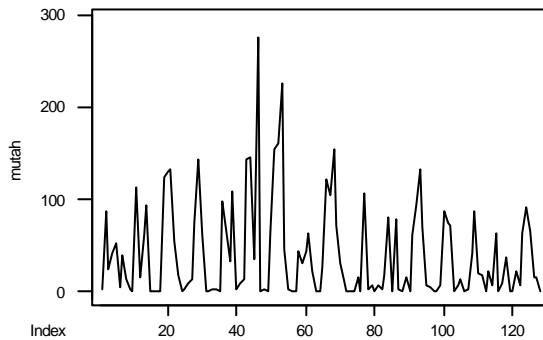
- 1) Model identification.
- 2) Parameter estimation [15].
- 3) Diagnostic checking [16,17,18].

By plotting original series, stochastic trends (nonstationarity) in the mean and variance may be revealed [13]. To determine the possible persistence structure in the data set, an autocorrelation function (ACF) and partial autocorrelation function (PACF)

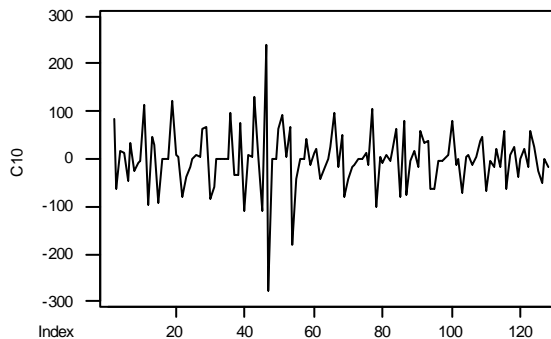
Analysis of Rainfall in Southern Area of Jordan

should be used [11]. The ACF and PACF give information about the non-seasonal and seasonal AR and MA operators for a time series. The ACF provides significant information about the correlation between pairs of observations that are k time units apart, called lag. The identification of the appropriate parametric time series model depends on the shape of the ACF [19].

Mutah rainfall time series analysis



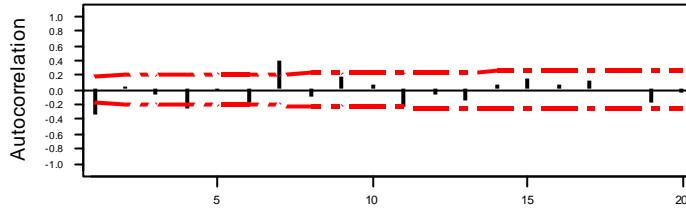
Taking the first difference makes data stationary in the mean and the variance. The time series plot for the first difference of the Mutah data is as follows:



In this case the data are stationary, ACF plot and PACF plot gives an indication about the best fitting model for this data.

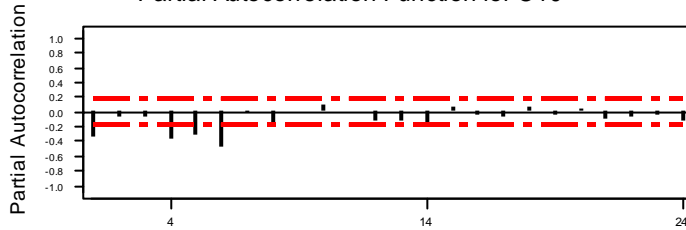
Tashtoush

Autocorrelation Function for C10



Lag	Corr	T	LBQ	Lag	Corr	T	LBQ	Lag	Corr	T	LBQ
1	-0.34	-3.83	15.01	8	-0.08	-0.71	51.96	15	0.14	1.14	72.10
2	0.05	0.51	15.34	9	0.18	1.55	56.61	16	0.07	0.56	72.86
3	-0.06	-0.62	15.83	10	0.06	0.52	57.17	17	0.11	0.89	74.79
4	-0.27	-2.71	25.38	11	-0.23	-1.90	64.64	18	0.00	0.01	74.79
5	-0.00	-0.04	25.38	12	-0.08	-0.64	65.53	19	-0.17	-1.32	79.15
6	-0.19	-1.78	30.06	13	-0.15	-1.18	68.64	20	-0.03	-0.26	79.33
7	0.39	3.66	51.01	14	0.06	0.45	69.09				

Partial Autocorrelation Function for C10



Lag	PAC	T	Lag	PAC	T	Lag	PAC	T	Lag	PAC	T
1	-0.34	-3.83	8	-0.14	-1.58	15	0.06	0.64	22	-0.06	-0.70
2	-0.07	-0.83	9	0.00	0.03	16	-0.05	-0.56	23	-0.03	-0.39
3	-0.08	-0.87	10	0.09	1.05	17	-0.06	-0.70	24	-0.12	-1.31
4	-0.36	-4.01	11	0.01	0.13	18	0.07	0.74			
5	-0.30	-3.39	12	-0.13	-1.47	19	-0.05	-0.61			
6	-0.48	-5.45	13	-0.12	-1.32	20	0.05	0.52			
7	-0.01	-0.06	14	-0.19	-2.17	21	-0.10	-1.13			

Based on these two plots the suggested model is $ARIMA(0,1,1)(3,2,3)_8$

Analysis of Rainfall in Southern Area of Jordan

ARIMA Model: Mutah

ARIMA model for Mutah

Final Estimates of Parameters

Type	Coef	SE Coef	T	P
SAR 8	-1.2027	0.1046	-11.50	0.000
SAR 16	-0.5313	0.1523	-3.49	0.001
SAR 24	-0.3376	0.0908	-3.72	0.000
MA 1	0.9405	0.0289	32.49	0.000
SMA 8	0.8000	0.0981	8.15	0.000
SMA 16	0.9327	0.1282	7.27	0.000
SMA 24	-0.7823	0.1002	-7.80	0.000

Differencing: 1 regular, 2 seasonal of order 8

Number of observations: Original series 184, after differencing 167

Residuals: SS = 269171 (backforecasts excluded)

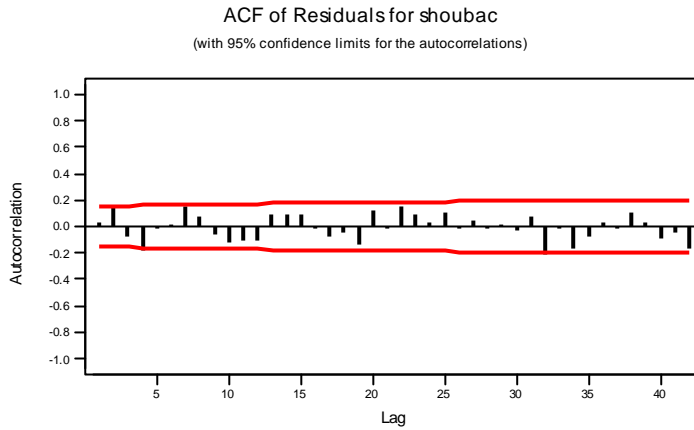
MS = 1682 DF = 160

Modified Box-Pierce (Ljung-Box) Chi-Square statistic

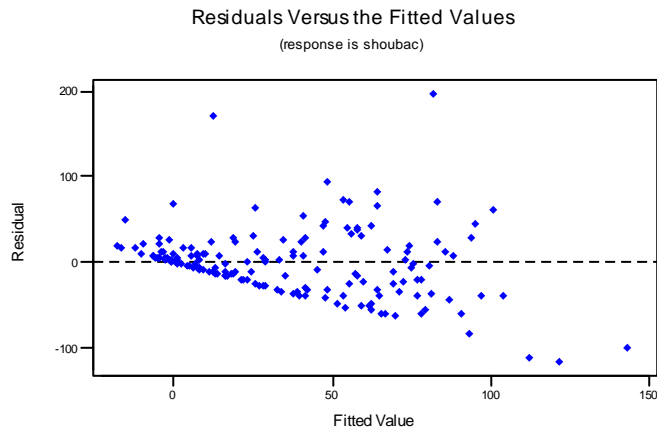
Lag	12	24	36	48
Chi-Square	24.7	44.1	64.3	85.1
DF	5	17	29	41
P-Value	0.000	0.000	0.000	0.000

Since the values of ACF residuals are between the limits as in the following figure, the suggested model seems to fit this data well.

Tashtoush

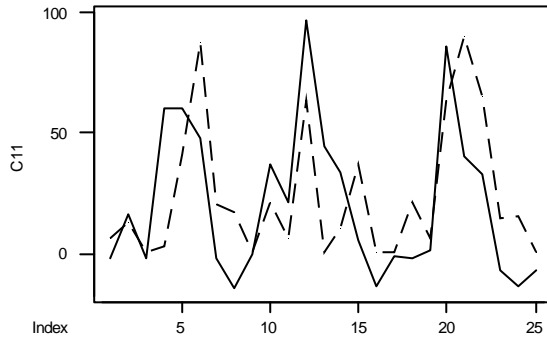


It is noticed from plotting the residuals with the fitted values for the last 25 observations that they are almost around zero except for some values.



By plotting the Actual values with the forecasted ones for the last 25 observations, it is clear that the model is almost well fitted for Mutah data.

Analysis of Rainfall in Southern Area of Jordan



The same analysis for the other stations has been done and the results are given below:

Rabba rainfall time series analysis

Based on similar analysis the suggested model is ARIMA(2,1,0)(2,2,1)₈

ARIMA Model: Rabba

Final Estimates of Parameters

Type	Coef	SE Coef	T	P
AR 1	-0.7684	0.0730	-10.52	0.000
AR 2	-0.3869	0.0729	-5.31	0.000
SAR 8	-0.5527	0.0770	-7.18	0.000
SAR 16	-0.3059	0.0760	-4.02	0.000
SMA 8	0.9444	0.0513	18.41	0.000

Differencing: 1 regular, 2 seasonal of order 8

Number of observations: Original series 184, after differencing 167

Residuals: SS = 518970 (backforecasts excluded)

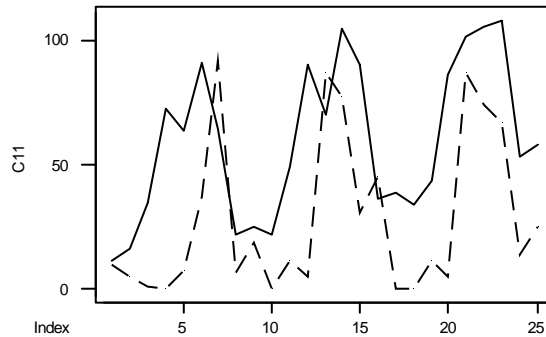
MS = 3204 DF = 162

Modified Box-Pierce (Ljung-Box) Chi-Square statistic

Lag	12	24	36	48
Chi-Square	20.3	38.7	44.2	61.1
DF	7	19	31	43
P-Value	0.005	0.005	0.059	0.036

Tashtoush

By plotting the Actual values with the forecasted ones for the last 25 observations, it is clear that the model is almost well fitted for Rabba data.



Hasa rainfall time series analysis

Based on similar analysis the suggested model is ARIMA(0,1,1)(1,1,1)4

ARIMA Model: Hasa

Final Estimates of Parameters

Type	Coef	SE Coef	T	P
SAR 4	-0.5100	0.0676	-7.54	0.000
MA 1	0.9457	0.0217	43.57	0.000
SMA 4	0.9027	0.0511	17.67	0.000

Differencing: 1 regular, 1 seasonal of order 4

Number of observations: Original series 176, after differencing 171

Residuals: SS = 18309.9 (backforecasts excluded)

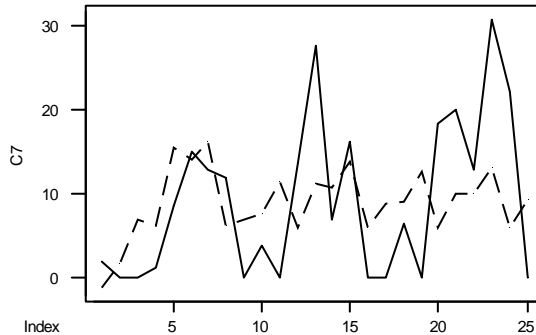
MS = 109.0 DF = 168

Modified Box-Pierce (Ljung-Box) Chi-Square statistic

Lag	12	24	36	48
Chi-Square	13.5	32.4	51.8	62.7
DF	9	21	33	45
P-Value	0.139	0.054	0.020	0.041

Analysis of Rainfall in Southern Area of Jordan

By plotting the Actual values with the forecasted ones for the last 25 observations, it is clear that the model is almost well fitted for Hasa data.



Maan rainfall time series analysis

Based on similar analysis the suggested model is ARIMA(2,1,0)(1,1,1)₄

ARIMA Model: Maan

Final Estimates of Parameters

Type	Coef	SE Coef	T	P
AR 1	-0.7591	0.0727	-10.45	0.000
AR 2	-0.2951	0.0739	-3.99	0.000
SAR 4	-0.2334	0.0781	-2.99	0.003
SMA 4	0.9703	0.0306	31.75	0.000

Differencing: 1 regular, 1 seasonal of order 4

Number of observations: Original series 184, after differencing 179

Residuals: SS = 24268.6 (backforecasts excluded)

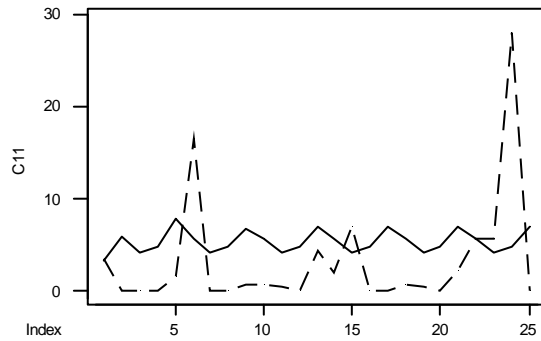
MS = 138.7 DF = 175

Modified Box-Pierce (Ljung-Box) Chi-Square statistic

Lag	12	24	36	48
Chi-Square	17.8	22.6	41.0	51.3
DF	8	20	32	44
P-Value	0.023	0.310	0.133	0.211

Tashtoush

By plotting the Actual values with the forecasted ones for the last 25 observations, it is clear that the model is almost well fitted for Maan data.



Shoubak rainfall time series analysis

Based on similar analysis the suggested model is ARIMA(0,1,1)(2,0,1)₄

ARIMA Model: Shoubak

Final Estimates of Parameters

Type	Coef	SE Coef	T	P
AR 1	-0.7092	0.0739	-9.60	0.000
AR 2	-0.2088	0.0735	-2.84	0.005
SAR 4	-1.1610	0.0800	-14.52	0.000
SAR 8	-0.1608	0.0790	-2.04	0.043
SMA 4	-0.9746	0.0355	-27.49	0.000

Differencing: 1 regular difference

Number of observations: Original series 184, after differencing 183

Residuals: SS = 322526 (backforecasts excluded)

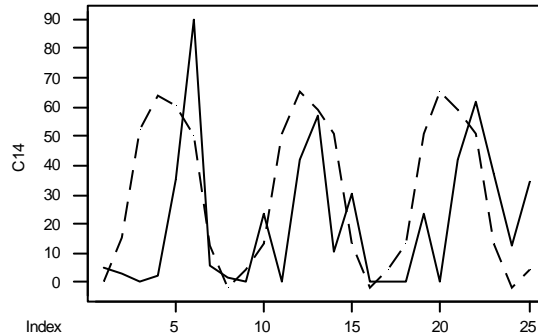
MS = 1812 DF = 178

Modified Box-Pierce (Ljung-Box) Chi-Square statistic

Lag	12	24	36	48
Chi-Square	23.2	44.0	54.3	68.5
DF	7	19	31	43
P-Value	0.002	0.001	0.006	0.008

Analysis of Rainfall in Southern Area of Jordan

By plotting the Actual values with the forecasted ones for the last 25 observations, it is clear that the model is almost well fitted for Shoubak data.



Tafelah rainfall time series analysis

Based on similar analysis the suggested model is **ARIMA(1,1,1)(3,3,3)4**

ARIMA Model: Tafelah

ARIMA model for Tafelah

Final Estimates of Parameters

Type	Coef	SE Coef	T	P
AR 1	-0.2621	0.1073	-2.44	0.016
SAR 4	-1.7317	0.0747	-23.17	0.000
SAR 8	-1.2634	0.1261	-10.02	0.000
SAR 12	-0.5303	0.0711	-7.46	0.000
MA 1	0.5745	0.0912	6.30	0.000
SMA 4	0.9302	0.0428	21.71	0.000
SMA 8	0.9247	0.0686	13.48	0.000
SMA 12	-0.8939	0.0510	-17.52	0.000

Differencing: 1 regular, 3 seasonal of order 4

Number of observations: Original series 184, after differencing 171

Residuals: SS = 233790 (backforecasts excluded)

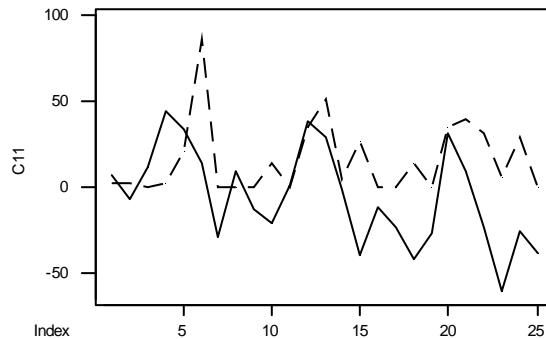
MS = 1434 DF = 163

Tashtoush

Modified Box-Pierce (Ljung-Box) Chi-Square statistic

Lag	12	24	36	48
Chi-Square	27.2	55.1	73.1	87.6
DF	4	16	28	40
P-Value	0.000	0.000	0.000	0.000

By plotting the Actual values with the forecasted ones for the last 25 observations, it is clear that the model is almost well fitted for Tafelah data.



Exponential smoothing

This is a very popular scheme to produce a smoothed Time Series. Exponential smoothing assigns exponentially decreasing weights as the observation get older. In exponential smoothing there is one or more smoothing parameters to be determined (or estimated) and these choices determine the weights assigned to the observations.

Single exponential smoothing

The model for this smoothing scheme is:

$$F_t = \alpha Y_t + (1 - \alpha)F_{t-1} \quad , \quad 0 < \alpha \leq 1 \quad t \geq 1 \quad (7)$$

Where:

F_{t-1} = forecast value for period t-1, y_t = actual value for period t,

F_t = forecast value for period t. α = smoothing constant.

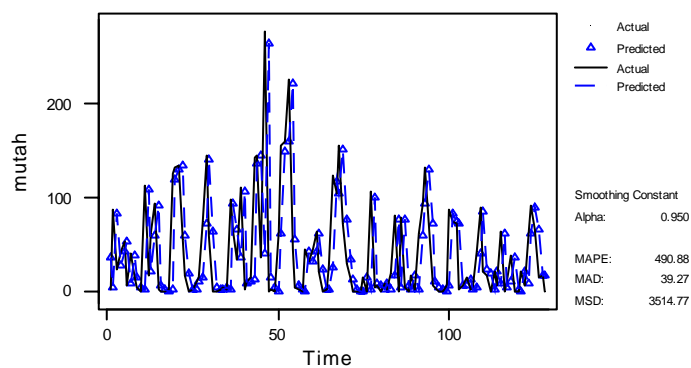
The forecast value is calculated using equation (7).

Analysis of Rainfall in Southern Area of Jordan

Table (4) The model parameters and the accuracy measures

Station	Alpha	Accuracy Measures		
		MAPE	MAD	MSD
Mutah	0.95	490.880	39.27	3514.77
Rabba	0.95	570.860	42.36	3769.46
Hasa	0.70	296.509	9.950	185.906
Maan	0.60	317.608	7.972	158.235
Shoubak	0.95	520.290	36.96	3040.74
Tafilah	0.80	643.530	27.82	1643.28

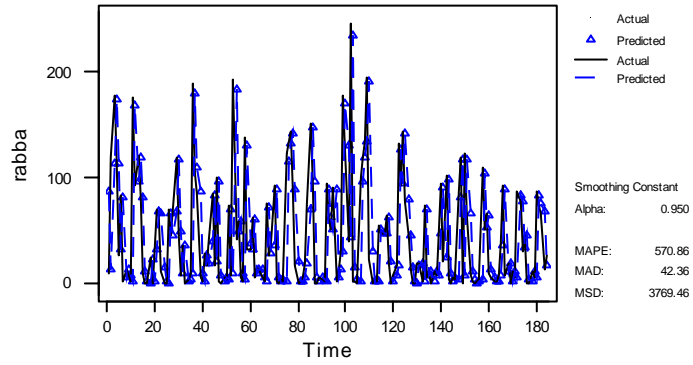
Single Exponential Smoothing



1) For Mutah station

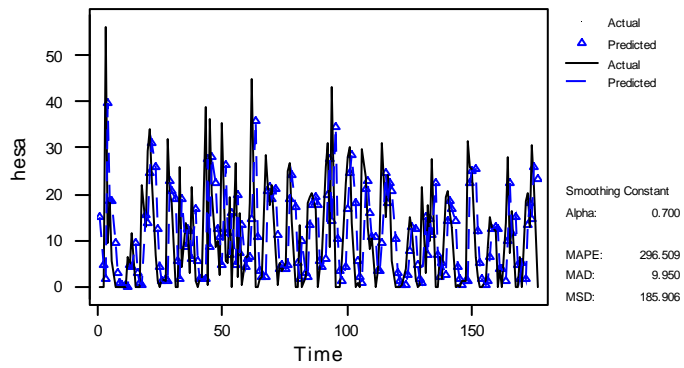
Tashtoush

Single Exponential Smoothing



2) For Rabba station

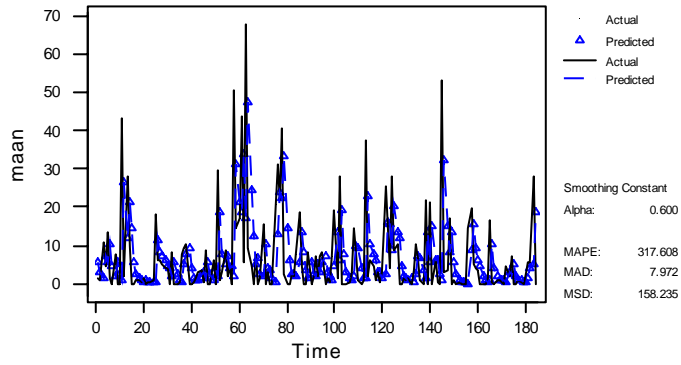
Single Exponential Smoothing



3) For Hasa station

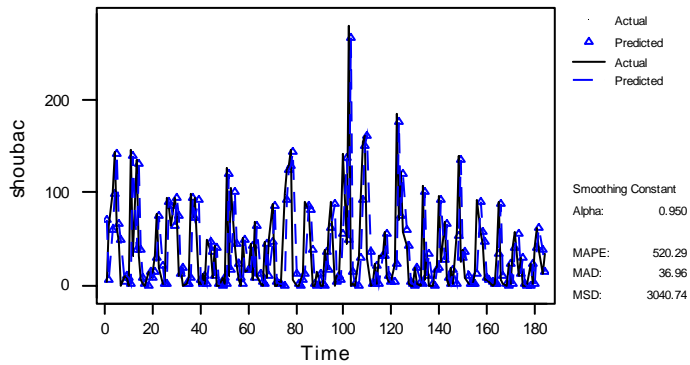
Analysis of Rainfall in Southern Area of Jordan

Single Exponential Smoothing



4) For Maan station

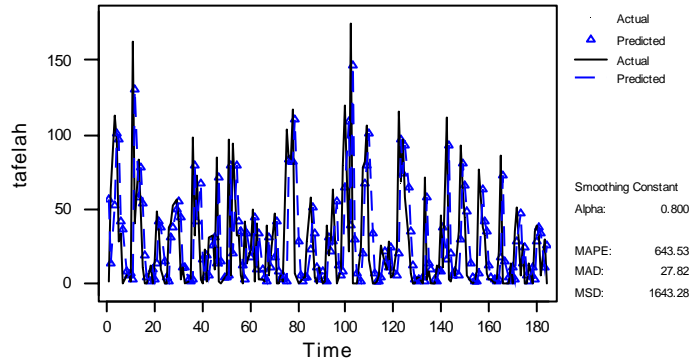
Single Exponential Smoothing



5) For Shoubak station

Tashtoush

Single Exponential Smoothing



6) For Tafela station

Double exponential smoothing

The model for this smoothing scheme is:

$$\begin{aligned}
 C_t &= \alpha Y_t + (1 - \alpha)(C_{t-1} - T_{t-1}) \quad , \quad 0 < \alpha \leq 1 \quad t \geq 1 \\
 T_t &= \gamma(C_t - C_{t-1}) + (1 - \gamma)T_{t-1}, \quad 0 < \gamma \leq 1 \\
 F_{t+1} &= F_t + T_t
 \end{aligned}
 \tag{8}$$

Where:

F_{t+1} = forecast value for period t+1, y_t = actual value for period t,

F_t = forecast value for period t. α = process smoothing constant,

γ = trend-smoothing constant, C_t = smoothing constant- process value for period t,

T_t = smoothing trend value for period t (forecasted value for period t), t= current time period.

The forecast value is calculated using equations (8).

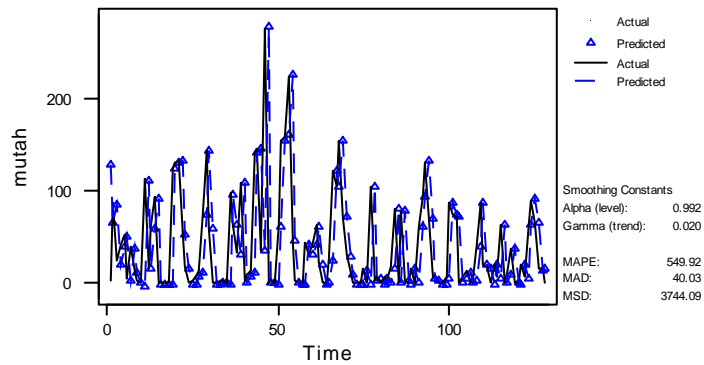
Table (5) The model parameters and the accuracy measures

Station	Smoothing Constants		Accuracy Measures		
	Alpha(level)	Gamma(trend)	MAPE	MAD	MSD
Mutah	0.991772	0.019683	549.920	40.030	3744.090
Rabba	0.986350	0.008190	597.990	44.870	4246.700

Analysis of Rainfall in Southern Area of Jordan

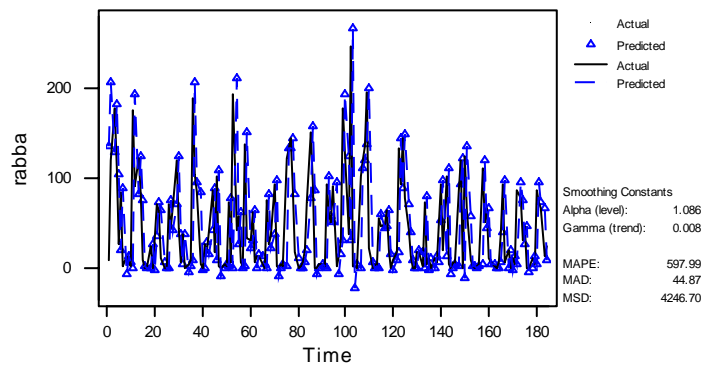
Hasa	0.991366	0.016907	328.275	10.746	238.995
Maan	0.864202	0.000157	354.349	8.475	198.207
Shoubak	0.997950	0.013420	491.950	37.280	3197.230
Tafilah	0.975619	0.015524	632.510	28.410	1867.720

Double Exponential Smoothing for mutah



1) For Mutah station

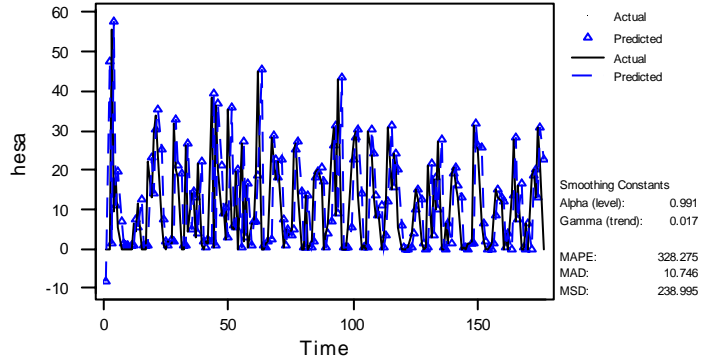
Double Exponential Smoothing for rabba



2) For Rabba station

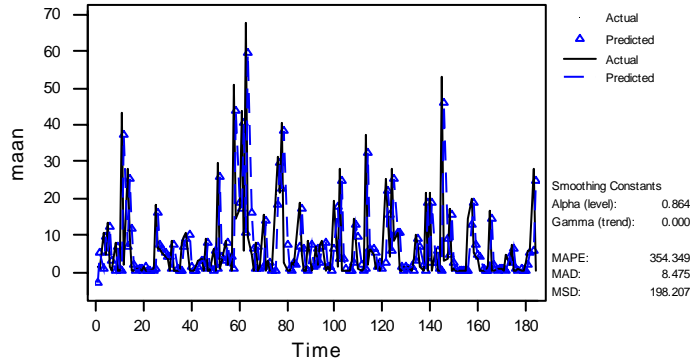
Tashtoush

Double Exponential Smoothing for hesa



3) For Hasa station

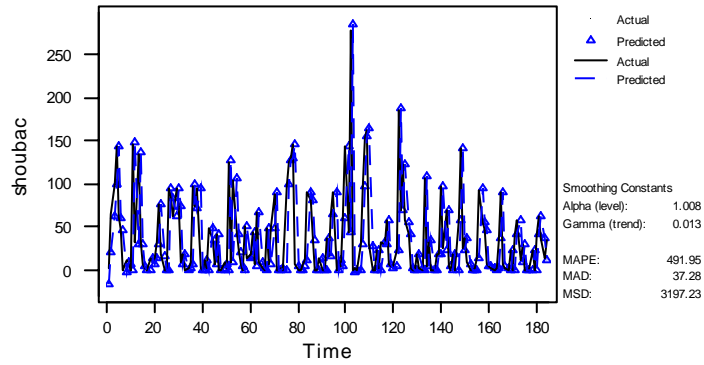
Double Exponential Smoothing for maan



4) For Maan station

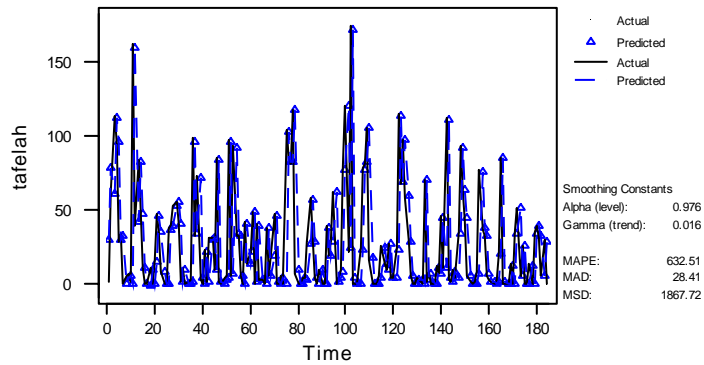
Analysis of Rainfall in Southern Area of Jordan

Double Exponential Smoothing for shoubac



5) For Shoubak station

Double Exponential Smoothing for tafelah



6) For Tafelah station

Winter's exponential smoothing

Now there are three equations, one for the (deseasonalized) level L_t , one for the trend T_t , and one for the seasonal index in period t , S_t :

Tashtoush

Over all smoothing
$$L_t = \alpha \frac{Y_t}{S_{t-M}} + (1 - \alpha)(L_{t-1} + T_{t-1})$$

Smoothing for trend
$$T_t = \gamma(L_t - L_{t-1}) + (1 - \gamma)T_{t-1}$$

Smoothing for the seasonal index
$$S_t = \delta \frac{Y_t}{L_t} + (1 - \delta)S_{t-M}$$

Value of forecast
$$Y_t = L_{t-1} + T_{t-1} + S_{t-M}$$

Here, M is the number of seasons, $M = 12$ for monthly data.

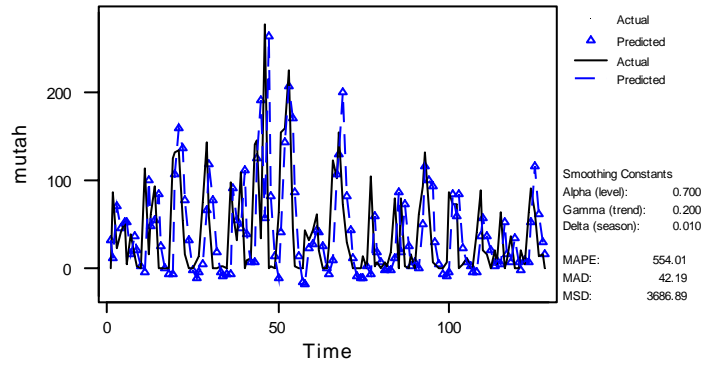
Exponential weighted moving average type (Holt-Winter) model used for forecasting the monthly rainfall in the six stations.

Table (6) The model parameters and the accuracy measures

Station	Smoothing Constants			Accuracy Measures		
	Alpha(level)	Gamma (trend)	Delta (seasonal)	MAPE	MAD	MSD
Mutah	0.70	0.20	0.01	554.01	42.19	3686.89
Rabba	0.80	0.20	0.01	407.29	40.12	3579.97
Hasa	0.70	0.20	0.01	317.592	10.949	212.320
Maan	0.80	0.20	0.01	398.064	9.069	211.602
Shoubak	0.90	0.20	0.02	501.60	38.83	3318.54
Tafilah	0.70	0.20	0.01	672.05	30.71	1880.26

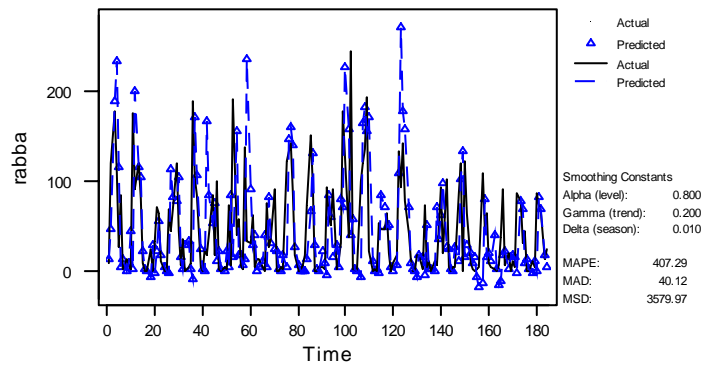
Analysis of Rainfall in Southern Area of Jordan

Winters' Multiplicative Model for mutah



1) For Mutah station

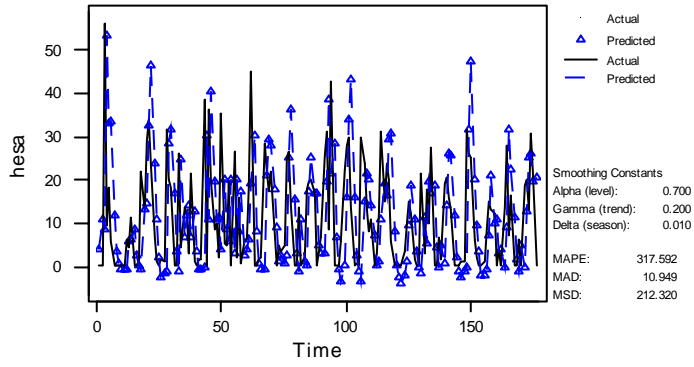
Winters' Multiplicative Model for rabba



2) For Rabba station

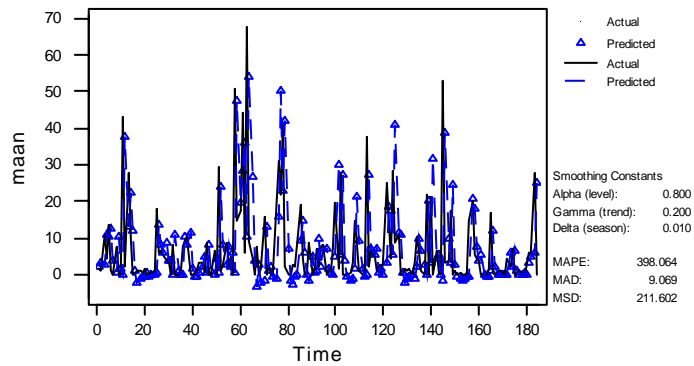
Tashtoush

Winters' Multiplicative Model for hesa



3) For Hasa station

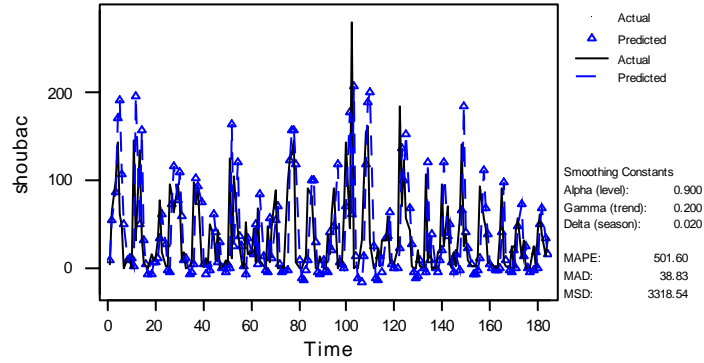
Winters' Multiplicative Model for maan



4) For Maan station

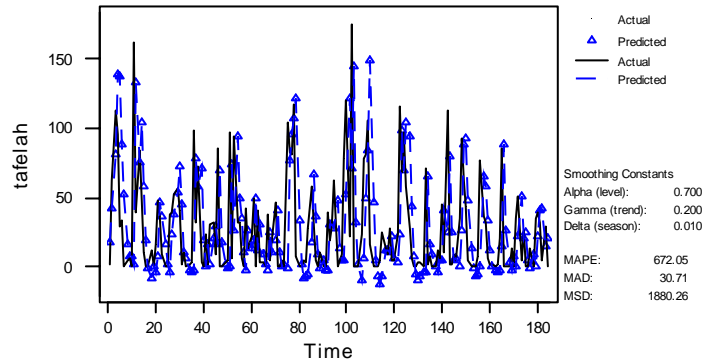
Analysis of Rainfall in Southern Area of Jordan

Winters' Multiplicative Model for shoubac



5) For Shoubac station

Winters' Multiplicative Model for tafelah



6) For Tafela station

Conclusion

The main objective is to obtain reliable estimates of monthly rainfall. The selection of the best model fitted to historical data is directly related to residual analysis. This study is concerned with testing residuals from an ARIMA model, which are the most popular for generating stochastically synthetic data, applied to monthly rainfall data from the 6 stations in the southern area of Jordan. Independence analysis of the residuals was

Tashtoush

examined by using the Ljung-Box statistic. To determine whether the residuals are normally distributed, the selected parsimony model for each data set among the ARIMA models fulfilled the diagnostic checks considered, showed that the assumptions concerning the residuals from the selected best ARIMA model held. Furthermore, comparisons of monthly mean and standard deviation values for the observed and predicted data from the ARIMA model showed that the predicted data preserved the basic statistical properties of the observed series. The simple linear regression approach was applied to explain the association between the observed and predicted monthly data sequences.

The fitted time series models perform close to or better than the regression model which may lead to poor performance when forecasting beyond the time period of the given data.

The Selection of the appropriate Exponential Smoothing Model based on the MAPE and MAD for data from mutah is (Single), Rabba is (Winter), Hasa (Single), Maan (Single), Shoubak (Double), and Tafelah (Double).

دراسة لتحليل الأمطار في جنوب الأردن

سليمان طشطوش

ملخص

تم استخدام نماذج متعددة لتقدير الأمطار والتي لها أهميتها في الدراسات المختلفة للمصادر الطبيعية والزراعة.

في هذا البحث تم استخدام ثلاث نماذج سلاسل زمنية لتقدير الأمطار الشهرية في المنطقة الجنوبية من الأردن. النماذج المستخدمة هي الإنحدار و بوكس-جنكنز (أريما) والتمهيد الأسّي. نتيجة الدراسة تشير إلى افضلية نموذج التمهيد الأسّي على نموذج الإنحدار. تم التحقق من دقة وفعالية نماذج التنبؤ المختلفة في التنبؤ بالامطار في منطقة الدراسة.

References

- [1] Salameh E. The climate of Jordan. Short summary extracted from the progress research report., (1997).
- [2] Al-Khashman A. O., The environmental state of the area extending between Wadi-El Hasa and Wadi Musa from the railway to Wadi Araba. Dissertation, Jordan University, Faculty of Graduate Studies,(2002).
- [3] Mc Kerchar A.I. and Delleur J.W., "Application of Seasonal Parametric Linear Stochastic Models to Monthly Flow Data", *Water Resources Research*, 10(1974) 246-255.
- [4] McLeod A.I., Hipel K.W. and Lennox W.C., "Advances in Box- Jenkins Modeling 2. Applications", *Water Resources Research*, 13(1977)577-586.
- [5] Fernando D.A.K. and Jayawardena A.W., "Generation and Forecasting of Monsoon Rainfall Data", 20th WEDC Conference, Colombo, Sri Lanka, (1994)310-313.
- [6] Venema H.D., Schiller E.J. and Adamowski K., "Evidence of Climate Change in the Senegal River Basin", *Water Resources development*, 12(1996) 531-546.
- [7] Chaloulakou A., Assimacopoulos D. and Lekkas T., "Forecasting Daily Maximum Ozone Concentrations in the Athens Basin", *Environmental Monitoring and Assessment*, 56(1999)97-112.
- [8] Ahmad S., Khan I.H. and Par_da B.P., "Performance of Stochastic Approaches for Forecasting River Water Quality", *Water Resources*, 35(2001) 4261-4266.
- [9] Yürekli K., Kurunç A., and Öztürk F., Testing The Residuals of an ARIMA Model on The Cekerek Stream Watershed in Turkey, *Turkish Journal of Engineering and Environmental Sciences*, 29(2005)61-74.
- [10] Sadhuram Y. and Ramana Murthy T. V., "Simple Multiple Regression Model for long range forecasting of Indian Summer Monsoon Rainfall", *Meteorol Atmos Phys* (2007), Printed in The Netherlands Regional Centre, National Institute of Oceanography, Visakhapatnam, India, (2007).
- [11] Janacek G. and Swift L., Time Series Forecasting, Simulation, Application, Ellis Horwood, New York, USA., (1993).
- [12] Sun H. and Koch M., 2001, "Case Study: Analysis and Forecasting of Salinity in Apalachicola Bay, Florida, Using Box-Jenkins Arima Models", *Journal of Hydraulic Engineering*, 127(2001)718-727.
- [13] Box G.E.P. and Jenkins G.M., Time Series Analysis Forecasting and Control, Holden-Day, San Francisco, USA.,(1976).
- [14] Newton H. L., TIMESLAB: A time series analysis laboratory, Wadsworth and Brooks /Cole Publishing Company, California, (1988).

Tashtoush

- [15] Zhang G.P., "Time Series Forecasting Using a Hybrid ARIMA and Neural Network Model", *Neurocomputing*, 50(2003)159-175, 74.
- [16] Hipel K.W. and McLeod A.I., Time Series Modeling of Water Resources and Environmental Systems. Development in Water Science, vol. 45, Elsevier Scientific Publishing Company, Amsterdam, The Netherlands, (1994).
- [17] Gibbons J.D., Nonparametric Methods for Quantitative Analysis. American Sciences Press, Inc., Ohio, USA., (1997).
- [18] Greene W.H., Econometric Analysis, Prentice Hall International, Inc., New Jersey, USA., (2000).
- [19] Brooks C., Introductory Econometrics for Finance, Cambridge University Press, UK., (2002).
- [20] Geurts M. and Kelly J., "Forecasting retail sales using alternative model. *International Journal of Forecasting* 2(1986)261-272.

Petrographical and Mineralogical Study of the Travertine in Deir Abu Said Area, NW Jordan

Nazem El- Radaideh and Hakam Mustafa*

Received on June 11, 2007

Accepted for publication on July 23, 2007

Abstract

The travertine deposits in Wadi Ain El-Tais, Deir Abu Said area have been formed, as indicated by field study, in fresh water environment by warm-Palaeosprings, and are characterized by cavernous topography. Five travertine facies could be differentiated: Algal facies (Cyanoids and rhodolites), Stromatolitic and small reed tufa facies, micritic masses and peloids facies, Chironomida faunal remnants facies and pebbly facies. These travertine deposits have been precipitated mostly, as indicated by field and petrographical study, as a result of biogenic activity, in which the main builders are Cyanobacteria, Chironomida and Algae. The inorganic processes are dominant only near the spring orifices. The carbonate of the travertine deposits consists of low-Mg calcite. The most common cement in Deir Said travertine is radially- fibrous, bladed calcite cement and to less extent calcite cement with triangular termination. The analyses show that the travertine deposits are mainly composed of CaO with an average content of 44.02 wt%, where CaCO₃ forms about 80.3 wt%, and they are poor in the trace elements Sr, Mn, and K and rich in Zn, Pb, Cu, and Mo with respect to normal carbonates

Keywords: Travertine, Tufa, Low Mg-calcite, Facies, Stromatolite, Cyanoid, Rhodolite, Peloid, Cyanobacteria, Chironomida, Deir Abu Said, Jordan.

Introduction:

The term travertine originates from the city name Tivertino, Italy where an extensive travertine deposits occur. However, these deposits have been referred to by many different names including tufa. There are, however, some differences in the basic characteristics of travertine and tufa; tufa has a higher porosity, woody texture, and is generally a cool fresh water deposit. Conversely, travertine is commonly deposited in warm water, and is more lithified. Atabey[1] stated that travertine is composed of diagenetic old calcareous tufa deposits with significant amounts of calcite spar added to its framework

Tufa and travertine are known to be formed in wide range of temperatures from 5 to 95 °C, but mostly between 10 to 30°C [2]. They can be formed on higher and lower plants, but most commonly on Cyanobacteria, algae, mosses, hepatics and insect larval

carapaces (Chironomida). Tufa and travertine may be deposited organically by photosynthesis of plants (biochemical processes) or inorganically by changes in water turbulence, temperature and /or pressure (physiochemical processes). They can be classified according to type of plants and algae involved in their precipitation or according to petrographic properties.

The travertine deposits in Deir Abu Said area have not been yet studied. Therefore the present study aims at investigating these deposits petrographically and mineralogically, in order to determine their characteristics and their origin.

Geological setting:

Deir Abu Said area is located in the NE part of Jordan, about 40 Km southwest of Irbid, between 35 50 to 35 54 N and 32 51 to 32 57 E (Fig.1).

The average elevation of Deir Abu Said area ranges from 300 – 350 m above sea level. In west of Deir Abu Said area, beside solidified limestone, oil shale, chalk marly limestone, marly deposits, of Late Cretaceous age, also alluvial, travertine and caliche deposits of Quaternary age are exposed. Structurally, the study area is bordered by major structures, the Ajlun structure in the south west of the study area and the Dead Sea transform in the west. This transform is a plate boundary between the Arabian plate and the Siani-Palestine subplate formed in Late Cenozoic as the breakup of the Arabian plate from the African plate took place. This prominent tectonism was associated with volcanic eruptions along the transform from Wadi El-Hasa to Yarmouk river.

The heat energy associated with the volcanic activity is and was partially transported to the surface by groundwater moving along faults, rising to the surface, flowing out spring orifices as hot water, and depositing travertine at the orifices and along the flow channels.

Methodology:

Field observations were made at several travertine sequences along the Wadi Ain ET-Tais (Figs.1 and 2). Although there is natural variation between individual bodies within the zone of travertine deposits, all of the deposits are broadly alike with respect to their morphology and the presence and distribution of travertine facies.

The exposed rocks have been described in the field using normal field techniques. Thirty oriented samples from Deir Abu Said area were subjected to the following investigations:

1. Petrographic study in thin sections, using polarizing transmitted light Microscope (PTLM). The relative abundance of the rock constituents was determined by a visual modal analysis. The samples were subsequently air dried and examined using a light microscope for organics, structures and fabrics. Fifteen of these were sub-sampled for thin section analysis, including staining using Feigl's solution and Alizarin Red S following the protocol in [3].

Petrographical and Mineralogical Study of the Travertine in Deir Abu Said Area, NW Jordan

2. X-ray diffraction method was used for the determination of the mineral composition of the tufa. Fifteen samples were examined using Philips vertical x-ray diffractometer under the following conditions:

-Radiation: Stabilized copper filtered $\text{CuK}\alpha$.

Time constant: 2.

Grain: 64.

Slit: 0.1

Speed: 2Φ /cm/minute.

3. AAS (Atomic Absorption Spectrophotometer).

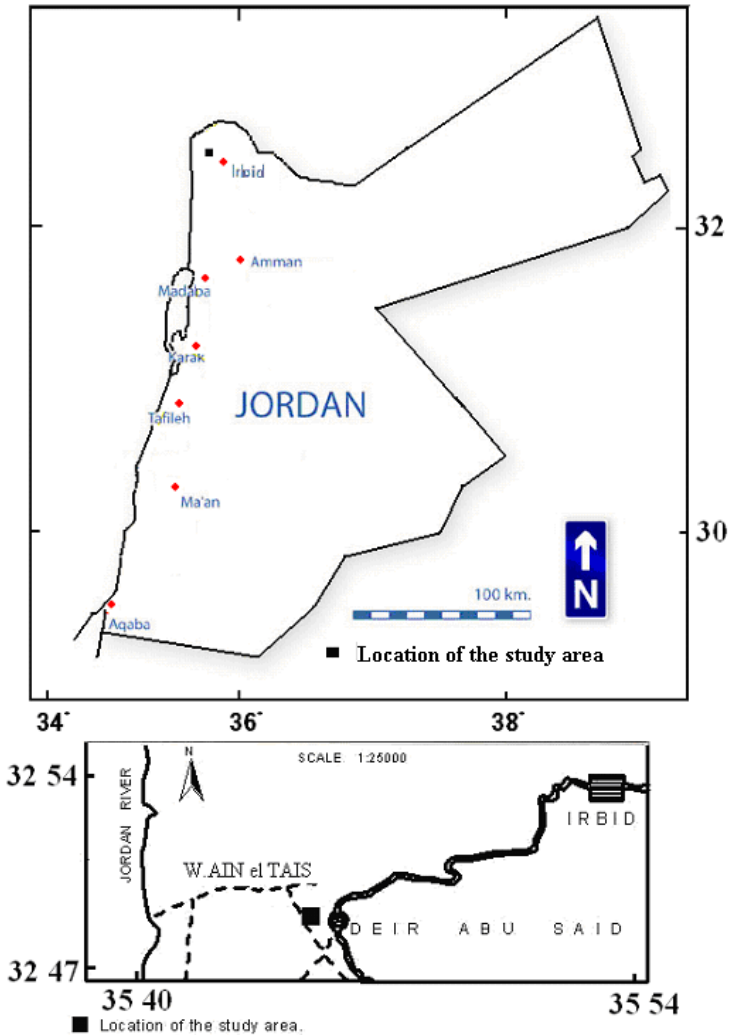


Figure 1: Location map of study area.

Description of Deir Abu Said travertine:

The composition of Deir Abu Said travertine is not widely diverse; it is composed of algal travertine, stromatolitic - small reed tufa, micritic masses with peloids, Chironomida-faunal remnants, Pebbly-fine gravel facies and cementing material. The lithological section of Deir Abu Said can be divided into lower, middle and upper members, depending on the presence or absence of stromatolitic structure. The following is a brief description of the nature, distribution and field characteristics of Deir Abu Said travertine; this 30m thick

Petrographical and Mineralogical Study of the Travertine in Deir Abu Said Area, NW Jordan

section crops out on the east bank of wadi Ain ET-Tais Palaeo-hot spring, some 3.0 km west of Deir Abu Said city (Fig.2).

Member(1):

2m: chalky marly limestone, overlain unconformably by 15 to 20 cm thin horizon of fine gravels.

10m: grayish white, massive, microcrystalline, very hard, fenestral cavernous, slightly laminated, weathered travertine composed of small encrusted plants (less than 10 cm in length and less than 3 cm in diameter) and irregular chaotic bodies (2 m high and 5 m long). The lowermost layers of this member are rich in small concentric precipitations of microcrystalline carbonate around fine (1 to 5cm) pebbles, composed mainly of chert, limestone and older tufa debris (Pl. 1, Fig.5). Several palaeocaves, vugs and karst are distributed within this part (Pl. 1, Fig.6 and Pl. 2, Fig. 7), (Fig.3).

Member (2):

8 m: grayish-white microcrystalline indurate thickly bedded porous, cavernous, vuggy travertine, with yellowish-brownish tint, and slightly weathered surfaces containing black-brownish irregular patches. It includes stromatolitic and laminated structures and irregular chaotic bodies. Upwards, there is a slight increase in the size of encrusted plants, which form cylindrical bodies (Pl.1, Fig.4), (Fig.3).

Member (3):

10m: grayish-white, massive, microcrystalline, indurate vuggy, cavernous tufa, consisting partly of stromatolitic and laminar beds, mainly in the lower most layer of this part (Pl.1, Fig.6). Thin horizon of red soil and caliche deposits overlie this member (Fig.3).

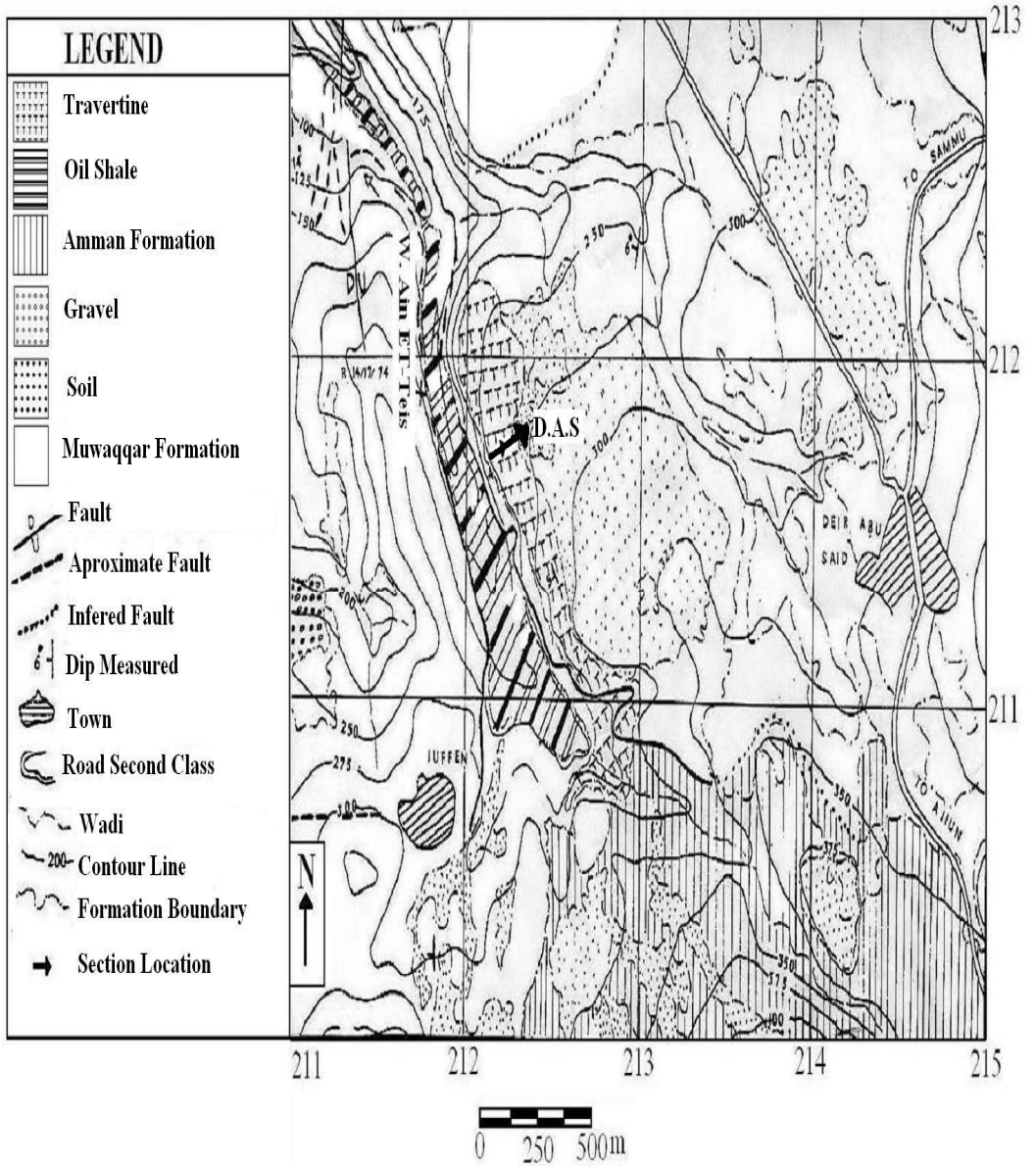


Figure 2: Geological map of Deir Abu Said area and location of lithological section.

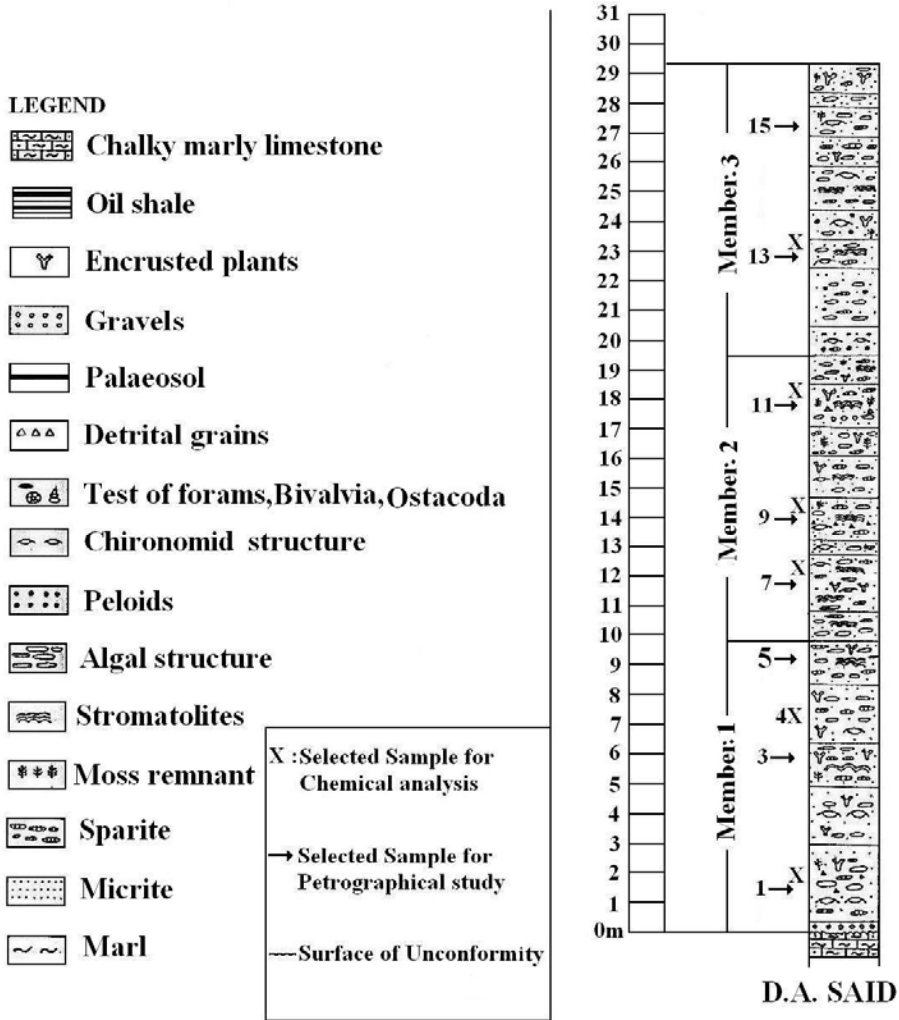


Figure.3: Section (1) in Deir Abu Said travertine.

Facies of Deir Abu Said Travertine:

- Algal facies

Cyanoids (Algaly coated grains)

Several samples of Deir Abu Said travertine show cyanoid structures (Pl. 2, Figs.8 and 9). These structures are concentrated in the middle member of the section; they are subspherical to spherical in shape, ranging in diameter from 0.1 to 1 mm, and have irregular and pumpy surfaces. They have internally concentric laminated structures, where the cores

are darker than the cortices, with internally wrinkly laminated mode of circumferences. The nuclei of these grains are not distinct; they may be composed of litho –or bioclasts. The cortices surround completely the cores. This indicates that such grains were moving during the growth of the coating material.

Love and Chafetz [4] described cyanoids and found that the dark laminae contain Cyanobacteria filaments; they distinguished several sizes of cyanoids; the larger ones have distinct nuclei. Few of the large coated grains show growths of bush-like shape of Cyanobacteria filaments growing vertically to the outer micritic laminae (Pl. 2, Fig.10).

Two modes of discontinuous laminae can be distinguished in these cyanoids; wrinkly and gently convex shaped (Pl. 2, Fig.11). The cyanoids of Deir Abu Said travertine are widespread.

Rhodolites

Rhodolites were distinguished only in one sample (sample 4) of Deir Abu Said travertine. They consist of algal nodules ranging in diameter from 0.6 to 1 mm and show internal weakly bounded laminae with microsparite between the filaments (Pl. 2, Fig.12).

Recent and fossil rhodolites are bulbous calcereous bodies spheroidal, ellipsoidal, discoidal or spindle-like created by undetached encrusting red algae.

- Stromatolitic and small reed tufa facies

Stromatolites are widespread in the middle and upper part of Deir Abu Said travertine making 20% and 15% of the rock respectively and uncommon in the lower part.

The stromatolitic structures are composed of alternations of dark and light laminae; the dark laminae consist of micritic material and minor amounts of iron oxides, while the light laminae are composed of microsparite. They show mostly gently convex (Pl.3, Fig.13) but also, wrinkly and wavy shaped laminae.

The dark and light laminae are equal in thickness ranging from 15 to 20 μm , so they are better named “microstromatolites”.

In Deir Abu Said travertine there are only traces of Cyanobacteria filaments; these are hardly distinguished within several bush-like structures. It is very difficult to distinguish genera, but undoubtedly, these Cyanobacteria are of filamentous type belonging to the order Oscillatoriales (Pl. 3, Fig. 14 and 15). It seems that the environmental conditions, which were prevailing during the formation of travertine in Deir Abu Said, like temperature, PH, salinity, light intensity, and other parameters were favorable for permitting Cyanobacteria to grow.

The encrusted tufa is laminated and rich in small reed moulds that have been cemented in situ, indicating deposition in low-gradient slack-water like pool environment. The tufa encrusts the reeds while simultaneously precipitating fine laminae, which frequently overlay fine gravels (Pl. 1, Fig. 5). This juxtaposition of these contrasting units would appear to mark a significant change in depositional environment from low-magnitude with low frequency floods that transport the fine gravels to a much lower-energy environment with more continuous steady flow where laminated tufa and reeds are commonplace. Similar situation was recorded by Pedley et al.[5], Garnett et al. [6] and Viles et al.[7].

Petrographical and Mineralogical Study of the Travertine in Deir Abu Said Area, NW Jordan

Other floral remnants are recorded in few samples in both lower and middle parts of Deir Abu Said travertine. They include encrusted stalks and leaves of microphyta like mosses and algae, the encrusted microphyta remnants show concentric structures but they lack well defined boundaries as a result of coalescence of adjacent structures (Pl. 3, Fig.16).

Some of the moulds are elongated, others are rounded, and the length of elongated moulds reaches more than 1 mm and the width ranges from 0.1 to 0.6 mm. While the rounded moulds are mostly less than 0.3 mm in diameter. These encrusted moulds are composed of alternating smooth wavy laminae of micrite and of sparry calcite crystals growing perpendicularly to the laminae surfaces (Pl. 3, Fig.17)

The individual laminae are ranging in thickness from less than 60 μm to 100 μm . Some of the vesicular moulds are still empty others are partially or completely filled by micrite and microsparite, as granular calcite cement (Pl. 3, Fig.18)

- Micritic masses and peloids facies:

Irregular masses of micrite are common, and to a lesser extent associated with some peloidal and pelletal structures. They are bounded by/or enclosed within other fabric elements like Chironomida tubes, cyanoids and other clasts.

These micritic masses are intimately intergrown with sparry or microsparry calcite usually in an irregular fashion (Pl. 2, Fig. 9 and Pl. 4, Fig. 19). Mostly, they show clotted or grumous textures. The micritic travertines are massive and comprise a very fine crystalline to cryptocrystalline (<10 μm in diameter) calcite cement. Limestones with less than 2% terrigenous sand and silt (mostly quartz and feldspar) are considered pure micritic travertines and generally are beige in color and weakly luminescent (brownish-orange).

No coccoid bacteria, and no structures related to bacteria could be identified within these micritic masses. Therefore, the formation of these micritic and some peloidal-pelletal structures are related to Chironomida. Commonly these peloidal- pelletal structures are associated with other coated grains (Pl.4, Fig.19).

- Chironomida -faunal remnants facies:

The chironomid tubes in Deir Abu Said travertine are arranged horizontally in parallel alignment within micritic and microsparry matrix. Traces of Ostracod shells are hardly distinguished and only recorded in few samples of the whole section. These shells are partially or completely filled with brownish micrite and to less extent with microsparite or well rhomb calcite crystals (Pl. 4, Figs.20 and 21). In addition, larval constructions are readily preserved in tufa and travertine deposits and are useful for identifying palaeo-hydraulic zones [8,9].

However, larval facies are absent from all published tufa models. Aquatic insect larvae have been noted in tufas forming in a number of cool temperate streams, but larval constructions are only present within tufa formed in the spring season [10,11]. Conversely, warm water in tropical environments ensures a large larval population potentially operates all year. Thus, larval facies are common throughout tropical tufa deposits. The larval tufa facies in Deir Abu Said travertine should be studied in details and included in models of semiarid travertine-tufa formation.

- Pebbly facies:

The modern channel of the Wadi Ain ET-Tais is comprised of detrital tufa deposits and loose, uncemented, poorly sorted coarse sub-rounded to rounded pebbles (Pl. 1, Fig.5). However, at few sites in Deir Abu Said section more than 50% of the clasts are subangular, indicating local inputs from hill slope materials (talus) and/or a limited fluvial reworking of the channel deposits. Measured pebbles *a*-axis dimensions in the contemporary channel and in travertine occurring irregular beds of cemented gravels ranged from 1 cm to 5cm (Pl. 1, Fig.5 and Pl. 4, Fig.22). Larger pebbles with *a*-axis up to about 7.0 cm occur in all members of the travertine. The cemented gravels usually have a clast-supported fabric, and are less rounded than the active wadi deposits.

Mineralogical investigation:

A scanning of 15 samples shows no variations in their carbonate mineralogy; X-ray analysis shows that low Mg-calcite is almost the only recorded carbonate mineral.

Traces of quartz were reported in one sample as non-carbonate mineral. Both staining of thin sections and X-ray analysis indicated that aragonite and dolomite are totally absent. The deposition of travertine had taken place generally in a freshwater environment by warm-palaeosprings as indicated by field study. However the petrographical study reveals that travertine formed mostly as a result of biogenic activity, in which the chief builders are Cyanobacteria, Algae, Chironomida and to less extent Ostracoda; these organisms have a tendency to select low-Mg calcite and calcite as skeletal materials.

Travertine and tufa deposits are principally composed of calcite with low magnesium content. In deposits originating from thermomineral springs, there are sometimes low levels of aragonite, and some deposits contain up to five percent silica [12].

Major elements study revealed that Deir Abu Said travertine is mainly composed of CaO with an average value of 44.02 wt. % where CaCO₃ content is about 80.3 wt. %. Trace element study revealed that Deir Abu Said travertine is poor in Sr, Mn, and K, and rich in Zn, Pb, Cu, and Mo with respect to normal carbonate.

Diagenesis:

The most common cement distinguished in Deir Abu Said travertine is radially-fibrous, bladed calcite cement (Pl.4, Figs.23, 24, and Pl.5, Fig.25) and to less extent calcite cement with triangular termination (Pl.5, Fig.25). Several vesicular structures, chironomid tubes and other moulds are partially or completely filled by sparry calcite cement, most chironomid tubes are filled partially or completely by well shaped rhombs of isopachous spars, growing mostly inward or partially outward (Pl.4, Figs.20 and 21). Few relict pore spaces are completely filled by equant euhedral sparry calcite cement rich in inclusions and crystallinities, showing drusy and granular appearance (Pl. 5, Fig.26). Few radial columnar crystals grow vertically to the organic substrate, show dragged terminations and tabular edges and are rich in inclusions and crystallinities (Pl. 5, Fig.27). The younger cement within Deir Abu Said travertine seems to be radial, fibrous, bladed and columnar sparry one, and the secondary cement is granular mosaic cement. Micritic cement can also be observed, showing clotted texture and fills irregularities within travertine structures (Pl. 4, Fig.19).

Discussion:

Micritic carbonate is common in Deir Abu Said travertine facies. The fast-flowing waters around the Palaeo-spring at the southwestern border of the section eventually reached its central and lateral portions and formed small, shallow ponds in which micritic travertine precipitated. At the borders of the section, far from the spring, conditions were favorable for tufa deposition. The presence of small reed moulds suggests the encrustation of macrophytes in small pools, probably as paludal tufas. Root sheaths probably formed around living and decaying roots; they are brownish and composed of fibrous calcite root casts which consist of mudstone or dull-luminescent calcite with triangular terminations (Pl. 5, Fig. 28). No relict organic root materials were found.

Moulds and prints within the tufas are created by disappearance of the original organic matter. The fossil deposits are also characterized by the presence of sparry crusts that originate from cementation and recrystallization of initial micritic cyanobacterial bushes. Furthermore, specific calcite crystals such as euhedral and needle fibre calcite have been recognized. These are interpreted to have formed during phreatic and vadose diagenesis [11].

Detrital grains and terrestrial faunal shells were transported into the tufa pools by distal alluvial fans (Pl. 5, Fig. 29). The surficial deposition of the carbonate lithoclast travertines in the Deir Abu Said section allowed for subaerial alteration in the micritic travertines, which led to desiccation-generated brecciation and the disruption of fabrics, as well as the formation of calcretes and palaeosols. These features indicate intermittent subaerial exposure and pedogenesis of the sediments during deposition. The lithoclast travertines at all members of the section indicate surficial reworking of previously deposited sediments.

Cyanobacteria and Chironomida played an important role in the formation of Deir Abu Said travertine, in the initial and late stages of travertine formation; they can thrive in a wide range of environmental conditions.

These organisms reduce the CO₂ content and play an important role in the precipitation of micrite, and formation sites of encrustation.

The carbonate buildup in freshwater environments takes place by the activity of microorganisms in four different ways, these are: (1) Trapping and binding of sediment particles by algal filaments and mucus at the algae surfaces. (2) Encrustation of the algae filaments with calcium carbonates. (3) Secretion of CaCO₃ within mucus (i.e. the trichomes of algae are embedded in mucus and calcite is precipitated along the sheaths of the trichomes within the mucus). (4) Cementation of CaCO₃. [13,14].

It seems that all the preceding mechanisms were effective during the deposition of Deir Abu Said travertine, with different intensity depending on the environmental conditions.

The travertine of Deir Abu Said seems to be deposited mostly in quiet water environment, as it is indicated by the presence of stromatolite structures especially in the middle part of the section, existence of micrite and the parallel alignment of unbroken Chironomida tubes. However, the environment parameters such as temperature, light, intensity, salinity, and PH were significantly varied during the deposition of the different parts of the section.

The absence of stromatolites in the lower part of Deir Abu Said sections indicates that the identified algae are probably of coccoid type, which is unable to build stromatolitic structure.

It seems that bacteria played no significant role in the formation of Deir Abu Said travertine, because no distinct clumps of bacteria or shrubby structure have been observed during the microscopic study.

The inorganic processes are dominant near the spring orifice as a result of fastly degassing of CO₂ while the biogenic processes increase down current where small pools are formed. The type and amount of associated organisms at the spring orifice is identified by many variables such as the amount of dissolved CO₂, temperature of water, PH, and salinity of water.

As the saturated groundwater issues from spring orifices, it is exposed to low partial pressure of CO₂ and became supersaturated with respect to CaCO₃. Removal or reduction of CO₂ to a minimum value could occur by rapid water turbulence, elevated temperature, and plant activity especially lower plants, mosses, Cyanobacteria and Algae.

Conclusion:

The Deir Abu Said travertine is composed mainly of stromatolite with small reed tufa, micritic masses-peloids, Chironomida -faunal remnants, pebbly-fine gravel facies and cementing materials. It can be considered as thermogene deposit according to Pentecost [15].

The deposit of the travertine constituents took place along the waterfall of Palaeo-hot spring at Wadi Ain ET-Tias, while the tufa facies deposited within a distal part in the cool pool environment.

Both staining of thin sections and X-ray analysis indicted that Deir Abu Said travertines are composed of low Mg-calcite.

Major elements study revealed that Deir Abu Said travertine is mainly composed of CaO with an average content of 44.02 wt. % where CaCO₃ content is about 80.3 wt. %.

Trace element study revealed that Deir Abu Said travertine is poor in Sr, Mn, and K, and rich in Zn, Pb, Cu, and Mo, with respect to normal carbonate.

It seems that the Deir Abu Said travertine mostly originated by the activity of biochemical processes over the physio-chemical processes, especially in the upper member where a high percent of plant imprints are detected (Pl. 1, Fig.1).

Deir Abu Said travertine is hard and thick bedded like the travertine deposits in Deir Alla and in other locations in Jordan. It is in Deir Alla removed in large blocks, cut into tiles and slabs, polished, honed, tumbled, sandblasted, or acid treated and used for different purposes: construction covering and cladding, internal floors and walls, bathrooms and as ornamental stones.

The quarry in Deir Alla produces 16000m² travertine annually. Jordanian travertine is exported to Italy, Spain, Portugal, and Russia, USA, Canada, Dominican, and Mexico, Australia, China, South Korea, Taiwan, and Hong Kong, Saudi Arabia, Bahrain, Kuwait, Qatar, Oman and UAE, Lebanon, Egypt, Tunis, Syria and Palestine, and to other parts of the world.

Huge travertine deposits occur in Turkey and Iran.

Acknowledgment:

The present study has been financially supported by the Yarmouk University (Project 2001/8), we wish to express our thanks for this support.

دراسة بتروغرافية ومعدنية الترفرتين في منطقة دير أبو سعيد- شمال غرب الأردن

ناظم الردايدة وحكم مصطفى

ملخص

بينت الدراسة الميدانية أن توضعات الترفرتين في وادي عين التيس تكونت في بيئة مياه حلوة من ينابيع حارة، وتمتاز بتضاريس كهفية. وقد ميزت خمس سحن ترفرتينية هي: السحنة الطحلبية المكونة من السيانونيدات والرودولائيات، والسحنة الستروماتوليتية النباتية، وسحنة الكتل الميكريتية البلويدية، وسحنة الشيرونوميديات المستحاثية الحيوانية والسحنة الحصوية. وبينت الدراسة الحقلية والبتروغرافية أن الجزء الأكبر من توضعات الترفرتين تكونَ بطريقة عضوية، حيث أن السيانونوبكتيريا والشيرونوميديا والطحالب هي المكونات الأساسية لها. وساد التكوين اللاعضوي فقط عند فوهات الينابيع. كما بينت أن كربونات الترفرتين تتكون فقط من الكلسايت قليل المغنيسيوم وأن المادة الإسمنتية مكونة غالباً من الكلسايت الشعاعي الحزمي النصلي وبشكل أقل من الكلسات ذي النهايات الثلاثية الشكل. وبينت التحاليل أن توضعات الترفرتين تتكون بشكل رئيسي من ما معدله 44.02% وزناً CaO، أو ما معدله 80.3% وزناً $CaCO_3$. كما أظهرت التحاليل أن الصخر فقير بالعناصر النادرة K, Mn, Sr، وغني بالعناصر النادرة Mo, Cu, Pb, Zn مقارنة بالصخور الكربوناتيية العادية.

References

- [1] Atabey E., The formation of fissure ridge type laminated travertine-tufa deposits microscopical characteristics and diagenesis, Kiersehir Central Anatolia: *Mineral Research and Exploration Bulletin*, 123-124 (2002) 59-65.
- [2] Heimann A., and Sass E., Travertine in the northern Hula Valley, Israel, *Sedimentology* 36 (1989) 95-108.
- [3] Hutchinson C.S., *Laboratory Handbook of Petrographic Techniques*, Wiley Interscience, New York, 1974.
- [4] Love K. and Chafetz H., *Petrology of Quaternary travertine deposits, Arbuckle Mountain, Oklahoma*, in Hermann, J.S., and Hubbard, D.A., (eds.), *Stream deposits in Virginia: Virginia Division of Mineral Resources, Publication 101(1990) 65-78.*

- [5] Pedley H.M., Andrews J., Ordonez, S., del Cura, M.A.G, Martin J.A.G. and Taylor D., Does climate control the morphological fabric of freshwater carbonates? A comparative study of Holocene barrage tufas from Spain and Britain, *Palaeogeography, Palaeoclimatology, Palaeoecology*, 121 (1996) 239–257.
- [6] Garnett E.R., Gilmour M.A., Rowe P.J., Andrews J.E. and Preece R.C., ²³⁰Th/²³⁴U dating of Holocene tufas: possibilities and problems, *Quaternary Science Reviews*, 23 (2004) 947–958.
- [7] Viles A. Taylor M.P. Nicoil K. and Neumann S., Facies evidence of hydroclimatic regime shifts in tufa depositional sequences from the arid Naukluft Mountains, Namibia, *Sedimentary Geology*, 195 (1-2) (2007) 39-53.
- [8] Carthew M.P. and Taylor R.N., Drysdale, Aquatic insect larval constructions in tropical freshwater limestone deposits (tufa): preservation of depositional environments, *General and Applied Entomology*, 31 (2002) 35–41.
- [9] Carthew K. ,Taylor, P. and Drysdale, R., An environmental model of fluvial tufas in the monsoonal tropics, Barkly karst, northern Australia, *Geomorphology*, 73 (1-2) (2006) 78-100.
- [10] Irion F. and Müller G., Mineralogy, petrology and chemical composition of some calcareous tufa from the Schwäbische Alb, Germany. In: Müller G. and Friedman G.M.(Eds.), *Recent Developments in Carbonate Sedimentology in Central Europe*, Springer-Verlag, Berlin, (1968) 157–171.
- [11] Janssen A., Swennen R., Podoor N., and Keppens E., Biological and diagenetic influence in Recent and fossil tufa deposits from Belgium. *ARTIC Sedimentary Geology*, 126 (1-4) (1999) 75-95.
- [12] Ramon J. edited by Scholle, Peter A. Bebout, Dan G. and Moore, Clyde H., *Travertines: Carbonate depositional environments*, [AAPG memoir 33]: Tulsa, Oklahoma. (1983) 64-72.
- [13] Szulc J. and Smyk B., *Bacterially controlled calcification of freshwater Schizothrix-stromatolites: an example from the Pieniny Mts, Southern Poland*. In: J. Bertrand-Sarfati and C. Monty, (Eds.) *Phanerozoic Stromatolites vol. II*, Kluwer Academic Publishers, Dordrecht (1994) 31–51.
- [14] Andrews J. E. and Brasier A. T., Seasonal records of climatic change in annually laminated tufas, *J. Quaternary Sci.*, 20 (2005) 411-421. ISSN 0267-8179.
- [15] Pentecost A., The Quaternary travertine deposits of Europe and Asia Minor, *Quaternary Science Reviews*, 14 (1995) 1005–1028

Plate (1), Figs: 1-6

Fig.1: Plant imprints.

Fig.2: Vugs and caves within the travertine beds.

Fig.3: Vugs and caves (microkarst morphology) within the travertine beds.

Fig.4: Small encrusted plants and laminated tufa including caves and vugs.

Fig.5: Thin horizon of friable fine gravels (lithoclastic travertine).

Fig.6: The upper part of photo shows laminated planner-stromatolitic travertine, with vuggy structure; X 40.

Plate (2), Figs: 7-12

Fig.7: Encrusted structures in situ within irregular chaotic travertine beds.

Fig.8: Smaller size of cyanoid structure bounded by micritic masses; X100.

Fig.9: Large cyanoid structure; X 40.

Fig.10: Medium sized coated grain; X 40.

Fig.11: Gently discontinuous concave and wrinkly shaped laminae within micritic microsparite matrix; X 100.

Fig.12: Rhodolites structure with micro-sparite cement between filaments; X 40.

Plate (3), Figs: 13-18

Fig.13: Gently convex alternating white and dark lamination; X 40.

Fig.14: Filamentous Cynobacteria surrounded by overgrowth of microsparite cement; X 40.

Fig.15: Traces of Cynobacteria of filamentous type; X 40.

Fig.16: Encrusted stalks and leaves of microphyta; X 40.

Fig.17: Alternating smooth wavy lamination of micrite and sparite, growing vertically to the lamina surface.

Fig.18: Partially micritized vesicular mould.

Plate (4), Figs: 19-24

Fig.19: Micritized masses with intergrowth of microsparite; X 40.

Fig.20: Micritezed Chironomida tubes partially filled with well rhomb of euhedral isopachous calcite cement; X 40.

Fig.21: Rhombohedral isopachous calcite crystals with inward growth within chironomid tubes; X 100.

Fig.22: Slightly cemented gravels facies.

Fig.23: Fibrous bladed calcite cement; X 40.

Fig.24: Radially fibrous calcite cement with tabular termination; X 40.

Plate (5), Figs: 25-29

Fig.25: Radially fibrous calcite cement with triangular termination, X100.

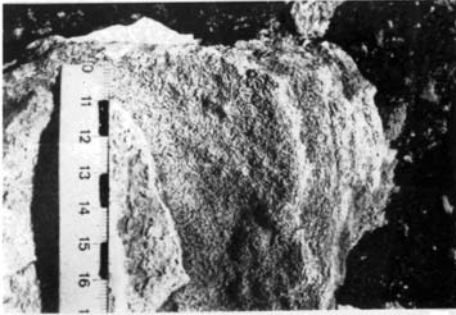
Fig.26: Drusy granular calcite cement; X 40.

Fig.27: Radially fibrous calcite cement.

Fig.28: Dully-luminescent with triangular terminations; X 40.

Fig.29: Detrital faunal shells; X 40.

Plate (1), Figs: 1- 6



1



2



3



4



5



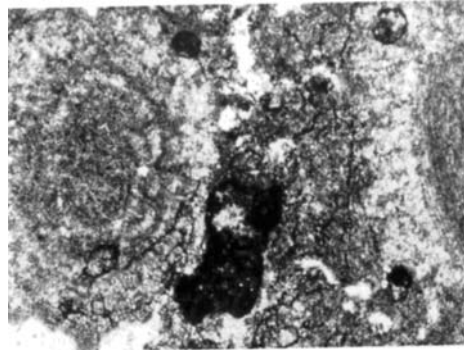
6

Petrographical and Mineralogical Study of the Travertine in Deir Abu Said Area, NW Jordan

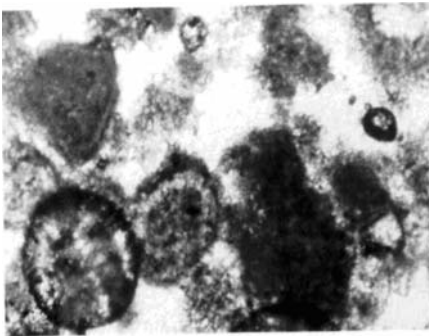
Plate (2), Figs: 7- 12



7



8



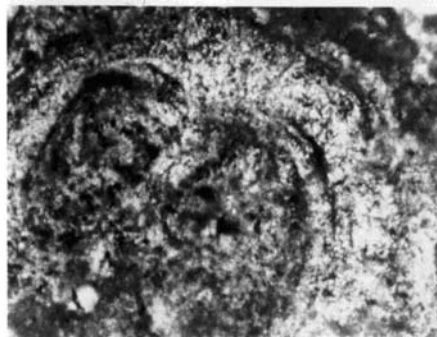
9



10

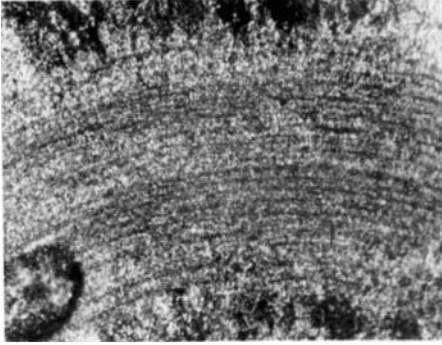


11

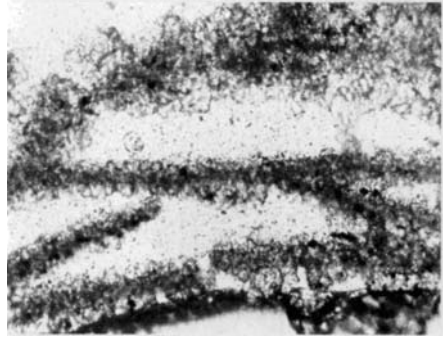


12

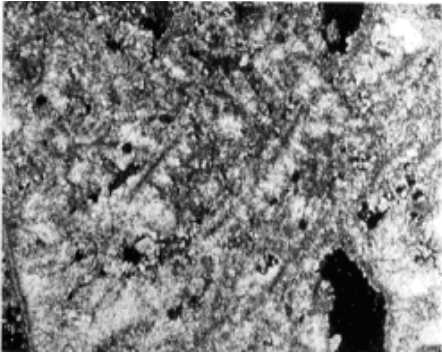
Plate (3), Figs: 13-18



13



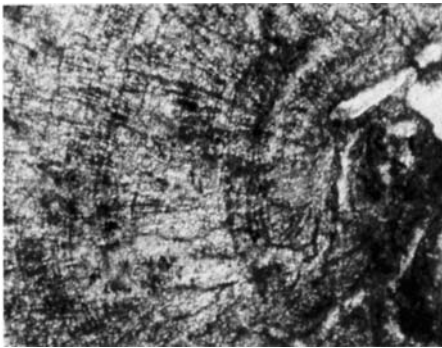
14



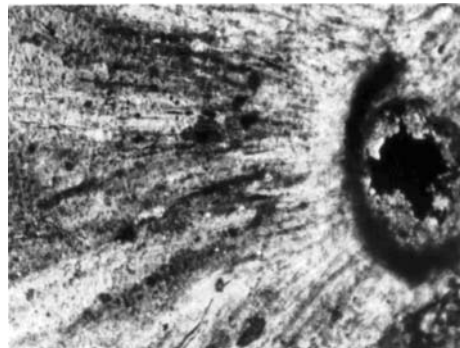
15



16



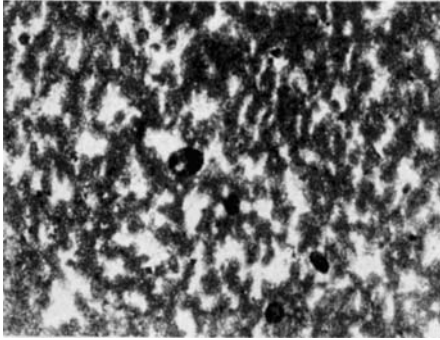
17



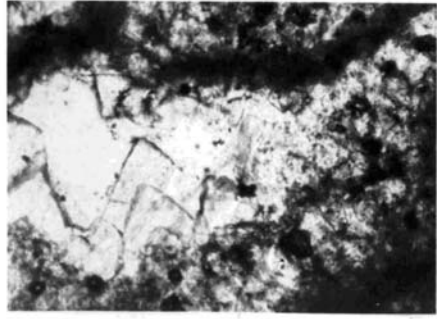
18

Petrographical and Mineralogical Study of the Travertine in Deir Abu Said Area, NW Jordan

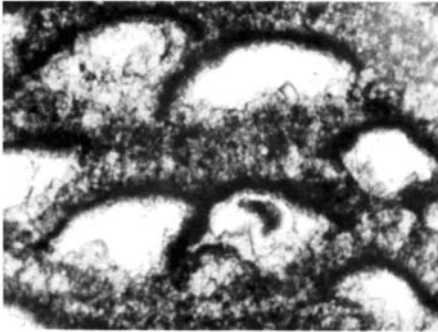
Plate (4), Figs: 19-24



19



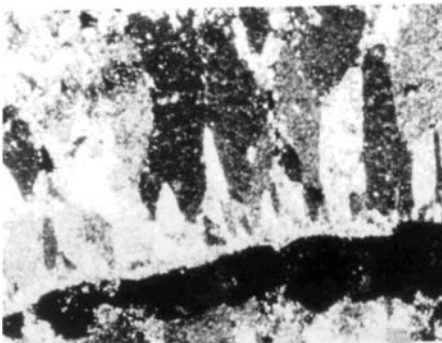
20



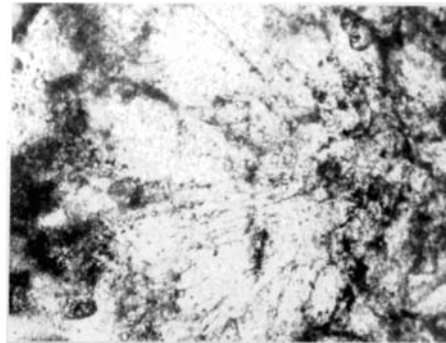
21



23

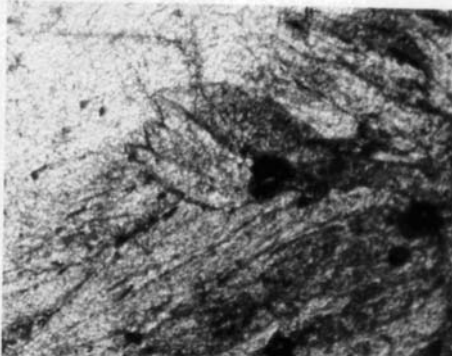


24

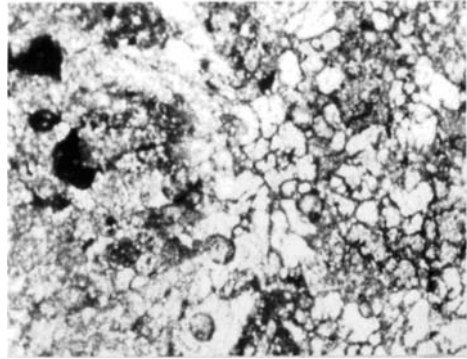


25

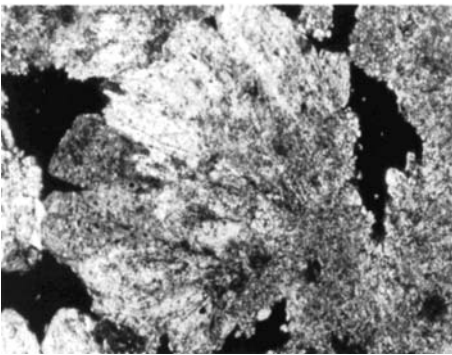
Plate (5), Figs: 25- 29



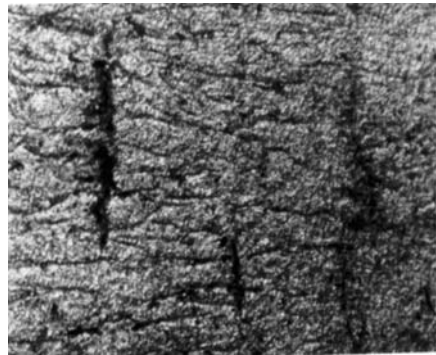
25



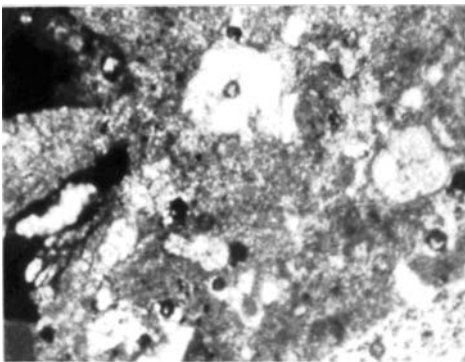
26



27



28



29

محتويات العدد

البحوث باللغة الانجليزية

* The Witten –Reshetikhin- Turaev Invariants of Lens Spaces	Khaled Qazaqzeh	425
* On Fibrewise τ – Paracompact Spaces	Abedallah D. AL-Momany	437
* Radon Measurements in Caves and Houses in Umm- Qais, Jordan	Khitam Khasawinah and Khalid Abumurad	459
* Critical Current Enhancement by Iron Doping in $Y_1Ba_2Cu_3O_{7-\delta}$ Superconducting System	Abdul Raouf El Ali (Al-Dairy) and Khitam Khasawinah	467
* Introducing English-Arabic Dictionary-Based Cross Language Information Retrieval	Awni Hammouri	477
* Parallel Graph Colouring Based on Saturated Degree Ordering	Ahmad Sharieh and Khair Eddin Sabri	489
* Automated Global Prayer Calls Using GPS	Zakaria Saleh	505
* Bayesian Prediction Interval from Grouped Data: Exponential Distribution	Moh'd Alodat, Khaled Aludaat and Tareq Alodat	517
* Up-Crossing Rates of Particular Non-Gaussian Processes	Moh'd Alodat and Khaled Aludaat	525
* Analysis of Rainfall in Southern Area of Jordan	Suleiman Tashtoush	533
* Petrographical and Mineralogical Study of the Travertine in Deir Abu Said Area, NW Jordan	Nazem El- Radaideh and Hakam Mustafa	565

التوثيق:

أ- توثيق المراجع والمصادر المنشورة: يتم ذلك داخل المتن باستخدام نظام الترقيم [1] بين قوسين.

- تعد قائمة بالمصادر والمراجع المنشورة في نهاية البحث حسب الترقيم الوارد في النص.

إذا كان المرجع كتاباً يكتب هكذا:

[] عزوز، دريد. ميكانيك الموائع، مديرية الكتب والمطبوعات، جامعة حلب، حلب، 1979.

وإذا كان المرجع بحثاً في دورية يكتب هكذا:

[] محمد، نوري صابر، قياس حساسية التخريز أثناء كسر الفولاذ الكربوني، دراسات: العلوم الهندسية والتكنولوجية، مج12، ع9، 1985، ص 24.

وإذا كان المرجع مقالة أو فصلاً في كتاب يكون كالتالي:

[] عبد الحافظ، سامي خضر. التشخيص المخبري للطفيليات، طرق زرع الطفيليات، اربد، جامعة اليرموك، 1986، ص 175-181.

ب- توثيق الهوامش والمصادر غير المنشورة: يتم ذلك في المتن بإثبات كلمة (هامش) متبوعة بالرقم المتسلسل للهامش داخل قوسين، هكذا: (هامش1). وتذكر المعلومات

التفصيلية لكل هامش في نهاية البحث تحت عنوان الهوامش وقبل قائمة المراجع:

هامش1: خضر، بسام راشد، قياس تركيز الرادون222 في هواء منازل مدينة اربد، الأردن، رسالة ماجستير غير منشورة، جامعة اليرموك 1990، ص 8-11.

مراجعات الكتب: تقبل للنشر في المجلة مراجعات الكتب الحديثة القيمة.

التصرف: يحق لرئيس التحرير إجراء التغييرات التي يراها ضرورية لأغراض الصياغة.

المستلآت: يمنح كل من ينشر بحثه نسخة واحدة من عدد المجلة الذي ينشر فيه البحث بالإضافة إلى عشرين مستلة منه.

ترسل البحوث والمراسلات إلى

رئيس تحرير مجلة

أبحاث اليرموك "سلسلة العلوم الأساسية والهندسية"

عمادة البحث العلمي والدراسات العليا

جامعة اليرموك

اربد-المملكة الأردنية الهاشمية

يمكن الحصول على أبحاث اليرموك من قسم التبادل في مكتبة جامعة اليرموك، أو عمادة البحث العلمي والدراسات العليا لقاء دينار للنسخة الواحدة.

الاشتراك السنوي: ديناران ونصف في الأردن، وثمانية دنانير أو اثني عشر دولاراً أمريكياً في الوطن العربي، وثمانية عشر دولاراً أمريكياً أو ما يعادلها في البلدان الأخرى.

بِسْمِ اللَّهِ الرَّحْمَنِ الرَّحِيمِ

أبحاث اليرموك

سلسلة العلوم الأساسية والهندسية

مجلة علمية محكمة

تنشر المجلة البحوث الأصلية التي تتوفر فيها

المنهجية السليمة، والتي لم تقدم للنشر في أي مكان آخر

قواعد وإجراءات النشر

- **اللغة:** تكتب البحوث باللغة العربية أو باللغة الإنجليزية ولا تستلم البحوث بغير هاتين اللغتين.
- **تقديم البحوث:** تقدم البحوث في أربع نسخ مطبوعة بفراغات مزدوجة وعلى وجه واحد، وهوامش حجم الواحد منها 2.5سم.
- يجب أن لا يزيد عدد صفحات البحث بما في ذلك الأشكال والرسوم والمراجع والجداول والملاحق عن (30) صفحة.
- يقدم الباحث ملخصين لبحثه في صفتين منفصلتين أحدهما باللغة العربية والآخر باللغة الإنجليزية في ما لا يزيد على 200 كلمة لكل منهما.
- يكتب عنوان البحث واسم المؤلف ورتبته العلمية والمؤسسة التي يعمل بها على صفحة منفصلة، ثم يكتب عنوان البحث مرة أخرى على الصفحة الأولى من البحث وعلى صفحة كل ملخص.
- يقدم البحث بعد الموافقة على نشره مطبوعاً ومحفوظاً على قرص كمبيوتر قياس 3.5 إنش متوافق مع أنظمة (IBM (Microsoft Word 2000, XP

الأشكال والرسومات:

- تقدم الأشكال والرسومات والجداول مرسومة بالحبر الأسود على ورق شفاف (Tracing Paper)، وفي صفحات منفصلة بحيث لا تتجاوز أبعاد هذه الأشكال والرسومات (19سم×12سم).
- أسماء الأعلام الأجنبية: عند ورود أسماء أعلام أجنبية في البحوث المقدمة بالعربية فإنها تكتب باللغة العربية تليها الأسماء بالإنجليزية بين قوسين.

هيئة التحرير

رئيس التحرير

الأستاذ الدكتور عبدالرحمن عطيات

الأعضاء

الأستاذ الدكتور مشهور الرفاعي	الأستاذ الدكتور عمر الريماوي
الدكتور محمد الشبول	الأستاذ الدكتور محمد أبو صالح
الدكتور محمد بلال الزعبي	الأستاذ الدكتور حامد زريقات

سكرتير التحرير

كاميليا عادل الحاج

© جميع حقوق الطبع محفوظة لجامعة اليرموك 2008
لا يجوز نشر أي جزء من هذه المجلة أو اقتباسه دون الحصول على
موافقة خطية مسبقة من رئيس التحرير

ما يرد في المجلة يعبر عن آراء أصحابه، ولا يعكس آراء
هيئة التحرير أو سياسة جامعة اليرموك

المراجعة اللغوية
الأستاذ الدكتور ابراهيم جبريل
قسم الكيمياء - جامعة اليرموك

تنضيد وإخراج
فاطمة يوسف عطروز

تصميم الغلاف
أحمد التميمي

ISSN 1023-0149

أبحاث اليرموك

سلسلة العلوم الأساسية والهندسية
مجلة علمية محكمة

1429هـ/2008م

العدد الثاني

المجلد السابع عشر

ISSN 1023-0149

منشورات جامعة اليرموك
عمادة البحث العلمي والدراسات العليا

أبحاث اليرموك

سلسلة العلوم الأساسية والهندسية
مجلة علمية محكمة

1429هـ/2008م

العدد الثاني

المجلد السابع عشر